OPTIMAL CONTROL OF A CONVENTIONAL HYDROPOWER SYSTEM WITH HYDROKINETIC/WIND POWERED PUMPBACK OPERATION

by

Fhazhil Said Wamalwa

Submitted in partial fulfillment of the requirements for the degree
Master of Engineering (Electrical Engineering)

in the

Department of Electrical, Electronic and Computer Engineering
Faculty of Engineering, Built Environment and Information Technology

UNIVERSITY OF PRETORIA

March 2017

SUMMARY

OPTIMAL CONTROL OF A CONVENTIONAL HYDROPOWER SYSTEM WITH HYDROKINETIC/WIND POWERED PUMPBACK OPERATION

by

Fhazhil Said Wamalwa

Promoter:	Prof. Xiaohua Xia
Co-Promoter:	Dr. Sam Sichilalu
Department:	Electrical, Electronic and Computer Engineering
University:	University of Pretoria
Degree:	Master of Engineering
Keywords:	Optimal control, hydraulic head, re-regulation reservoir, minimum environmental flow; hydrokinetic, optimal pump scheduling, optimal pumpback operation, hydropeaking, cascade pumping.

The need to ease pressure from the depleting fossil fuel reserves coupled with the rising global energy demand has seen a drastic increase in research and uptake of renewable energy sources in recent decades. Of the commonly exploited renewable energy resources, hydropower is currently the most popular resource accounting for 17% of the world's total energy generation, a portion which translates to 85% of the renewable energy share. However, despite the huge potential, hydropower is dependent on the availability of water resource, which is affected by climate change. During wet seasons, hydropower system operators are faced with a deluge of floods which results in excess power generation and spillage. The situation reverses in dry seasons where system operators are compelled to curtail power generation because of low water levels in the hydro reservoirs. The later situation is more pronounced in drought prone regions such as Southern Africa where some hydropower plants are completely shut down in dry seasons due to water shortage.

This dissertation focuses on the application of optimal control to hydropower plants with pumpback

retrofits powered by on-site hydrokinetic and wind power systems. The first section of this work develops an optimal operation strategy for a high head hydropower plant retrofitted with hydrokinetic-powered cascaded pumpback system in dry season. The objective of pumpback operation is to recycle a part of the downstream discharged water back to the main dam to maintain a high water level required for optimal power generation. The problem is formulated as a discrete optimisation problem to simultaneously minimise the grid pumping energy demand, minimise the wear and tear associated with the switching frequency of the two pumps in cascade, maximise restoration of the reservoir volume through pumpback operation and maximise the use of on-site generated hydrokinetic power for pumping operation. Simulation results based on a practical case study show the pumping energy saving advantages of the cascaded pumping system as compared to a classical pumped storage (PS) system.

The second section of this work develops an optimal control system for assessing the effects of ecological flow constraints to the operation of a hydropower plant with a hydrokinetic-wind powered pumpback retrofit. The aim of the control law in this case is to use the allocated water to optimally meet the contractual obligations of the power plant. The problem is formulated as a discrete optimisation problem to maximise the energy output of the reservoir subject to some defined technical and hydrological constraints. In this system, pumping power is met primarily by the wind power generator output supplemented by the on-site generated hydrokinetic power. The excess hydrokinetic power is exported to the grid to meet the committed demand. Three different optimisation scenarios are developed: The first scenario is the baseline operation of the hydropower plant without any intervention. The second scenario incorporates the hydrokinetic-wind-powered pumpback operation in the optimal control policy. The third scenario includes the downstream flow constraint to the optimal control policy of the second optimisation scenario. Simulation results based on a practical case study show that ecological flow constraints have negative effects to the economic performance of a hydropower plant.

ACKNOWLEDGEMENTS

This masters dissertation is a product of two years of hard work and immense support from many people. My deepest appreciation goes to my supervisor, Professor Xiaohua Xia, whom I am deeply indebted for academic guidance, motivation and support. Professor Xia, I would like to express my sincere gratitude to you for accepting me into your dynamic research team and your command in science will forever remain a source of motivation for me in my future academic journey going forward from this point. Special thanks also goes to my co-supervisor, Dr. Sam Sichilalu. This dissertation would not be possible without your contribution and persistent support. I would also like to express my deepest gratitude to all members of the EEDSM research group for their general camaraderie and for being part of my life for the last two years. They include Dr. Sam Sichilalu, Dr. Lijun Zhang, Dr. Xianming Ye, Dr. Farshad Barzegar, Evan Wanjiru, Bo Wang, Daoyuan Zhang, Jun Mei, Herman Castens, Alice Ikuzwe, Charles Kagiri, Sandro Masaki, Mpyana Bajany and Sedigheh Taghizadeh. I am also deeply indebted to my family including my mama, Everlyne Marita, my loving wife Glotilda Chelimo, my little son, Josemarie Wamalwa and my little daughter, Gianna Mary, for their love, encouragement and source of motivation during the two years that I have been working on this degree. I am deeply indebted to my single mother for the encouragement and motivation. Despite the fact that you barely went beyond primary school, you believed in the transforming power of education and even at age 72, you continued being a source of wisdom and encouragement for me during the two year journey. I am equally indebted to my wife for her support, care and for taking care of the family while I was away. The little Gianna has a special place in my heart because she was just three months old when I embarked on this journey. Despite being just two and a half years old, it has been an amazing experience engaging her on calls every evening before sleeping. I also want to acknowledge MasterCard Foundation and the EEDSM centre at the University of Pretoria for financial support and academic mentorship that enabled me to complete this degree. Lastly, I would like to thank God for guidance in everything that was accomplished during this period.

LIST OF ABBREVIATIONS

A_c	cross sectional area of the penstock (m^2)
A_u	base area of the main dam model (m^2)
A_m	base area of the intermediate reservoir model (m^2)
A_r	base area of the re-regulation reservoir model (m^2)
A_t	true or accepted value
A_{hk}	area swept by the hydrokinetic turbine rotor (m^2)
A_{wt}	area swept by the wind turbine rotor (m^2)
C_p	Betz Limit
E_g	total daily energy produced by the hydro-turbine generator (MWh)
E_{HK}	total daily energy produced by the HK system in a day (MWh)
E_{hk}	total daily hydro-turbine energy consumed by pumping system (MWh)
E_{hg}	total daily hydrokinetic energy exported to the grid (MWh)
E_{gk}	total daily grid energy supplied to the pumping system (MWh)
E_{opt}	total daily optimal energy output of the system (MWh)
HK	hydrokinetic
HKEC	hydrokinetic energy conversion
HKT	hydrokinetic turbine
HPP	hydropower plant
H_i	net differential head of pump Ki; $i = 1,2$ (m)
$h_o(t)$	net head of the hydropower system (m)
$h_m(t)$	water level in the intermediate reservoir (m)
$h_r(t)$	re-regulation reservoir water level (m)
$h_u(t)$	water level in the main dam model (m)
h_{ref}	anemometer reference height (m)
J	objective function
min ; max	minimum and maximum of the variables
masl	meters above sea level
MILP	mixed integer linear program
MINLP	mixed integer nonlinear program
MIQP	mixed integer quadratic program

N	total number of sampling intervals
n_{hk}	a variable denoting the number of HK generators
n_{wt}	a variable denoting the number of wind power generators
$P_{HK}(t)$	total HK generator power output (MW)
$P_{HK,r}$	nominal power rating of a single HK generator
OC	optimal control
PS	pumped storage
PSO	particle swarm optimisation
$P_g(t)$	hydro-turbine power output (MW)
$P_{g,r}$	hydropower plant's rated power output (MW)
$P_{gk}(t)$	grid power import for pumping operation (MW)
$P_K(t)$	power demanded by the pumpback system (MW)
P_{Ki}	power demanded by pump Ki; $i = 1,2$ (MW)
$P_{hg}(t)$	excess HK power supplied to the grid (MW)
$P_{hk}(t)$	a fraction of HK power supplied to the pumping system (MW)
$P_{WT,r}$	rated power output of the wind generator (MW)
$P_{ld}(t)$	instantaneous system load (MW)
$q_o(t)$	turbine discharge rate (m^3/s)
q_{in}	main dam in-stream flow rate (m^3/s)
q_k	flow rate of pump K (m^3/s)
q_r	controlled re-regulation reservoir discharge rate (m^3/s)
RPM	revolution per minute
R_{wt}	rotor diameter of wind turbine (m)
u_i	control switch for pump Ki; $i = 1,2$
v	desired wind speed at hub height, h_{hub} (m/s)
v_{ref}	wind speed at the reference height (m/s)
v_r	rated wind speed (m/s)
v_i	cut-in wind speed (m/s)
v_o	cut-out wind speed (m/s)
υ	river current velocity (m/s)
υ_r	rated speed of water (m/s)
WEC	wind energy conversion

$W_u(t)$	instantaneous volume of water in the main dam (m^3)
$W_m(t)$	instantaneous volume of water in the intermediate reservoir (m^3)
$W_r(t)$	instantaneous volume of water in the re-regulation reservoir (m^3)
ω	weighting factor
t_s	system sampling period (h)
Z_m	experimental measured values
η_e	electrical efficiency of the hydro-generator
η_m	mechanical efficiency of the hydro-turbine
η_k	combined efficiency of pump K and its motor drive
η_{wt}	overall efficiency of the wind power system
ρ_a	density of air (kg/m^3)
ρ_w	density of water (kg/m^3)
$\sigma_{m,dev}$	standard deviation
λ	ground surface friction coefficient
χ	Weibull shape parameter

TABLE OF CONTENTS

LIST OF FIGURES

CHAPTER 1 INTRODUCTION

1.1 PROBLEM CONTEXT AND MOTIVATION

The depleting fossil fuel reserves coupled with their externalities such as global warming underscore the need to explore and exploit clean and sustainable energy sources. To this end, the last five decades have seen increased research and utilisation of hydro, solar and wind as renewable alternatives to conventional sources. Some of the commonly cited advantages of renewable energy sources include environmental friendliness, natural abundance and their comparatively low operational costs when compared to their conventional counterparts. Despite increasing interests in solar and wind, hydropower is currently the most popular renewable energy resource thanks to its operational flexibility, ability to adapt quickly to changes in system load demand and its relatively high reliability. Currently, hydropower contributes 17% of the world's electrical energy demand, a portion which accounts for 85% of the renewable energy share [1]. Its share in the global energy matrix is projected to double by 2050 because of its ability to stabilise supply-demand variations caused by high penetration of the intermittent solar and wind [1]. However, the achievement of this projected growth may be hampered by the projected global decline in precipitation in the next four decades [1, 2, 3, 4]. The effects of climate change on hydropower generation have already been experienced in some vulnerable regions such as Southern Africa. Some countries in this region such as Tanzania, Zimbabwe, and Zambia have experienced a drastic decrease in hydropower generation in dry seasons in recent years due to the increase in prolonged droughts events. For instance, low water levels in the Kariba dam during prolonged droughts experienced in recent years resulted in massive power shortages in Zambia and Zimbabwe. In Tanzania, many hydropower plants (HPPs) were shut down in 2015 because of low

[1] https://www.iea.org/topics/renewables/subtopics/hydropower/

reservoir water levels resulting in an acute power shortage [2]. The effects of climate change and the increase in human settlement in the Pangani basin in Tanzania have resulted in over-allocation of water for irrigation farming resulting in an acute water shortage for hydropower generation. One of the affected power systems in Tanzania is the Pangani hydropower system. Due to the water shortage, the 91.5 MW Pangani hydropower system has been generating below 30% of its installed capacity in dry seasons in recent years. The anticipated decrease in precipitation in Southern Africa underscores that hydropower generation problem in the already affected countries is bound to decrease further [1]. This impending crisis, underscores the need to explore integrated water conservation and optimal control strategies that can optimise the performance of hydropower facilities.

One of the commonly encountered problems in the operation of hydropower systems is handling of conflicting objectives, which often times make the optimal control (OC) problem large scale and hard to solve. Because of their flexibility to respond to changes in system load demand and their comparatively low operational cost, impounded hydropower plants are commonly used as peaking plants in hydrothermal systems. In single purpose hydropower plants, the optimal control problem entails adjusting the turbine discharge rate to maximise hydropower generation when it is most profitable, such as during high peak-price hours [5]. In de-regulated markets with time differentiated energy prices, this operation strategy, referred as hydropeaking in technical literature, entails storage of sufficient water in the plant reservoir during off-peak hours for peak generation to maximise revenue generation. However, in practice, dams serve other purposes including provision of an aquatic habitat for downstream aquatic species, provision of water for irrigation farming, recreational navigation, and water abstraction for both domestic and industrial use. Therefore, practical optimal operation of a hydropower dam requires a balance between maximum revenue generation and protection of the downstream riverine ecosystem.

Without environmental regulatory policies, hydropeaking has the potential to cause downstream flooding with negative effects to aquatic biodiversity [6], riparian farming and recreational navigation [7]. To minimise these environmental effects, downstream ecological flow constraints are integrated into the OC policies of hydropower plants (HPPs), which often times reduce their operational

[2] http://www.telegraph.co.uk/news/worldnews/africaandindianocean/tanzania/11923748/Tanzania-turns-off-hydropower-as-drought-bites.html

flexibility to respond to changes in energy price signals and hence a reduction in revenue generation [8, 9]. The effects of minimum ecological flow constraints are more pronounced in systems with big disparities between peak and off-peak power demand in dry seasons; a scenario that requires HPP operators to store sufficient water during off-peak hours for optimal peak generation. These conflicting objectives underscore the need to assess the economic impacts of ecological flow policies and develop mitigation strategies that can optimise the utility of hydropower reservoirs with minimal effects to the downstream riverine ecosystem.

Many studies in the current literature on the optimal operation of hydropower plants have focused on water resource planning [10, 11, 12], optimal reservoir discharge [13] and scheduling of hydropower generators [14, 15, 16, 17] to maximise their beneficial use. Some studies have investigated the effects of incorporating ecological flow constraints in the OC policies of hydropower reservoirs [8, 18, 19]. In these studies, the commonly investigated environmental regulatory policies are minimum flow requirements and the ramp rate constraints [8]. A few works in the current literature have studied the effects of pumpback operation between the afterbay and the main storage reservoir to the energy yield of hydropower reservoirs [20, 21]. However, the problem of optimal control of the pumping operation to minimise the pumping energy demand has not been well studied. For instance, in [20, 21], the authors propose the pumpback operation during off-peak hours to store sufficient water in the hydro reservoir for peak generation. In this case, the rationale of pumping operation is justified by the difference between peak and off-peak energy prices to off-set the high pumping losses of the system. This system is uneconomical in high head applications where high pumping losses are more than the peak and off-peak price differences. The use of grid energy for such energy intensive pumping operation is also economically unattractive. There is no work in the current literature that has explored the use of alternative renewable energy alternatives for pumpback operation as applied in optimal control of hydropower systems.

This dissertation identifies optimal control of hydropower plants with hydrokinetic and wind powered pumpback operation as a potential area of increasing the energy yield of a hydropower reservoir in dry seasons. From the afterbay of conventional HPPs, water flows freely downstream with approximately 45% of the gravitational potential energy released from the reservoir. A fraction of this free energy can be tapped using the hydrokinetic energy conversion (HKEC) system to power the pumpback operation.

1.2 RESEARCH OBJECTIVE AND QUESTIONS

The main research objective of this dissertation is to optimise the energy output of HPPs in dry seasons using hydrokinetic/wind powered pumpback operation. To achieve this objective, the following specific objectives are stated:

1. To investigate the effects of pumpback operation to the energy output of a HPP in dry season.

2. To investigate and validate the energy saving potential of the cascaded pumpback system as compared to the classical pumped storage system.

3. To model an on-site hydrokinetic and wind power system for powering the pumpback operation of a HPP in the dry season.

4. To investigate the effects of minimum ecological flow constraints to the performance of a HPP with a pumpback retrofit.

In order to achieve the above stated objectives, the following research questions will be addressed in this dissertation:

1. What is the impact of pumpback operation to the daily energy yield of a hydro reservoir in the dry season?

2. What are the energy saving advantages of a cascade pumpback system as compared to a classical PS system for high head applications?

3. What are the effects of downstream flow constraints to the performance of a hydropower reservoir?

1.3 HYPOTHESIS AND RESEARCH APPROACH

This dissertation develops an optimal control strategy for maximising the economic value of the available water in a hydropower reservoir with and without downstream flow policies in dry seasons. The first section, presented in chapter 3, proposes a cascade pumping strategy to minimise the overall pumping energy demand of the pumpback system. The second part, presented in chapter 4, investigates the effects of environmental flow constraints on the performance of a hydropower system with hydrokinetic-wind powered pumpback operation over a 24 h control horizon. To minimise reliance on the much needed grid power for pumping operation, an on-site hydrokinetic and wind power system is proposed for powering the pumpback operation in both system. An optimal control policy is developed for the operation of the resultant hydropower system under the two optimisation cases. The following hypotheses are stated:

1. Pumpback operation improves the energy output of the hydropower reservoir in dry seasons.

2. Cascade pumping reduces the daily pumping power and energy demand of the pumpback system.

3. Integrating downstream flow constraints to the optimal control policy of a hydropower reservoir has negative impacts on its daily energy yield.

4. The optimal control of the proposed system improves the overall daily energy yield of the reservoir operated with and without ecological flow constraints.

The following approaches will be used to achieve the afore-listed research objectives:

- Literature review- A literature survey will be carried out to identify previous research works that relate to the proposed optimal control system as well as establish a body of knowledge on the optimal operation of hydropower reservoirs. Pertinent to the literature survey is the establishment of the existing optimisation approaches applied to the optimal control of hydropower plants with and without ecological flow policies.

- Mathematical model formulation- This will entail developing mathematical models that characterise the operation of each of the sub-systems of the proposed hydropower plant. These models

include the pumpback model for both classical pumped storage and cascaded pumping system, the hydropower reservoir model with and without environmental regulatory policies and the on-site hydrokinetic and wind power system for powering the pumpback operation.

- Simulation and results- Different optimisation scenarios of a hydropower plant with pumpback operation will be developed. The first scenario, presented in chapter 3, will entail the optimal control of a HPP with a cascaded pumpback retrofit powered by the on-site hydrokinetic power system. To validate the operational advantages of a cascaded pumpback system, its simulation results based on a suitable case study will be compared with the performance of a classical pumped storage (PS) system. The second optimisation scenario, presented in chapter 4, will assess the effects of ecological flow constraints on the performance of a hydropower plant with hydrokinetic-wind powered pumpback operation. In the second scenario, three optimisation models will be developed and analysed: The first model will present the baseline operation of the plant in the case study without any intervention, supplying power to meet a deterministic time-varying consumer load in the dry season. The second model will present a hydropower plant with a hydrokinetic-wind-powered pumpback operation to investigate the effects of pumpback operation to the performance of the plant. The third model will incorporate both pumpback operation and downstream flow constraints in the optimal control policy of the plant. The objective of the latter case is to assess the effects of pumpback operation to the performance of the plant in question.

- Case study- The proposed optimal control systems will be applied to suitable case studies and the simulation results will be used to validate the research hypotheses as well as answer the proposed research questions set out in this dissertation.

1.4 RESEARCH GOALS

This research aims at achieving the following goals:

1. To maximise the daily energy output of a hydropower reservoir in dry seasons.

2. To investigate the comparative advantages of a classical single pump and cascaded pumping systems as applied in the optimal control of hydropower plants.

3. To investigate the effects of downstream ecological flow constraints to the performance of a hydropower plant with a pumpback retrofit powered by on-site hydrokinetic and wind power systems.

1.5 RESEARCH CONTRIBUTION

The main contribution of this dissertation is developing a cascade pumpback model as a water conservation strategy for a high head hydropower plant to minimise the pumping power and overall pumping energy demand of the system. The dissertation also proposes the use of on-site hydrokinetic and wind power systems for pumping operation to minimise reliance on the grid power. In the course of the research, the following papers were developed:

1. Fhazhil Wamalwa, Sam M.Sichilalu, Xiaohua Xia, Optimal control of hydrokinetic-powered pumpback system for a hydropower plant in dry season: A case study, *Energy Procedia* 105 (2017):94-101

2. Fhazhil Wamalwa, Sam M.Sichilalu, Xiaohua Xia, Optimal control of conventional hydropower plant retrofitted with a cascaded pumpback system powered by an on-site hydrokinetic system, *Energy Conversion and Management* 132 (2017):438-451.

3. Fhazhil Wamalwa, Sam M.Sichilalu, Xiaohua Xia, Effects of downstream flow constraints on the performance of a hydropower system with hydrokinetic-wind powered pumpback operation, *Energy* (Submitted April 2017).

4. Fhazhil Wamalwa, Sam M.Sichilalu, Xiaohua Xia, Optimal energy mix of a micro-hydro-wind-grid system powering a dairy farm in Western Cape, South Africa, *9th International Conference on Applied Energy-ICAE2017*, August 21-24 2017, Cardiff, UK.

1.6 OVERVIEW OF STUDY

Chapter 1 of this dissertation has introduced the background as well as the motivation of the research work. It has covered the study objectives, research questions, goals and a brief overview of the approach to be followed in the research. Chapter 2 will review the current literature to establish the bounds of knowledge on optimal control of hydropower systems with pumpback operation. Pertinent to literature study is the establishment of relevant theoretical knowledge and mathematical models of the various components of the proposed hydropower systems including conventional hydropower systems, hydrokinetic and wind energy systems as well as the pumpback system. At the end of literature review, a research gap to be addressed in the dissertation is established. Chapter 3 presents an optimal control system for a conventional hydropower plant with a cascaded pumpback retrofit powered by an on-site hydrokinetic energy conversion system. The main objective of this chapter is to establish the performance advantages of a cascaded pumpback system over a classical pumped storage system. Chapter 4 presents an optimal control system for assessing the effects of ecological flow constraints to the performance of a hydropower plant with a pumpback retrofit powered by on-site hydrokinetic-wind hybrid power system while chapter 5 presents the conclusion of the dissertation and the recommendations for future research directions.

CHAPTER 2 LITERATURE STUDY

2.1 CHAPTER OBJECTIVES

This chapter presents a review of the current literature on the optimal control of hydropower systems. In chapter 1, pumpback operation was identified as a potential strategy for improving the energy output of hydro reservoirs in dry seasons. To minimise the use of grid imported power for pumping operation, the previous chapter also proposed the hydrokinetic and wind as potential distributed renewable energy (DRE) resources for powering the pumpback operation. Hence, this chapter introduces the general theoretical concepts of the various system components of a hydropower scheme with a pumpback retrofit powered by the hydrokinetic and wind energy resources.

2.2 CONVENTIONAL HYDROPOWER SYSTEMS

Hydropower is one of the oldest and the most advanced renewable energy resources in the world. It was first generated in 1878 to power a single electric lamp in Northumberland, England [1] but currently, hydropower has evolved to account for 17% of the world's total energy and 85% of the renewable energy share [1]. A hydropower system converts the kinetic energy of moving water into mechanical and subsequently into electrical energy by use of a hydro-turbine generator. In general, hydropower plants (HPPs) can be classified either on the basis of their sizes or on the basis of their deployment technology. On the basis of their sizes, hydropower plants can be classified into five categories: Large (more than 30 MW), Small (1 MW–30 MW), Mini (100 kW–1 MW), Micro (10 kW–100 kW) and Pico (less than 10 kW) hydro plants.

[1] https://www.hydropower.org/a-brief-history-of-hydropower

On the basis of their deployment technology, they can be classified into conventional plants, pumped storage (PS) plants and hydrokinetic (HK) power plants. Conventional hydropower plants can be classified further into impounded and diversion plants. An impounded HPP also referred as a peak HPP is made by creating a dam on the course way of a river to temporarily store water that would be released controllably through a penstock to power a hydro-turbine generator. On the other hand, a diversion HPP (also referred as run-off-river HPP), which is the most popular technology, is made by diverting a part of the river flow either directly into an off-site reservoir/canal or a penstock for electricity generation before releasing the diverted water back to the downstream river flow. The key feature of a conventional HPP is the water head which is the vertical height between the water surface in the dam and the hydro-turbine generator. The ability of Peak HPPs to hold water and regulate its release in response to system demand makes them dispatchable to some extent [22]. On the other hand, the water discharges from the run-of-river HPPs follow the natural river flow making them non-dispatchable [22].

Unlike a conventional HPP which is characterised by natural in-stream flows, a PS plant is a 'closed' system with minimal to zero natural inflows. It makes use of two reservoirs, one situated at a higher elevation than the other. In pumping mode, a PS system converts electrical energy into gravitational potential energy stored in an upper reservoir which is re-converted back to electrical energy in generation mode. PS systems are mainly used as giant utility-scale energy storage facilities for excess off-peak energy in systems with big disparities between peak and off-peak load demand and also for mitigating the power variability of intermittent renewable resources such as solar and wind [23, 24, 25]. When a PS is used as a storage facility for surplus off-peak energy, the surplus electrical energy is used to pump water from the lower reservoir to the upper reservoir which is released during peak hours via a hydro-turbine generator to generate electricity. The PS technology is currently the most matured energy storage technology and widely used in utility-scale applications because of its high energy density; with a current installed capacity of 130 GW as of 2016 [26]. In deregulated energy markets, PS systems can be operated as merchant entities to exploit price arbitrage opportunities resulting from inter-temporal energy price variations to make profits [27, 28]. In this case, the rationale of operating PS systems as merchant entities is based on the assumption that the peak and off-peak energy price differences outweigh the round-trip system losses. Otherwise, it would be uneconomical to a operate PS system considering that pumping energy is always more than the generated energy due to system round trip losses. PS facilities can also be deployed as long term giant energy storage facilities in power systems with surplus hydroelectric energy during rainy seasons [29].

2.2.1 Hydropower plant models

There are many hydropower plant models in the current literature generally classified as linear (non-elastic) and non-linear (elastic) models [30, 31, 32]. The linear models use linearised equations at operating point while the non-linear models use non-linear equations of mechanical power and the relationship between the turbine discharge, the system head and gate opening [30]. These models are further sub-classified as with and without surge tank effects. They are further categorised as with elastic and non-elastic water column in the penstock as shown in Figure 2.1. Hydro turbines are also classified into two main categories; the impulse type such as the Pelton wheel turbine and the reaction type such as the Francis and Kaplan [31].

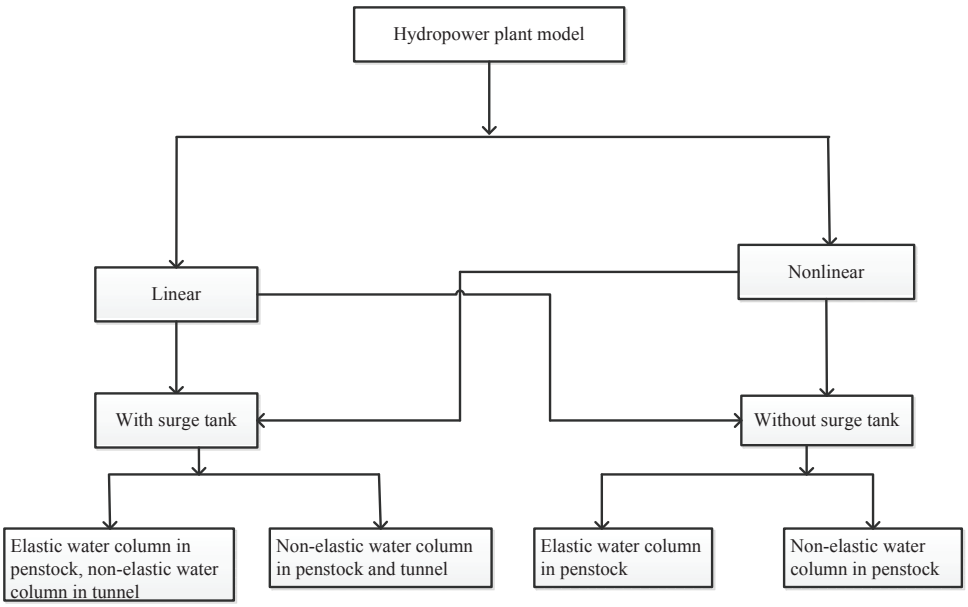

Figure 2.1. An overview of the various hydropower plant models

Since, the core objective of this dissertation is on optimal reservoir operation (not the generator performance), the hydropower model with non-elastic water column effect is adopted for modelling simplicity. Such a model assumes negligible hydraulic resistance, inelastic penstock wall and incompressible water flow, turbine output is proportional to the product of head and volumetric flow, and velocity of water is proportional to gate position.

Figure 2.2 shows the typical schematic of a conventional hydropower plant. As shown, it comprises a hydro reservoir (the main dam), the surge tank, the penstock and the hydro turbine generator system. The main function of a surge tank is to regulate the water flow during load reduction and sudden increase in the load on the hydro generator (water flow transients in penstock) and thus reducing the pressure on the penstock. The generator and the turbine are connected directly by a vertical shaft.

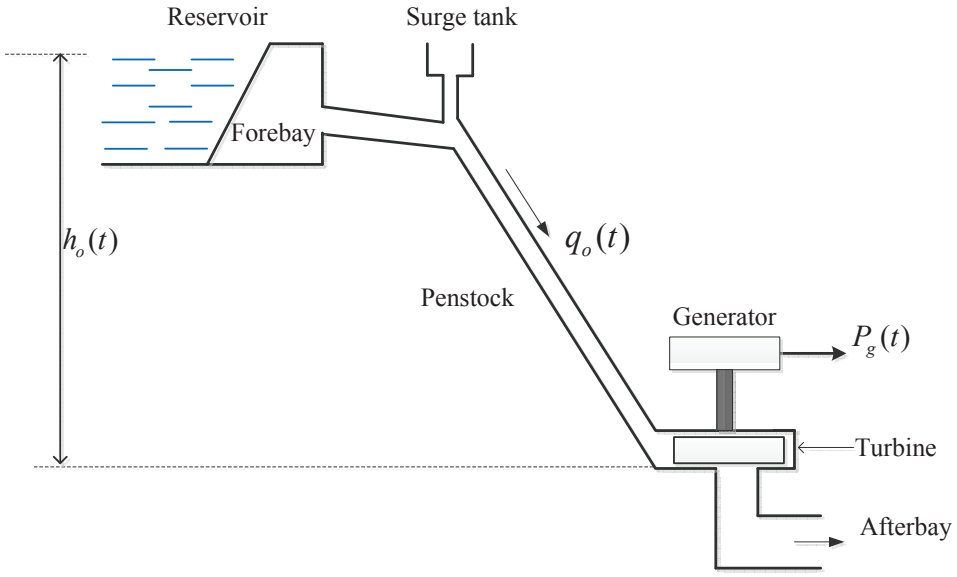

Figure 2.2. Layout of a conventional hydropower system

The most general model of a hydropower plant starts with hydraulic and then mechanical power modelling. The hydraulic power is developed when a volume of water falls from the plant reservoir through a height via the penstock. The hydro-turbine converts this kinetic energy of falling water into mechanical energy which is subsequently converted into electrical power output. In general, the theoretical electrical power out of a conventional hydropower system, $P_g(t)$ (MW), is a non-linear function of the turbine discharge rate, $q_o(t)$, and the net hydraulic head of the system, $h_o(t)$, given by the following expression [33]:

$$P_g(t) = \rho_w g \eta_m \eta_e h_o(t) q_o(t) \times 10^{-6}, \tag{2.1}$$

where $\rho_w = 1000$ kg/m^3 is the density of water, $g = 9.81$ m/s^2 is the gravitational acceleration constant while η_m and η_e are respectively, the mechanical and electrical efficiency of the hydropower system.

2.3 HYDROKINETIC POWER SYSTEMS

Unlike the conventional hydropower systems that require water heads, hydrokinetic (HK) systems are designed to extract the kinetic energy of water currents at very low to zero heads [34]. Hydrokinetic energy conversion (HKEC) systems are generally classified into two main categories depending on where they are deployed; namely marine and riverine HKEC systems. Marine HKEC systems are deployed in marine environments and they include tidal stream, ocean wave, ocean current and ocean thermal HKEC systems while riverine HKEC systems are deployed in rivers to harness the kinetic energy of the river currents [35]. The various HKEC technologies are discussed in [34]. The energy extraction efficiency of HK system depend on the turbine designs which are categorised into horizontal axial turbines (two-blade turbine, three-blade turbine, multi-blade turbines) and vertical axial turbines [34]. A state of the art review of the technological developments of the hydrokinetic turbines is presented in [36]. One of the problems associated with the use of axial flow HK turbines is the interruption of power generation caused by the attachment of the debris onto the turbine which impairs its deployment in rapid rivers with debris. The problem causes frequent stoppage of the turbine by the operator to remove the debris. This problem has been mitigated by a turbine designed with swept-back blades that allow it to automatically shed the debris [37]. The operation principle of a hydrokinetic turbine is similar to that of a wind turbine except that the HK turbine is powered by the kinetic energy of water currents. Therefore, the theoretical power output of a HKEC system is expressed as follows:

$$P_{HK}(t) = 0.5\rho_w A_{hk}\eta_{hk}C_p\upsilon^3 \times 10^{-6}, \tag{2.2}$$

where $P_{HK}(t)$ (MW), A_{hk} and υ are respectively, the total instantaneous power output of the HKEC system, the area swept by the HK turbine rotor and the river current speed. The coefficient η_{hk} denotes the combined efficiency of the HK turbine and the HK generator while C_p is the turbine power coefficient, also known as the Betz limit [34]. Despite having a similar working principle, a HK turbine

produces far more power than a wind turbine of the same dimension because water has a higher energy capacity than wind; water is about 835 times denser than the wind. HK turbines extract energy from the water currents by reducing the speed of flowing water. To ensure flow continuity, there is a theoretical limit to the amount of kinetic energy of a flowing water that can be extracted by a hydrokinetic turbine; known as the Betz limit [34].

2.4 WIND POWER SYSTEMS

Wind is one of the oldest energy sources that have been exploited immensely to power technological developments throughout many civilisations. It was traditionally used to power sailing ships and windmills but the development of a wind turbine led to the current upsurge in the use of wind to generate electricity [38]. Besides environmental friendliness, the popularity of wind energy is owed to its natural abundance and low operational costs of wind power systems when compared to conventional systems. However, one of the limitations of wind power systems is the large area required by wind turbines and thus, they are mostly deployed in rural areas with large open spaces [39]. Wind resource is also intermittent in nature. That is, the power output of a wind generator varies with changes in wind speed which is weather-dependent and thus non-dispatchable. This drawback can be mitigated by deploying wind energy resource in hybrid integrations with other renewable resources and by use of energy storage devices (ESDs), which in this dissertation is the pumped storage system. Therefore, besides boosting the overall performance of the resultant hybrid power system, the use of wind-generated electricity to power the pumping system will also mitigate its variability.

Generally, wind turbines are classified into two categories; horizontal axial (with the rotational axis parallel to the ground) turbines and vertical axial (rotational axis is perpendicular to the ground) turbines [38]. Vertical axial turbines have the omnidirectional advantage; they can be powered by the wind from all directions. However, they suffer from low energy conversion efficiency, low starting torque and low power production because of low wind speeds closer to the ground [40]. They are commonly used in small-scale residential applications such as roof-top installations. On the other hand, horizontal axial turbines have a comparatively higher energy extraction efficiency and they are commonly used in large-scale wind power installations due to their ability to produce more power at a given wind speed when compared to their vertical axial counterparts. In this dissertation, horizontal axial turbines are used.

The power output of a wind turbine is dependent on the wind speed at the given location, air density, the area swept by the turbine rotor and the energy extraction efficiency of the turbine as specified by the manufacturer [41]. When modelling a horizontal axial turbine wind power system, it is important to determine the wind speed at the hub height, h_{hub}, since that is the actual wind speed that interacts with the turbine rotor to produce power. In general, the theoretical power output of a wind turbine, $P_{WT}(t)$ (MW), is expressed as follows [41]:

$$P_{WT}(t) = 0.5\rho_a A_{wt}\eta_{wt}C_p v^3 \times 10^{-6}, \tag{2.3}$$

where ρ_a is the air density, A_{wt} is the area swept by the wind turbine rotor while η_{wt} is the overall efficiency of the wind energy conversion (WEC) system. The quantity v denotes the wind speed at the desired height, h_{hub}, which is normally taken at 10 m as the standard height. In this dissertation, the power law expression for the hub height wind speed used in [40] is adopted:

$$v = v_{ref}\left(\frac{h_{hub}}{h_{ref}}\right)^{\lambda}, \tag{2.4}$$

where v_{ref} denotes the wind speed at the reference height, h_{ref}, while the exponent λ denotes the coefficient of the ground surface friction which is a function of the hub height, time of day and the season of the year, the temperature, the wind speed and the nature of the terrain classified as rough or smooth. Typical values of λ are given in [38] classified on a range of $\frac{1}{7}$ to $\frac{1}{4}$ depending on the nature of the terrain. In this dissertation, $\lambda = \frac{1}{7}$ is used as a typical value commonly adopted for open land WEC installations. The desired wind speed, v, obtained from equation (2.4) is the actual wind speed for computing the power generated by a wind generator.

2.5 THE PUMPBACK SYSTEM

Many hydropower plant operators in drought-prone regions, such as Southern African, are normally compelled to curtail power generation in dry seasons due to low water levels in the hydro reservoirs. This problem has become more pronounced in Southern Africa in recent years with Zimbabwe, Zambia and Tanzania worst affected in the face of prolonged droughts occasioned by the on-going climate change. To mitigate such situations, some works in the current literature have proposed pumpback

operation during off-peak hours to maintain a high reservoir water level for optimal and safe operation of the HPPs in peak hours [20, 21]. In general, the pumping power of a pump, $P_K(t)$ (MW) is directly proportional to the discharge capacity of the pump, $q_k(t)$, and the hydraulic head of the pumping system, H, expressed as follows:

$$P_K(t) = \frac{9.81 H q_k(t)}{\eta_k} \times 10^{-3}, \tag{2.5}$$

where the coefficient η_k is the combined efficiency of the pump, K, and its motor drive.

2.6 OPTIMISATION APPROACHES IN HYDROPOWER SYSTEMS

Optimisation is the process of finding the best solution that minimises or maximises a given objective function subject to a set of constraints [42]. The solution that satisfies the set constraints is called an optimal solution. An optimisation problem which is solvable subject to some defined constraints is referred to as a constrained optimisation problem. In some cases, the optimisation problems do not have constraints: such problems are referred to as unconstrained optimisation problems. Optimisation problems can also be classified as single objective or multi-objective problems with the later class having more than one objective to be optimised simultaneously. Multi-objective optimisation problems are generally complex and hard to solve as compared to single objective problems. In many multi-objective optimisation problems, it is difficult to get a single optimal solution that optimises all the objective vectors simultaneously and as a result, the optimal solutions are commonly referred to as Pareto optimal or non-inferior solutions. Which means, improvement of the performance index of one objective is pitched against the performance indices of other objectives in the multi-objective function [42].

Many optimisation problems in hydropower systems are generally multi-objective problems because hydropower dams are, in most practical cases, multi-purpose reservoirs. Besides hydropower generation, rivers serve other purposes such as downstream recreational navigation, provision of a habitat for aquatic biodiversity, water abstraction for irrigation farming as well as the abstraction for both domestic and industrial use. Therefore, practical optimisation in hydropower systems entails the search for optimal solutions that balance multiple conflicting objectives.

In many optimal control studies in hydropower systems, the commonly investigated objectives include maximisation of the energy output of the reservoir and minimisation of operational costs of the system. In general, variations in many studies in the current literature include the objective to be optimised, system size and configuration, control horizon (short term and long term), handling of uncertainties and problem dimensionality such as single-reservoir and multi-reservoir systems [43] which often determine the optimisation techniques employed. The main sources of uncertainties in the operation of hydropower plants (HPPs) are water inflow, energy price and load variability. This section focuses on reviewing research works on optimal operation and control of hydropower systems.

One of the operational problems in hydropower systems that have received substantive attention in the current literature is water resource planning. In many studies, the problem is formulated as a multi-objective optimisation problem with conflicting sub-objectives [10, 11, 12, 44, 45]. In [10], a water resource allocation problem to maximise water use for irrigation, hydropower generation and navigation is formulated as a multi-objective problem and solved as a linear program subject to technical and hydrological constraints. A similar water allocation problem is solved in [11] using dynamic programming approach to maximise revenue from the generated hydropower while minimising costs of meeting contractual power demand from alternative energy sources subject to both environmental and system regulatory constraints. In [5], the authors propose an optimal control model for assessing the opportunity cost of ramp rate restrictions on the operation of a HPP under a contract to supply a deterministic but time-varying consumer load. The problem is formulated as a nonlinear scheduling program to meet the load demand at all times subject to both technical and operational (including ramp rate) constraints over a 120 h control horizon.

Another important operational aspect of a hydropower system that has been studied widely in the current literature is scheduling and dispatch. In many studies, the scheduling objective is to maximise the profitability of a HPP in de-regulated energy markets subject to energy price uncertainties as well as in-stream flow variability as summarised in [46]. In hydrothermal systems, scheduling objective is to minimise the operational cost of the hybrid system [47]. A stochastic dynamic programming strategy is proposed in [16] for short-term scheduling of a HPP to maximise revenue generated from the sale of energy in a pool-based market. In [48] a linear program is employed to solve the problem of maximising the energy output of a head-dependent HPP subject to reservoir storage and penstock release constraints. In [49] a short-term optimal scheduling strategy for a coupled multi-reservoir multi-unit hydropower system is presented for maximising profit in a day-ahead market taking into consideration detailed

constraints of each reservoir and generator unit as well as forbidden discharge between cascaded reservoirs. The problem is formulated as a multi-objective mixed-integer nonlinear program (MINLP) to maximise expected revenue and minimise generator start-up costs. A similar multi-reservoir multi-unit scheduling problem with spatial-temporal coupling between and among reservoirs: the turbine discharge from an upstream reservoir forms the in-stream flow into the downstream reservoir, is solved as a mixed integer linear program (MILP) in [50] to maximise revenue generated from sale of energy in a pool-based energy market with deterministic time-varying 24 h price forecasts. In [49, 50], integer variables are used to represent the ON-OFF behaviour of each hydropower generator in the multi-unit system. However, the discretisation of the non-linear hydropower function employed in mixed integer linear programming to model the hydraulic head variations increases the computational complexity of solving the scheduling problem, more so over a short-term control horizon. These limitations of mixed integer nonlinear programming can be surmounted by employing mixed-integer quadratic programming (MIQP) technique that captures the non-linear relationship between hydropower generation and the turbine discharge as well as the hydraulic head variations [51].

In hydrothermal systems, the commonly pursued optimisation objective by many system operators is meeting system load demand at minimal operational costs [47, 52]. The various techniques and approaches to solving the hydrothermal scheduling problem are reviewed in [53]. A review of the application of dynamic programming, mixed integer programming, evolutionary algorithms (simulated annealing and genetic algorithm), Lagrangian relaxation technique, interior-point and artificial intelligence approaches (neural networks) to solve scheduling and unit commitment problems in hydrothermal systems is presented in [53]. In [54], a short-term scheduling strategy for minimising the operational cost of a hydrothermal system based on a nonlinear network flow concept subject to system transmission and other physical and operational constraints is presented. The optimisation objective is to maximise the use of hydropower generators in the system to minimise the thermal fuel costs in the overall system. The authors in [55] present an optimal scheduling strategy for hydro and thermal generators in a large hydrothermal system taking into account the system demand and hydrological variability. A similar large-scale operational cost minimisation hydrothermal scheduling problem is solved in [56] using stochastic dual dynamic programming approach over a long-term control horizon. In [57], the noise annealing network approach is applied employed to solve the cost minimisation problem in a large hydrothermal system subject to the system's load balance, hydrological constraints and technical constraints of the thermal generators. In [52], a mixed integer linear programming approach is employed to solve the cost minimisation problem in a hydrothermal power system over a short-term

planning horizon subject to both hydrological constraints of the hydro system and thermal generators' technical constraints. The general large-scale non-linear planning problem is first decomposed into small sub-problems for each of the hydro units in the system and solved using mixed integer linear programming approach.

Optimal control of pumped storage (PS) systems as merchant entities in pool-based energy markets is also a well-studied problem in the current literature [52, 58, 59, 60, 61, 62, 63]. In these cases, PS facilities are used to store cheap-to-buy-off-peak energy which is then recovered during peak time and sold at high peak prices to make profits [58]. The rationale of operating a PS system is based on the assumption that the peak and off-peak price differences are higher than the round-trip system losses. Otherwise, it would be uneconomical to operate a PS facility except where it is purely used for storing energy for mitigating the peak and off-peak system demand variations as well as enhancing dispatchability of intermittent renewable resources [59].

In [60], MILP is used to solve the scheduling and the unit commitment problem of a head-dependent multi-unit PS power system to maximise profit in a deregulated energy market over a short-term control horizon. The problem is first formulated as a MINLP owing to the nonlinear power function of a hydropower system and then converted into a MILP by enhanced linearisation technique. A Lagrangian relaxation technique is employed in [61, 62] to optimally schedule a large hydrothermal power system with PS facilities to minimise the net thermal operational costs of the resultant system subject to physical and operational constraints. Particle Swarm optimisation (PSO) and genetic algorithm are employed in [64] and [65] respectively to solve the short-term scheduling problem of a multi-reservoir hydrothermal system to minimise the operational costs of the resultant hybrid system subject to both hydrological as well as thermal constraints of the systems. The problem is formulated as a large-scale hard to solve non-linear problem taking into account the spatial-temporal coupling among the cascaded reservoirs, the head-dependent nonlinear hydropower function and the valve-point loading effect in the thermal plant's fuel cost function.

In the afore-studied literature, the complexity of the optimisation problems varies depending on their nature (number of reservoirs involved), constraints and the number of objectives involved. For instance, when compared to single-reservoir problems, multi-reservoir problems are more complex due to hydraulic coupling between and among adjacent reservoirs [43, 65] and higher dimensionality which make these type of problems large scale and hard to solve [33, 43]. In many optimisation studies

involving multi-reservoir multi-purpose systems, trade-offs and compromises are made in search of optimal operation policies which are often difficult to get [45]. However, for modelling simplicity, this dissertation focuses on the optimal control of a single reservoir HPP. The above-referenced studies are based on 'business-as-usual' scenarios with regard to water availability. None of them has tackled the problem of mitigating the variability of water availability between wet and dry seasons; a problem commonly experienced by the HPP operators in drought-prone regions such as Southern Africa. Where the pumpback operation is proposed such as in [20, 21], optimal control of pumping operation to minimise pumping energy demand is not considered. Therefore, the next chapter considers a cascaded pumpback retrofit to a conventional high head hydropower plant to maximise the energy yield of the system at minimal pumping power and energy demand.

2.7 SUMMARY

This chapter presented a literature survey on optimal control of hydropower systems. Pertinent to the review is the establishment of the bounds of theoretical as well as practical knowledge on the components of the optimal control model proposed in the previous chapter. This entails a review on conventional hydropower plants, the wind energy system and the hydrokinetic energy conversion systems. The last section of the chapter presents a review on the various optimal control approaches of hydropower systems in the current literature. The next chapter will present an optimal scheduling strategy of a conventional hydropower plant retrofitted with the hydrokinetic-powered cascaded pumping retrofit.

CHAPTER 3 OPTIMAL CONTROL OF A HYDROPOWER PLANT WITH A HYDROKINETIC-POWERED CASCADED PUMPBACK RETROFIT

3.1 CHAPTER OVERVIEW

This chapter presents an optimal scheduling strategy for a conventional high head hydropower plant retrofitted with a cascaded pumpback system. The aim of the pumpback operation is to maintain a high reservoir water level required for optimal power generation. The general optimal control (OC) problem is formulated as a discrete mixed integer nonlinear optimisation program to; minimise grid pumping energy demand; minimise wear and tear associated with the switching frequency of the pumping system; maximise restoration of the volume of the hydro reservoir; and maximise the use of hydrokinetic (HK) power for pumping operation. The proposed optimal control is applied to a suitable case study and the simulation results compared with the performance of a classical pumped storage model to validate the economic advantages of cascaded pumping as a water conservation measure applied in hydropower system.

3.2 INTRODUCTION

In predominantly hydropower systems with big disparities between peak and off-peak power demand, pumpback operation during off-peak hours has been proposed in [20, 21] as a potential operational strategy for increasing the energy yield of the hydro reservoirs. In [20], the pumpback operation is employed to optimise the energy output of a hydropower plant (HPP) over a 12-month control horizon

with seasonal changes in in-stream flows as a source of uncertainty. The drawback of this pumping approach is the sole reliance on grid energy for pumping operation and high pumping energy demand over the control horizon; minimisation of pumping energy is not considered in the optimisation model. In [21], a pumpback retrofit is proposed for a high head application to maximise the energy output and revenue of a HPP in a day ahead market with deterministic time-varying energy prices over a 24 h control horizon with a constant in-stream flow. In this case, the high head losses associated with a single high lift pump has the potential to undermine the economic viability of the model. In this chapter, we propose a cascaded pumping strategy for minimising the pumping power and pumping energy demand of the pumpback system for high head hydropower application.

Cascading the pumpback operation reduces the overall pumping problem into a multi-pump problem which can be solved to minimise the pumping power and pumping energy demand through optimal scheduling over a given control horizon, 24 h in this chapter. Defining a pump switch as a state transition from OFF to ON state [66], the optimal control problem of the pumping system to minimise the pumping energy demand is solved in [67, 68]. Since pumping energy demand over a given control period is proportional to the number of switches or the cumulative operating hours of the pumping system, minimisation of the number of switches of a pump over a given control period has the potential to minimise the wear and tear of the pump [66, 69]. This chapter presents the first attempt at implementing cascaded pumping strategy for the pumpback operation to optimise the performance of a hydropower reservoir.

The main contribution of this chapter include: (1) The use of alternative hydrokinetic energy for pumpback operation, (2) cascading the pumpback operation to minimise pumping power and pumping energy demand for high head applications and (3) minimisation of the wear and tear of the pumps by minimising their switching frequency. The work presented in this chapter has been published in [70].

3.3 MATHEMATICAL MODEL FORMULATION

There are various hydropower facility models in the current literature, generally classified as linear and non-linear as described in section 2.2.1. Some dynamic models such as the one employed in [21, 71] considers a dynamic mechanical turbine efficiency expressed as a function of rotor angular speed,

turbine blade radius, turbine flow rate and the reservoir head, which makes the models complex. In this dissertation, the simplified model employed in [18], which assumes a fixed mechanical turbine efficiency, is used for modelling simplicity since the objective of the study is to optimise the reservoir performance, and not the generator performance.

3.3.1 Schematic model layout

The layout of the proposed hybrid hydropower system with a cascaded pumpback retrofit is shown in Figure 3.1. As shown, the pumpback system comprises two pumps, $K1$ and $K2$, inter-staged with an intermediate reservoir, M. The pumps are powered exclusively by the hydrokinetic (HK) power, $P_{hk}(t)$, supplemented by the grid power import, $P_{gk}(t)$. In cases when the total HK power, $P_{HK}(t)$, is more than the total pumping power demand, the excess HK power, $P_{hg}(t)$, is supplied to meet the contractual grid demand. In the figure, $h_o(t)$, $h_u(t)$ and $h_m(t)$ are respectively, the hydraulic head of the dam, the height (depth) of water in the dam and the water level in the intermediate reservoir at time t. The hydrokinetic power system comprises n_{hk} HK generators installed downstream the power plant to harness a part of the kinetic energy of free-flowing water to power the pumpback system. The pumps, $K1$ and $K2$, are powered through their respective switches, u_1 and u_2.

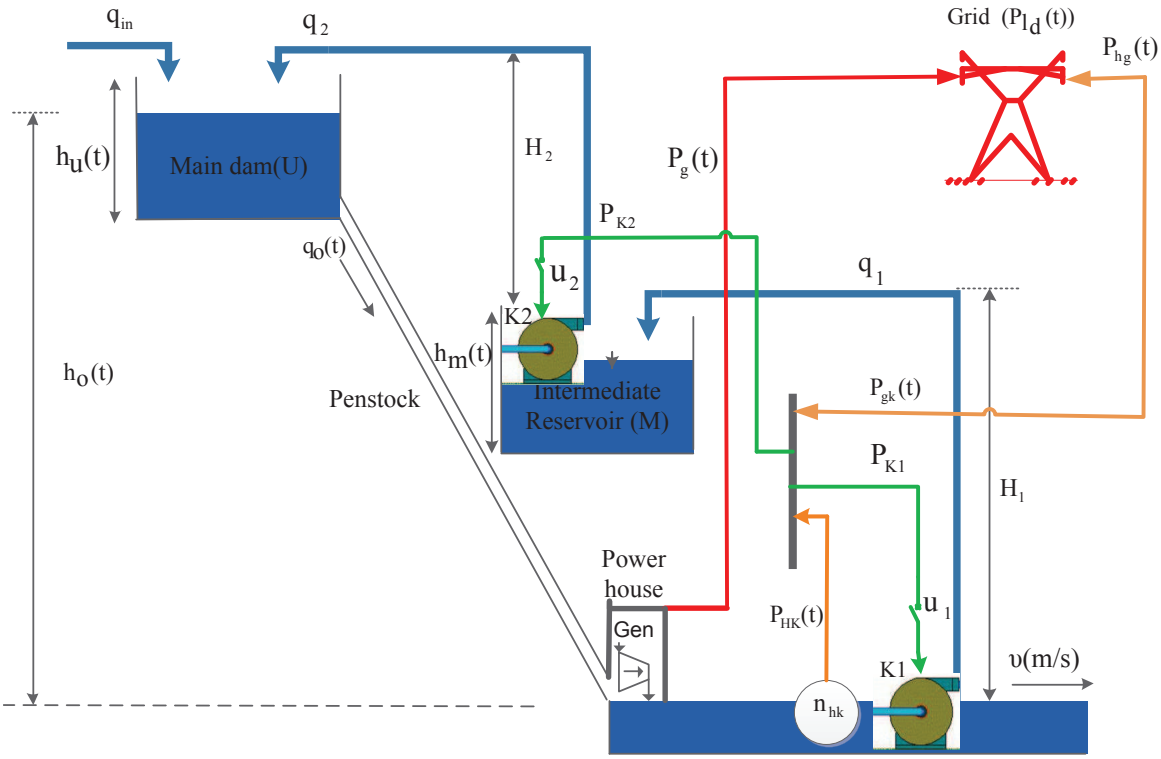

Figure 3.1. Schematic layout of the system with cascaded pumpback operation

In Figure 3.1, $P_g(t)$, $P_{K1}(t)$ and $P_{K2}(t)$ denote respectively, the hydro-turbine generator power output and the pumping power demands for pumps $K1$ and $K2$. On the other hand, q_{in}, q_1, q_2 and $q_o(t)$ are respectively, the constant river in-stream discharge, the flow rate of pumps $K1$, the flow rate of pump $K2$ and the turbine discharge rate expressed in m^3/s. The speed of water downstream, υ (m/s), is assumed constant over a short-term (24 h) control horizon considered in this dissertation. In the proposed OC system, the downstream river flow is assumed un-regulated and therefore, the plant operator has full flexibility to adjust $q_o(t)$ in response to changes in system load demand to optimise the value of the reservoir water. The control variables of the model include $q_o(t)$, $n_{hk}(t)$, $P_{hk}(t)$, $P_{gk}(t)$, $P_{hg}(t)$, $u_1(t)$ and $u_2(t)$ while $h_u(t)$ and $h_m(t)$ constitute the state variables of the model.

3.3.2 Model operation constraints and assumptions

In this chapter, a typical day in the dry season with low constant in-stream flow, q_{in}, is assumed. To optimise the economic value of the available water, it is assumed in the case study that there is no

spillage and all water discharged from the reservoir is utilised for hydropower generation. Also, for a short control horizon, 24 h in this chapter, it is assumed that evaporation and precipitation effects on both the intermediate reservoir and main dam water surface are negligible and can be ignored.

For modelling simplicity, cylindrical models for both the main dam and the intermediate reservoir with base areas; A_u and A_m respectively are assumed in this chapter. Given the hypothetical cylindrical models, the reservoir water level (height) can be expressed as a function of the available amount of water. Therefore, if the volume of water in the main dam at a time t is expressed by $W_u(t)$, then the height of water in the main dam, denoted by $h_u(t)$, can be expressed as follows:

$$h_u(t) = \frac{W_u(t)}{A_u}. \tag{3.1}$$

Similarly, if the instantaneous volume of water in the intermediate reservoir is denoted by $W_m(t)$, then its level (height), $h_m(t)$, can be written as follows:

$$h_m(t) = \frac{W_m(t)}{A_m}. \tag{3.2}$$

Further, in the case study, it is assumed that a hypothetical contract exists for the HPP operator to supply power to a customer with a deterministic time-varying load profile. The contract specifies the amount of power to be supplied at each time t. Therefore, the HPP operator is under an obligation to meet the daily load demand of the customer, the grid in this case, using the allocated water for that particular day. No power generation above contracted demand is permitted. The HPP operator has two options of meeting the power demand of the hypothetical contract; full supply from the hydro generation or a combination of HPP generation with a supplementary supply from the on-site hydrokinetic power system.

3.3.3 Sub systems

3.3.3.1 Hydro reservoir

If the density of water $\rho_w = 1000$ kg/m^3 and the gravitational acceleration constant $g = 9.81$ m/s^2, then the theoretical power output of a conventional hydropower system, $P_g(t)$ (MW), can be expressed as a non-linear function of the system head, $h_o(t)$, and the turbine discharge rate, $q_o(t)$ [33] expressed as follows:

$$P_g(t) = 9.81\eta_m\eta_e q_o(t)h_o(t) \times 10^{-3}, \quad q_o^{min} \leq q_o(t) \leq A_c\sqrt{2gh_o^{max}}, \tag{3.3}$$

where η_m and η_e are respectively, the mechanical and electrical conversion efficiency of the hydro-turbine generator, q_o^{min} is the minimum turbine discharge rate, h_o^{max} is the maximum head of the system before spillage occurs while A_c is the cross-sectional area of the penstock.

For a short scheduling period, 24 h in this chapter, with negligible precipitation and evaporation effects to and from the water surface, the water mass balance of the main dam can be represented by the battery state of charge model in [72]. Therefore, the level of water in the main dam at any given time t can be expressed in continuous time domain as follows:

$$h_u(t) = h_u(0) + \frac{1}{A_u}\int_{t_0}^{t}\big(q_{in}(t) + q_2u_2(t) - q_o(t)\big)dt, \tag{3.4}$$

where $h_u(t)$ and $h_u(0)$ are respectively, the water level in the dam at time t and the initial level in the dam at time $t_0(t = 0)$. The quantities q_{in}, q_2 and q_o are respectively, the river in-stream flow, the discharge rate of pump $K2$ and the turbine discharge rate expressed in m^3/s. $u_2(t)$ is a binary variable [0,1] denoting the ON/OFF state of the switch of pump $K2$. Equation 3.4 shows that the level of water in the dam at time t, i.e, $h_u(t)$, is equal to the level at time t_0, i.e, $h_u(0)$, plus the net sum of the inflows and outflows during the time interval $[t_o,t]$, i.e $\int_{t_0}^{t}(q_{in}(t) + q_2u_2(t) - q_0(t))dt$.

For optimal operation of the reservoir, its water level at any given time t is constrained to lie within a minimum value, h_u^{min}, and a maximum value, h_u^{max}, given by the following expression:

$$h_u^{min} \leq h_u(t) \leq h_u^{max}. \tag{3.5}$$

3.3.3.2 Intermediate reservoir

In the proposed optimal control system, the intermediate reservoir provides a temporary storage for cascading the operation of the two pumps, $K1$ and $K2$. Similarly, following the assumptions described in section 3.3.2, the water mass balance of the intermediate reservoir can be expressed in terms of reservoir height as follows:

$$h_m(t) = h_m(0) + \frac{1}{A_m}\int_{t_0}^{t} \big(q_1 u_1(t) - q_2 u_2(t)\big)dt, \tag{3.6}$$

where $h_m(t)$ and $h_m(0)$ are respectively, the height of water in the reservoir at the end of time t and the level at the initial time, t_0. The quantity q_1 denotes the discharge rate of pump $K1$ controlled by a binary switch $u_1(t)$. In the same vein, the water level in the intermediate reservoir at any given time is constrained to lie within a minimum level, h_m^{min}, and a maximum level, h_m^{max}, expressed as follows equation (3.7):

$$h_m^{min} \leq h_m(t) \leq h_m^{max}. \tag{3.7}$$

3.3.3.3 Cascaded pumping system

The objective of the pumpback operation is to maintain a high water level in the hydro reservoir to optimise its power generation; the amount of water discharged for each unit of hydropower generated is inversely proportional to the level of water hydro reservoir. The proposed optimal control model employs the constant speed pumps assumed to work at their full rated capacity and controlled by ON/OFF switches, u_1 and u_2. Therefore, the pumping power demand of each pump depends only on the ON/OFF state of the control switches expressed as follows:

$$P_{Ki}(t) = \frac{9.81 H_i q_i u_i(t)}{\eta_{ki}} \times 10^{-3}, \quad i = 1,2, \tag{3.8}$$

where $P_{Ki}(t)$ (MW), H_i, q_i and u_i are respectively, the power demand, the hydraulic head , the flow rate and the control switch of pump Ki at time t. The coefficient η_{ki} denotes the combined efficiency of pump Ki and its motor drive. In the proposed model, the pumping power demand of the pumps is met primarily by the power flow from the HK power system, $P_{hk}(t)$. In cases when the on-site generated HK power is less than the pumping power demand, grid power, $P_{gk}(t)$, will be imported to offset the deficit. Therefore, the pumping power balance is expressed as follows:

$$P_{hk}(t) + P_{gk}(t) = P_{K1} u_1(t) + P_{K2} u_2(t), \tag{3.9}$$

where P_{K1} and P_{K2} are the nominal power rating of pumps $K1$ and $K2$ respectively.

3.3.3.4 Hydrokinetic power system

In the proposed optimal control model, the hydrokinetic power system, comprises n_{hk} HK generators in parallel installation downstream the river. The theoretical power output of the HK power system, $P_{HK}(t)$, is given by equation (3.10).

$$P_{HK}(t) = P_{HK,r} n_{hk}(t), \tag{3.10}$$

where $P_{HK,r}$ is the nominal power rating of each of the HK generators. In the proposed OC model, a fraction of the HK power, $P_{hk}(t)$, is supplied to meet the pumping power demand of the pumpback system and the excess HK power above the pumping power demand, $P_{hg}(t)$, is supplied to meet the contractual grid demanded from the HPP operator. Therefore, the power balance of the hydrokinetic system is expressed as follows:

$$P_{HK}(t) = P_{hk}(t) + P_{hg}(t). \tag{3.11}$$

3.4 DISCRETE MODEL FORMULATION AND OPTIMISATION

If we consider the discrete time instant j from $t = 0$ with the sampling time interval t_s, the water mass balance of the dam expressed by equation (3.4) can be re-expressed in discrete time domain by the following equation (3.12):

$$h_{u,j+1} = h_{u,j} + \frac{t_s}{A_u}\left(q_{in} + q_2 u_{2,j} - q_{o,j}\right), \tag{3.12}$$

where $h_{u,j+1}$ and $h_{u,j}$ are respectively, the water level in the main dam at the end of the discrete time $j+1$ and the level at the end of the previous time period, j. Equation (3.12) can be expressed iteratively by equation (3.13) as follows:

$$\begin{aligned}
j = 0; \quad & h_{u,1} = h_{u,0} + \frac{t_s}{A_u}\left(q_{in} + q_2 u_{2,0} - q_{o,0}\right), \\
j = 1; \quad & h_{u,2} = h_{u,1} + \frac{t_s}{A_u}\left(q_{in} + q_2 u_{2,1} - q_{o,1}\right), \\
j = 2; \quad & h_{u,3} = h_{u,2} + \frac{t_s}{A_u}\left(q_{in} + q_2 u_{2,2} - q_{o,2}\right), \\
& \vdots \\
& h_{u,j} = h_{u,0} + \frac{t_s}{A_u}\left(q_{in} + q_2 \sum_{i=1}^{j} u_{2,i} - \sum_{i=1}^{j} q_{o,i}\right), \quad (1 \le i \le j).
\end{aligned} \tag{3.13}$$

Equation (3.13) is the discrete time domain expression of the state dynamics of the main dam. Therefore, the water level constraint of the main reservoir can be expressed in discrete time domain as follows:

$$h_u^{min} \le h_{u,0} + \frac{t_s}{A_u}\left(q_{in} + q_2 \sum_{i=1}^{j} u_{2,i} - \sum_{i=1}^{j} q_{o,j}\right) \le h_u^{max}. \tag{3.14}$$

Similarly, the state equation (3.6) of the intermediate reservoir can be re-expressed in discrete time domain as follows:

$$h_{m,j+1} = h_{m,j} + \frac{t_s}{A_m}\left(q_1 u_{1,j} - q_2 u_{2,j}\right), \tag{3.15}$$

which can be expressed iteratively as follows:

$$\begin{aligned}
j=0; \quad & h_{m,1} = h_{m,0} + \frac{t_s}{A_m}\left(q_1 u_{1,0} - q_2 u_{2,0}\right), \\
j=1; \quad & h_{m,2} = h_{m,1} + \frac{t_s}{A_m}\left(q_1 u_{1,1} - q_2 u_{2,1}\right), \\
j=2; \quad & h_{m,3} = h_{m,2} + \frac{t_s}{A_m}\left(q_1 u_{1,2} - q_2 u_{2,2}\right), \\
& \vdots \\
& h_{m,j} = h_{m,0} + \frac{t_s}{A_m}\left(q_1 \sum_{i=1}^{j} u_{1,i} - q_2 \sum_{i=1}^{j} u_{2,i}\right), \quad (1 \leq i \leq j),
\end{aligned} \tag{3.16}$$

where $h_{m,j+1}$ and $h_{m,j}$ are respectively, the height of water in the intermediate reservoir at the end of discrete time period $j+1$ and the previous time period j. Similarly, the water level constraint of the intermediate reservoir is expressed in discretised form as follows:

$$h_m^{min} \leq h_{m,0} + \frac{t_s}{A_m}\left(q_1 \sum_{i=1}^{j} u_{1,j} - q_2 \sum_{i=1}^{j} u_{2,j}\right) \leq h_m^{max}, \tag{3.17}$$

where h_m^{min} and h_m^{max} are respectively, the minimum and the maximum operational bounds of the intermediate reservoir.

3.4.1 Objective function

The objective function is expressed in discrete time domain by equation (3.18). The first term, $t_s \sum_{j=1}^{N} P_{gk,j}$, minimises the grid pumping energy demand. The second part, $t_s \sum_{j=1}^{N} (s_{1,j} + s_{2,j})$, minimises the switching frequency of the two pumps, $K1$ and $K2$, to reduce wear-and-tear. The third term, $t_s \sum_{j=1}^{N} q_2 u_{2,j}$, maximises the restoration of the water volume in the main reservoir through pumpback operation while the fourth term, $t_s \sum_{j=1}^{N} P_{hk,j}$, maximises the use of hydrokinetic energy to power the pumpback system. Objective function:

$$\min \quad J = t_s \left(\omega_1 \sum_{j=1}^{N} P_{gk,j} + \omega_2 \sum_{j=1}^{N} (s_{1,j} + s_{2,j}) - \omega_3 \sum_{j=1}^{N} q_2 u_{2,j} - \omega_4 \sum_{j=1}^{N} P_{hk,j} \right), \tag{3.18}$$

where J is the objective function to be optimised and $\sum_{i=1}^{4} \omega_i = 1$ is the weighting factors that determine the relative importance of each of the objective terms. The control horizon is 24 h with a sampling time, $t_s = 0.25\ h$. $j = 1, \ldots, N$ is sampling interval and $N = 96$ is the total number of samples. In general, the maintenance cost of a pump relates to wear and tear associated with the number of ON/OFF switches of the pump [73]. Therefore, minimising the switching frequency of the pumps reduces their associated wear and tear costs. In this chapter, the Pretorian method developed and employed in [74] is adopted for minimisation of the switching frequency of the cascaded pumps. This approach introduces an auxiliary variable, s, represented by a value of 1 whenever a transition from OFF to ON state of a pump occurs. Minimising the state transitions of s reduces the switching frequency of the pump by augmenting the adjacent ON/OFF switches and consequently reducing the overall number of switches of each of the pumps over the 24 h control horizon.

The objective function expressed by equation (3.18) is solved subject to the following constraints:

$$P_{g,j} + P_{hg,j} = P_{ld,j}, \tag{3.19}$$

$$P_{HK,j} = P_{hk,j} + P_{hg,j}, \tag{3.20}$$

$$P_{hk,j} + P_{gk,j} = P_{K1}u_{1,j} + P_{K2}u_{2,j}, \tag{3.21}$$

$$h_u^{min} \leq h_{u,0} + \frac{t_s}{A_u}\left(q_{in} + q_2\sum_{i=1}^{j} u_{2,i} - \sum_{i=1}^{j} q_{o,i}\right) \leq h_u^{max}, \tag{3.22}$$

$$h_m^{min} \leq h_{m,0} + \frac{t_s}{A_m}\left(q_1\sum_{i=1}^{j} u_{1,i} - q_2\sum_{i=1}^{j} u_{2,i}\right) \leq h_m^{max}, \tag{3.23}$$

$$P_g^{min} \leq P_{g,j} \leq P_g^{max} \quad ; \quad 0 \leq q_{o,j} \leq A_c\sqrt{2gh_o^{max}}, \tag{3.24}$$

$$P_{HK}^{min} \leq P_{HK,j} \leq P_{HK}^{max} \quad ; \quad n_{hk}^{min} \leq n_{hk,j} \leq n_{hk}^{max}, \tag{3.25}$$

$$P_{hg}^{min} \leq P_{hg,j} \leq P_{hg}^{max}, \tag{3.26}$$

$$P_{hk}^{min} \leq P_{hk,j} \leq P_{hk}^{max}, \tag{3.27}$$

$$P_{gk}^{min} \leq P_{gk,j} \leq P_{gk}^{max}, \tag{3.28}$$

$$u_{i,j} - s_{i,j} \leq 0, i = 1,2 \quad s_{i,j} \in [0,1], \tag{3.29}$$

$$u_{i,j} - u_{i,j-1} - s_{i,j} \leq 0, \quad i = 1,2, \tag{3.30}$$

$$u_{i,j} \in [0,1], \quad i = 1,2, \quad (1 \leq j \leq N), \tag{3.31}$$

The equalities (3.19) and (3.20) are respectively, the grid and the hydrokinetic power balances. Equality expressed by equation (3.19) shows that the power supplied to the grid is the sum of the hydro turbine generator output and the excess hydrokinetic power. Equality expressed by equation (3.21) shows that the total pumping power of the pumpback system is the sum of the HK power supplied to the pumps and the supplementary grid power import. Inequalities (3.22) and (3.23) are respectively, the state constraints of the dam and the intermediate reservoir bounded by their respective minimum and maximum allowable limits. Inequalities (3.24), (3.25), (3.26), (3.27) and (3.28) are respectively, the control variables bounds for: the hydro-turbine generator power output which depends on the turbine flow rate bounds, the total HK power output, the surplus HK power exported to the grid, the HK power supplied to meet the pumping power demand and the supplementary grid power imported to offset pumping power deficit. The inequality (3.29) initialises the auxiliary variable $s_{i,j}$ as the initial status of $u_{i,j}$ while the inequality (3.30) favours the control with less switching frequency. These auxiliary constraints allow the objective function expressed by equation (3.18) to simultaneously optimise its four defined objective terms. Equation (3.31) is a binary control variable constraint for the switches, u_1

and u_2, which control pumps $K1$ and $K2$ respectively.

3.4.2 Algorithm formulation and implementation in MATLAB

The proposed OC model yields a constrained mixed integer linear problem which can be solved using any mixed integer linear programming (MILP) solvers such as 'intlinprog' in MATLAB. In this dissertation, the *OPTI toolbox* SCIP (Solving Constraint Integer Programs) solver is employed because of its fast optimisation speed and robust ability to handle constrained problems. SCIP is currently, the fastest non-commercial solver with a complete suite for solving both mixed integer (linear and non-linear) programming and linear programming problems [1]. SCIP integrates constraint programming (CP) for solving constrained optimisation problems and mixed integer programming (MIP) used for solving mixed integer optimisation problems with some of the decision variables taking integer values at the optimal solution [75]. The canonical form of a MILP is expressed as follows:

$$\min \quad f^T \mathbf{X} \quad \text{subject to} \quad \begin{cases} \boldsymbol{AX} \leq \boldsymbol{b} \\ \boldsymbol{A}_{eq}\boldsymbol{X} = \boldsymbol{b}_{eq} \\ \boldsymbol{L}_B \leq \boldsymbol{X} \leq \boldsymbol{U}_B, \end{cases} \tag{3.32}$$

where $\boldsymbol{AX} \leq \boldsymbol{b}$ denotes the inequality constraints, $\boldsymbol{A}_{eq}\boldsymbol{X} = \boldsymbol{b}_{eq}$ the equality constraints and $\boldsymbol{L}_B \leq \boldsymbol{X} \leq \boldsymbol{U}_B$ denotes the lower and the upper bounds of the control variables. The constraints 3.25 and 3.31 are respectively, integer and binary constraints that make the problem a candidate for MILP; in this case SCIP is preferred because of its speed and robust ability to satisfy constraints.

The control variables of the OC model are as follows: binary variables, $u_{1,j}$ and $u_{2,j}$, real number variables; $q_{o,j}$, $P_{hk,j}$, $P_{hg,j}$ and $P_{gk,j}$, an integer variable, $n_{hk,j}$, and the auxiliary variable, $s_{i,j}$ (i=1,2).

The objective function expressed by equation (3.18) is expressed in canonical form by equation (3.32).

[1] http://scip.zib.de/

The vector **X** contains all the control variables of the model expressed by equation (3.33).

$$\mathbf{X} = \Big[u_{1,1}...u_{1,N},\quad u_{2,1}...u_{2,N},\quad n_{hk,1}...n_{hk,N},\quad q_{o,1}...q_{o,N},\quad P_{hk,1}...P_{hk,N},\quad P_{gk,1}...P_{gk,N},\quad P_{hg,1}...P_{hg,N},\quad s_{1,1}...s_{1,N},\quad s_{2,1}...s_{2,N}\Big]'_{9N\times 1}. \tag{3.33}$$

From the objective function equation (3.18):

$$f^T = \Big[0_1...0_N,\quad -\omega_3 q_{2,1}... - \omega_3 q_{2,N},\quad 0_1...0_N,\quad 0_1...0_N,\quad \omega_{1,1}...\omega_{1,N},\quad \omega_{1,1}...\omega_{1,N},\quad 0_1...0_N,\quad \omega_{2,1}...\omega_{2,N},\quad \omega_{2,1}...\omega_{2,N}\Big]_{1\times 9N}. \tag{3.34}$$

The lower and the upper bounds of the control variables are expressed by equation (3.35) and equation (3.36) respectively.

Lower bounds

$$lb^T = \Big[0_1...0_N,\quad 0_1...0_N,\quad 0_1...0_N,\quad 0_1...0_N,\quad 0_1...0_N,\quad 0_1...0_N,\quad 0_1...0_N,\quad 0_1...0_N,\quad 0_1...0_N\Big]_{9N\times 1}. \tag{3.35}$$

Upper bounds

$$ub^T = \Big[1_1...1_N,\quad 1_1...1_N,\quad 30_1...30_N,\quad 45_1...45_N,\quad \sum_{i=1}^{2} P_{Ki,1}... \sum_{i=1}^{2} P_{Ki,N},\quad \sum_{i=1}^{2} P_{Ki,1}... \sum_{i=1}^{2} P_{Ki,N},\quad n_{hk}P_{HK,1}...n_{hk}P_{HK,N},\quad 1_1...1_N,\quad 1_1...1_N\Big]_{9N\times 1}. \tag{3.36}$$

The detailed formulation of the inequality and equality constraints of the problem are attached to Addendum A.

3.4.3 Case study

The case study is based on Pangani fall hydropower plant (HPP), one of the three HPPs that form a cascade of the Pangani hydropower system located on Pangani River in Tanzania. The first one is Nyumba ya mungu (NyM) plant, a 2×4 MW hydropower plant located at NyM dam which discharges into the 2×10.5 MW Hale HPP. From the Hale power plant, water flows into the Pangani fall dam that feeds the 2×34 MW Pangani fall HPP which drains into the Indian Ocean 64 km downstream. The Pangani hydropower system has a total installed capacity of 91.5 MW. However, the generation capacity drops to 30% during dry seasons due to low water levels in the dams; a situation which has worsened in recent years due to prolonged droughts [2] caused by the on-going climate change. Hydropower generation of the Pangani fall HPP has declined in the last 10 years [76] and reached the lowest point in 2014 with a production level of 25 MW; a situation that threatened its shutdown [3]. In this chapter, pumpback operation to maintain a high water level to optimise the hydropower generation of the reservoir is proposed. To minimise the pumping power and energy demand of the system, a cascaded pumping strategy is proposed. To validate the economic advantages of the cascaded pumping system over the classical PS system, the performance of the hydropower plant is simulated over a 24 h control period. The simulation assumes a normal average day in dry and rainy seasons with a constant in-stream discharge.

3.4.3.1 Pangani fall hydropower plant

The Pangani fall dam has a live capacity of 0.8×10^6 m^3. The reservoir has a maximum and minimum hydropower operating level by volume of 1.7×10^6 m^3 and 0.9×10^6 m^3 respectively. The plant is installed with 2×34 MW SAV340/110/14 generators with a nominal capacity of 2×40 MVA and a power factor of 0.85. The plant turbines' speed is 428 revolutions per minute (rpm) [77]. In this case study, an initial volume of 1.1×10^6 m^3 is assumed, which is a typical average capacity of Pangani fall reservoir in dry season. For modelling and control simplicity, a cylindrical model with a base radius of 71.36 m and a design depth of 68.75 m are assumed. In the table, $P_{g,r}$ denotes the rated power output of the HPP.

[2] http://www.iucn.org/dbtw-wpd/edocs/2007-002.pdf

[3] http://www.theeastafrican.co.ke/news/Tanzania-to-switch-off-all-hydropower-stations/-/2558/2905900/-/ep5kq9/-/index.html

Table 3.1 shows the salient features of Pangani fall HPP with the height given in meters above sea level (masl) [77].

Table 3.1. Salient features of Pangani fall hydropower plant

Res-vol (m^3)	h_u^{max} (masl)	h_u^{min} (masl)	h_o (masl)	$P_{g,r}$ (MW)	q_o^{min} (m^3/s)	q_o^{max} (m^3/s)	q_{in} (m^3/s)
1.4×10^6	177.5	176.0	170.0	68.0	9.0	45.0	12.5

3.4.3.2 Intermediate reservoir parameters

The intermediate reservoir is used to create a temporary storage for continuous pumping operation of the two pumps , $K1$ and $K2$, in cascade as shown in Figure 3.1. An optimal scheduling strategy that alternates the operation of the two pumps has the potential to minimise the pumping power demand as well as the overall pumping energy over the given control horizon. For optimal pumping operation, the intermediate reservoir is sized by rule of thumb to ensure 12 h continuous outward pumping by pump $K2$ without restorative inward pumping by pump $K1$ and 12 h inward pumping by pump $K1$ without discharge by pump $K2$. Since the two pumps, $K1$ and $K2$, are sized equally, the maximum capacity of the intermediate reservoir can be approximated to 2.4×10^5 m^3 with a design radius of 35.60 m and a design height of 60.0 m. Table 3.2 shows the design specifications of the intermediate reservoir.

Table 3.2. Design specifications of the intermediate reservoir

Design shape	Design capacity (m^3)	Radius (m)	Design height (m)	h_m^{max} (m)	h_m^{min} (m)
Cylindrical	2.40×10^5	35.6	60.0	60.0	10.0

3.4.3.3 Cascaded pumping system parameters

In the case study, the SJT vertical turbine pumps from Sulzar Ltd are employed. They have a performance range of upto 17.3 m^3/s, maximum head of 110.0 m and pressure of upto 64.0 bar[4]. Table 3.3 shows the specifications of the pumps used in the case study.

[4]https://www.sulzer.com/en/Products-and-Services/Pumps-and-Systems/Vertical-Pumps/Vertical-Wet-Pit-Pumps/SJT-Vertical-Turbine-Pumps

Table 3.3. Design Specifications of the pumping system

q_1 (m^3/s)	q_2 (m^3/s)	H_1 (m)	H_2 (m)	Head range (m)	Pressure (bar)	η_k (%)
5.5	5.5	85.0	85.0	upto 110.0	up to 64.0	90.0

3.4.3.4 Hydrokinetic generator parameters

The hydrokinetic system used in this case study comprises the CC035A river-in-stream turbine models developed by the Clean Current Renewable Energy Systems Inc [5] and the flooded, permanent magnet generators. The CC035A turbine has a rotor diameter of 3.50 m and requires a minimum river depth of 7.0 m for effective deployment. The technical specifications of the HK turbines used in this chapter are given in Table 4.2.In the table, η_t and η_g are respectively, the efficiency of the mechanical gear box of the turbine and the electrical efficiency of the system. The Betz limit, C_p, is factored in the power output model expressed by equation (3.10).

Table 3.4. Hydrokinetic turbine specifications

Model	n_{hk}	$P_{HK,r}$ (kW)	A_w (m^2)	v_r (m/s)	η_w (%)	η_g (%)	C_p
CC035A	26.0	65.0	9.6	3.0	90	85	0.45

Each of the CC035A HK turbine model has a rated power output of 65.0 kW and a nominal speed of 75 revolution per minute (rpm). It operates optimally in a current speed range of 1.50-3.70 m/s.

3.4.3.5 Uncertainty analysis of the demand load

There are several techniques used in sensitivity (uncertainty) analysis in a given model to determine its viability and reliability at the design stage. In this chapter, the methodology used in [78] is adopted for ascertaining the confidence level of the load in the case study. The random error (noise) in addition to the instrument's absolute uncertainty is introduced in the load demand which in this case is the recorded load profile of the hydropower plant referred to as the measured value. The true (accepted) values are then estimated from the measured (corrupted) values. The resulting difference between

[5] http://www.cleancurrent.com/river-turbines

measured and true values is due to random errors. For analysis purposes, random errors are generated in MATLAB software with a distribution mean of 0 and standard deviation of 1 which is then multiplied by the absolute uncertainty of the watt-meter $\sigma_{m,meas} = \pm 0.01$; a value which is often given by the manufacturer of the demand measuring instrument.

$$Z_m = A_t + RAND_m * \sigma_{m,dev}, \tag{3.37}$$

where Z_m, A_t, $RAND_m$ and $\sigma_{m,dev}$ are respectively, the measured value of mth measurement, the true value, the random noise and the standard deviation of the mth measurement while $m = 1,\ldots,24$ is the number of measurements. The Pangani fall hydropower load demand profile is analysed for sensitivity and the results are shown in Table 3.5. Further analysis is done to determine the relative uncertainty of each given measurement.

$$\text{Relative uncertainty } (\%) = \frac{\text{Absolute uncertainty}}{\text{Measured value}}. \tag{3.38}$$

In this case, the weakest link rule [6] is applied where the measurement with the largest relative uncertainty is picked from Table 3.5. In this case, the largest relative uncertainty is 0.022% which is used to determine the absolute uncertainty of the final objective function.

[6] http://www2.fiu.edu/ dbrookes/ExperimentalUncertaintiesCalculus.pdf Date accessed 10.10.2016

Table 3.5. Uncertainty analysis of the Pangani fall HPP on load demand profile

Measured values (MW)	Rand error	$\sigma_{m,dev}$	True values (MW)	Absolute uncertainty	Relative uncertainty
50	0.534	0.01	49.995	(50 ±0.01)	0.020%
50	0.885	0.01	49.991	(50 ±0.01)	0.020%
50	0.899	0.01	49.991	(50 ±0.01)	0.020%
50	0.626	0.01	49.994	(50 ±0.01)	0.020%
60	0.138	0.01	59.999	(60 ±0.01)	0.017%
60	0.218	0.01	59.998	(60 ±0.01)	0.017%
60	0.182	0.01	59.998	(60 ±0.01)	0.017%
60	0.042	0.01	60.000	(60 ±0.01)	0.017%
60	0.107	0.01	59.999	(60 ±0.01)	0.017%
60	0.616	0.01	59.994	(60±0.01)	0.017%
60	0.940	0.01	59.991	(60±0.01)	0.017%
60	0.355	0.01	59.996	(60±0.01)	0.017%
65	0.411	0.01	64.996	(65 ±0.01)	0.015%
65	0.984	0.01	64.990	(65 ±0.01)	0.015%
65	0.946	0.01	64.991	(65 ±0.01)	0.015%
65	0.677	0.01	64.993	(65 ±0.01)	0.015%
45	0.988	0.01	44.990	(45 ±0.01)	0.022%
45	0.767	0.01	44.992	(45 ±0.01)	0.022%
45	0.337	0.01	44.997	(45 ±0.01)	0.022%
45	0.662	0.01	44.993	(45 ±0.01)	0.022%
45	0.244	0.01	44.998	(45 ±0.01)	0.022%
45	0.296	0.01	44.997	(45 ±0.01)	0.022%
45	0.680	0.01	44.993	(45 ±0.01)	0.022%
45	0.528	0.01	44.995	(45 ±0.01)	0.022%

The simulation is performed for both measured and true values, A_t, to establish the confidence level of the results of the proposed model. The measured and true value simulation results are presented in Figure 3.5 and Figure 3.6 respectively in sub-section 3.5.1.3.

3.5 RESULTS AND DISCUSSION

The proposed optimal control (OC) is simulated for two scenarios: The first scenario simulates the performance of the system on a typical day in the dry season with low in-stream flow, simulating a typical dry season case. The second scenario simulates the performance of the system on a typical

day in the rainy season with high in-stream discharge. To validate, the performance advantages of the cascaded pump-back system, simulation for a single pump classical PS system is also carried out for the two scenarios. The comparison of the performance of the two systems is presented in sub-section 3.5.1.6.

3.5.1 Operation scenario I

3.5.1.1 Optimal switching of the pumpback system

switching operation of the pumping system

In this operation mode, the switching of the pumping system is unconstrained. This is achieved by setting the weighting factors $\omega_1 = \omega_3 = \omega_4 = 0.33; \omega_2 = 0$. The results of the switching operation of the pumps of this operation mode and the resultant change in water level of the intermediate reservoir are shown in Figure 3.2. The lower bound of the intermediate reservoir is set at 10.0 m while the initial water level is set at 15.0 m. Also shown in the top row graphs of Figure 3.3 is the power demand of each of the two pumps, which is 4.82 MW whenever they are in operation, otherwise it is zero.

As shown in the figure, the OC switches ON pump $K2$ between 00:00 and 01:30 to optimise restoration of the main dam water level. However, when the water level of the intermediate reservoir approaches the minimum limit, the OC switches OFF $K2$ and in turn switches ON $K1$ to restore its volume. The OC is seen to alternate the operation of pumps $K1$ and $K2$ in short intervals, after every 15 minutes, between 02:30 and 05:30 to optimise the water level of the main dam. As a result, the optimal water level of the intermediate reservoir, R_{opt}, remains constant at the minimum level of 10.0 m, shown in the second row of Figure 3.2. Afterwards, the OC operates pump $K1$ for a longer period, between 05:30 and 11:00, to ensure a high water level in the intermediate reservoir before bringing in $K2$ for onward pumping to the main dam. As a result, the water level of the intermediate reservoir rises from 10.50 m to 23.66 m between 05:00 and 11:00 as shown in Figure 3.2. Subsequently, the OC alternates the operation of $K1$ and $K2$ for the remainder of the control horizon to ensure a high water level in the main dam at low pumping power and energy demand. As shown, in the second row of Figure 3.2, R_{opt} decays to a minimum level of 10.0 m due to the pumping action of $K2$. The results of Figure 3.2 show the effects of the unconstrained operation of the pumpback system: There is high switching frequency

of the two pumps in cascade resulting in high wear and tear. Throughout the control horizon, the OC switches ON pumps $K1$ and $K2$ 11 and 12 times respectively. The wear and tear associated with the high switching frequency of the system can be minimised by augmenting the adjacent switches with short intervals between them into one and reducing the overall number of switches throughout the control period.

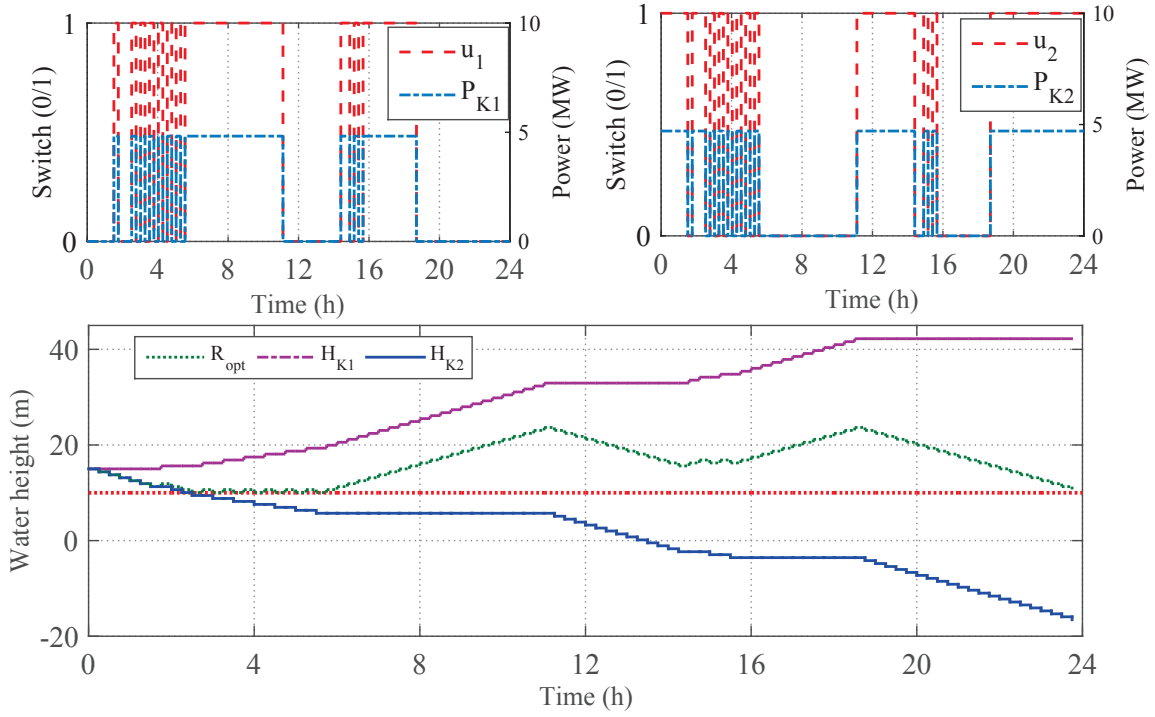

Figure 3.2. Optimal operation without switching constraint

Optimal control with minimum switching frequency

In this operation strategy, an auxiliary variable, $s_{i,j}$, $[i = 1,2]$ that minimises the number of switches of the pumps in the 24 h control period is introduced in the optimisation objective function as shown in equation (3.18). This is achieved by setting the objective weights $\omega_1 = \omega_2 = \omega_3 = \omega_4 = 0.25$. The results of this operation mode are shown in Figure 3.3. Because of the low initial water level in the intermediate reservoir, the OC switches ON pump $K1$ from 00:00 to 11:00 to raise its water level before bringing in pump $K2$ for onward pumping to the main dam. After 11:00, the OC switches OFF pump $K1$ and in turn switches ON $K2$ for the remainder of the day to keep a high water level in the main dam in order to optimise the performance of the HPP. As shown, the reservoir water level would

fall below its minimum level at 13:00 if pump $K2$ was operated before $K1$. The water level drops to the minimum level of 10.0 m at the end of the day. The second-row graph shows the change in water level of the intermediate reservoir as a result of the pumping actions of pumps $K1$, H_{K1}, and pump $K2$, H_{K2}. R_{opt} (m) is the optimal intermediate reservoir water level due to the combined pumping actions of the two pumps, $K1$ and $K2$. As shown in the figure, H_{K1} rises steadily to 50.0 m by 11:00 before restoration of the dam water level commences. During this period, the overall water level, R_{opt}, is equal to H_{K1} because pump $K2$ is in OFF mode. At the end of the control horizon, the intermediate reservoir water level drops to 10.0 m, proving that the OC meets all the operational constraints of the system. In general, the OC scheduling strategy is observed to alternate the operation of pumps $K1$ and $K2$ in order to minimise the overall pumping energy demand. This is one of the main advantages of the cascaded pumpback system over the classical single pump PS system.

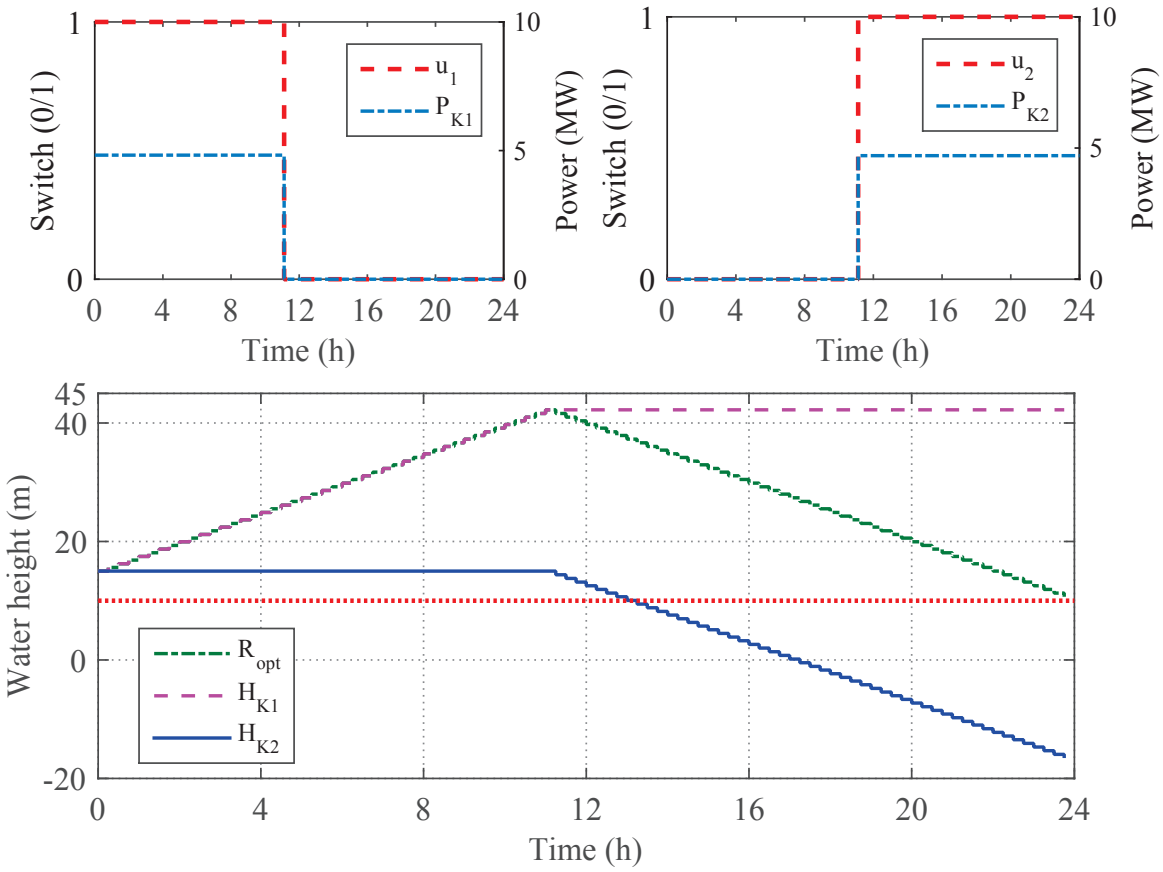

Figure 3.3. Optimal operation of the system with switching constraint

3.5.1.2 Water level and flow rates of the main dam

The optimal flow rates and the corresponding change in water level of the main dam are shown in Figure 3.4. In the figure q_o and q_2 are respectively, the turbine flow rate for hydropower generation and the discharge rate of pump $K2$ while q_{inflow} denotes the combined in-stream discharge and flow rate of pump $K2$, $q_{in} + q_2$. As shown in the figure, q_{inflow} is 12.5 m^3/s whenever $K2$ is in OFF mode and 18.0 m^3/s whenever $K2$ is in ON mode. The turbine flow rate, q_o, varies in response to the changes in hydropower generation level, P_g. In this case, q_o is 20.9 m^3/s between 00:00 and 00:15 but rises to 24.46 m^3/s between 00:15 and 02:00 in response to an increase in P_g as shown in Figure 3.5. A decrease in P_g between 02:00 and 04:00 results in a corresponding decrease in q_o from 24.46 m^3/s to 20.9 m^3/s. An increase in P_g between 04:00 and 06:00, shown in Figure 3.5, results in a corresponding increase in q_o as shown in Figure 3.4. Subsequently, the OC varies q_o in response to changes in P_g throughout the remainder of the control horizon. The optimal water level in the dam, H_{opt}, is as a result of the change due to the combined inflows, H_{inflow}, less the change due to turbine discharge, H_{out}. The baseline case is depicted by H_{out} which is the change in the water level of the main reservoir in the absence of the proposed pumpback operation. As shown in Figure 3.4, H_{opt} drops from the initial level of 176.0 m to 117.1 m at the end of the day. For the baseline case, the water level in the dam, H_{out}, would drop from 176.0 m to 101.9 m. However, the pumpback system maintains a high water level in the dam to optimise the performance of the plant throughout the control horizon. H_{inflow} shows the would be water level in the dam if there was inflows without turbine discharge, q_o. In this case, the water level of the dam would rise from 176.0 m to 257.3 m leading to an overflow at the end of the day.

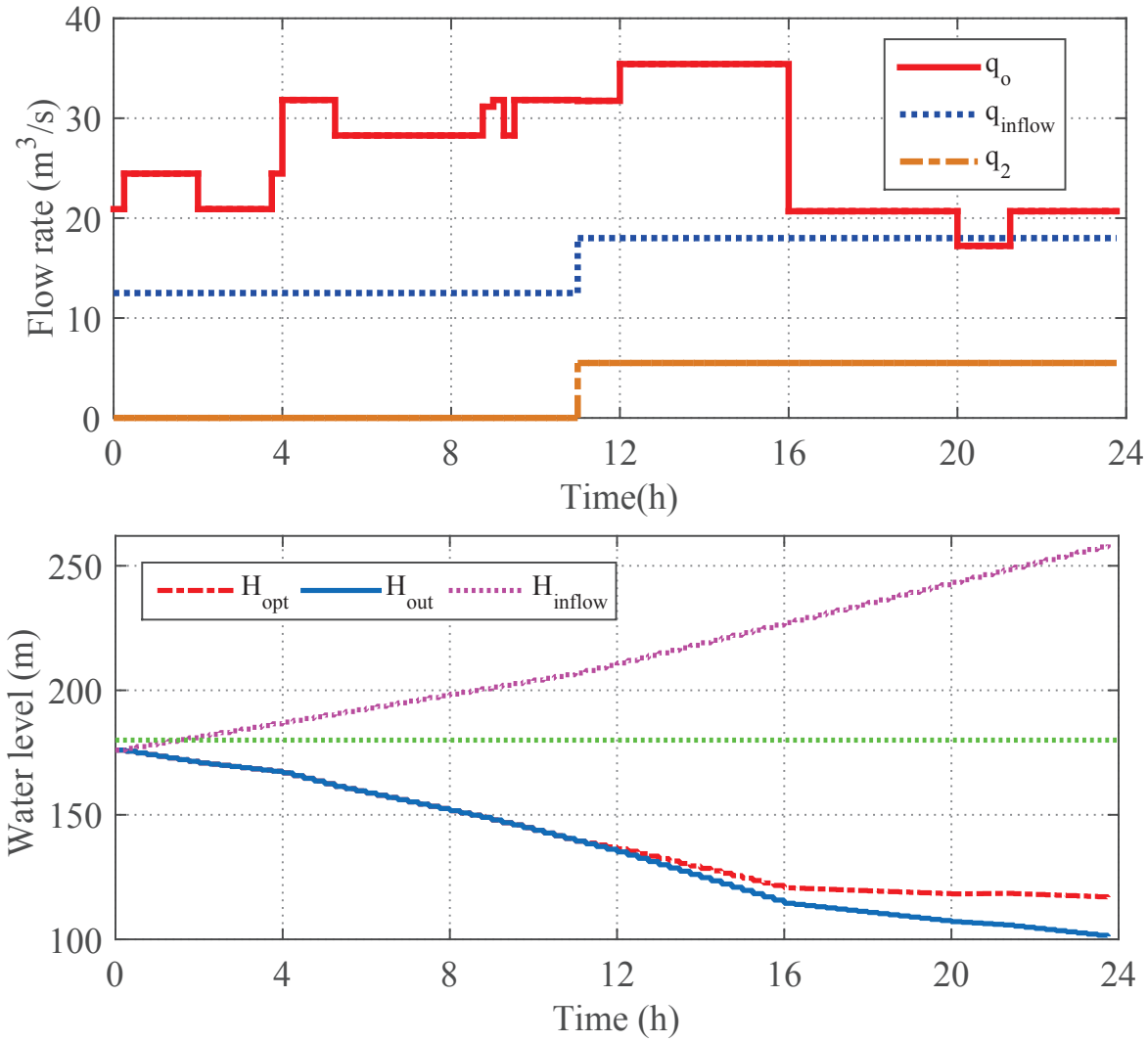

Figure 3.4. Flow rates and changes in water level of the main dam in dry season

3.5.1.3 Optimal power flows of the system

Figure 3.5 shows the results of the optimal power flows of the system based on the measured values for the objective weights $\omega_1 = \omega_2 = \omega_3 = \omega_4 = 0.25$. As shown in Figure 3.5, the OC alternates the use of P_{hk} and P_{gk} in meeting pumping power demand throughout the control horizon. For instance, between 00:00 and 00:15, the pumping power demand of 4.82 MW is met by 1.47 MW supplied by P_{hk} and 3.35 MW from P_{gk}. However, the OC opts to meet the pumping power demand fully by P_{hk} between 00:15 and 02:00, between 04:00 and 06:16, between 08:45 and 16:15, between 16:30 and 20:00 and between 21:00 and 24:00, otherwise it is met fully by the grid import power, P_{gk}. This can

be attributed to the lower grid load demand hence the grid power, P_{gk}, while much of the produced HK power, P_{hg}, is fed into the grid to conserve water in the main dam. The total grid pumping energy in the case study is 35.74 MWh.

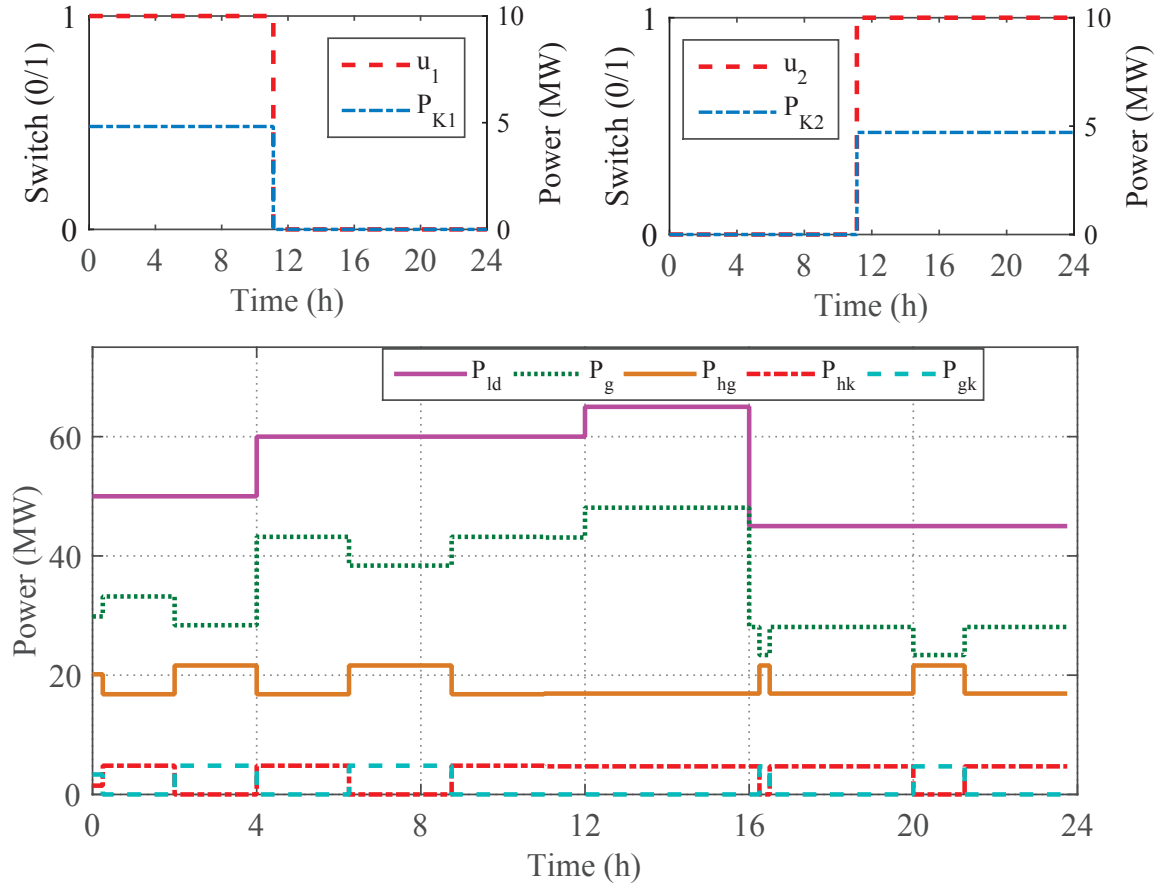

Figure 3.5. Optimal power flows of the system in dry season

As shown as well in Figure 3.5, all the on-site generated HK power of 21.62 MW is exported to the grid between 02:00 and 04:00, between 06:15 and 08:45, between 16:15 and 16:30, and between 20:00 and 21:15 as the OC opts to meet the pumping power demand by the grid import power, P_{gk}. On the other hand, P_g varies in response to changes in grid load demand supplemented by P_{hg}. For instance, P_g supplies 29.85 MW supplemented by P_{hg} of 20.15 MW to meet the committed demand of 50.0 MW between 00:00 and 00:15. However, a decrease in P_{hg} from 20.15 MW to 16.8 MW at 00:15 against a constant P_{ld} of 50.0 MW results in a corresponding increase in P_g from 29.85 MW to 33.2 MW. This inverse complementary relationship between P_g and P_{hg}, especially between 06:15 and 08:45, between 16:15 and 16:30, and between 20:00 and 21:15, is one of the advantages of the proposed

optimal control model. A decrease in P_g in response to an increase in P_{hg} conserves water in the dam and consequently optimising the energy output of the hydro reservoir.

3.5.1.4 Uncertainty analysis on optimal power flows

Visual inspection of Figure 3.6 of true value power flows shows a close match of the power flows from the measured values, shown in Figure 3.5. However, there are some minor observable differences in pumping power demand between the two cases. When true values are used as shown in Figure 3.6, the OC opts to meet the pumping power demand using P_{gk} between 00:00 and 00:15, between 03:15 and 04:00, between 06:15 and 09:30, between 12:30 and 13:00 and between 20:00 and 21:45 otherwise it is met by P_{hk}.

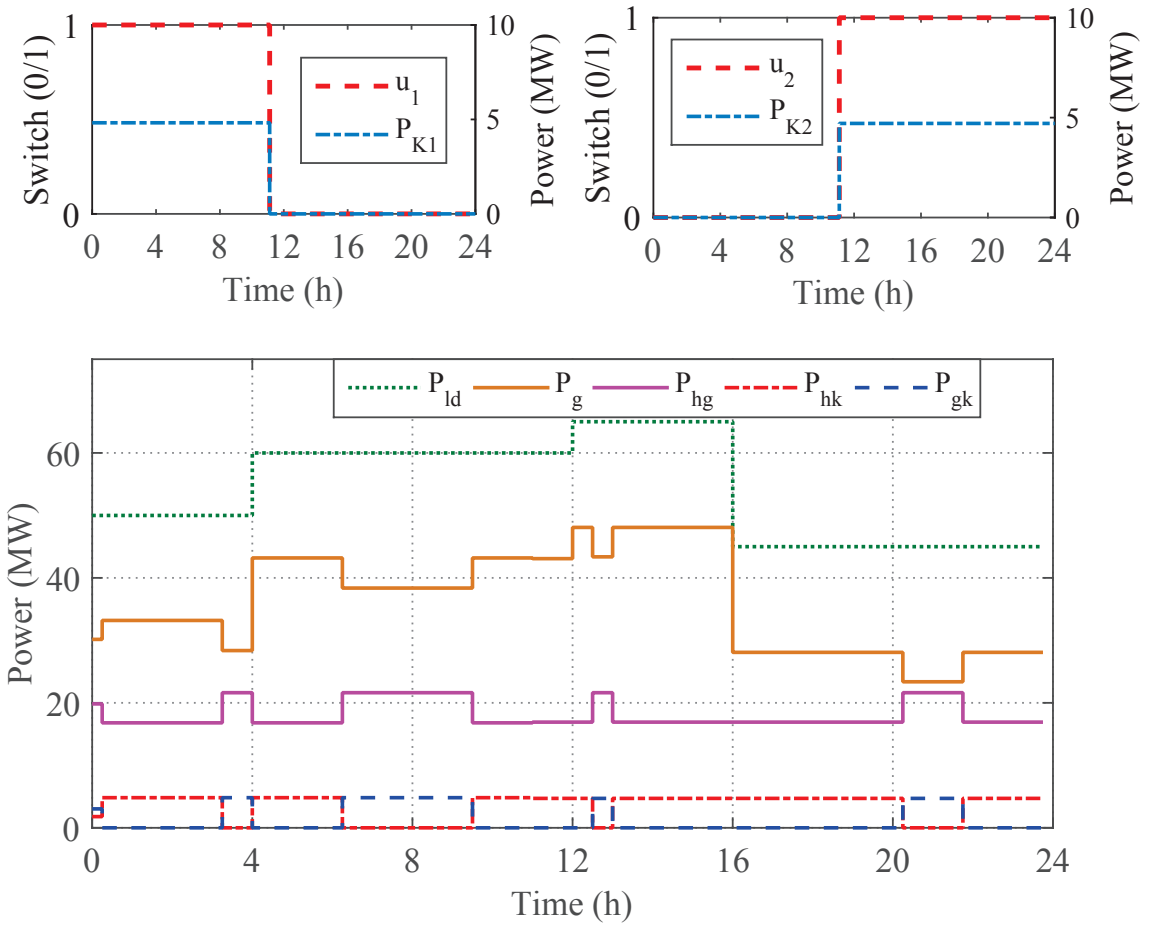

Figure 3.6. Sensitivity on the optimal power flows of the cascaded system in dry season

The net effect between the two cases is a slight difference in daily grid pumping energy, E_{gk}. The case based on true values results in E_{gk} value of 35.6 MWh as compared to the measured value of 35.74 MWh.

3.5.1.5 Optimal daily energy production in dry season

Table 3.6 shows the optimal energy flows of the proposed OC system with a hydrokinetic-powered pumpback retrofit for a typical day in dry season. As shown in the table, weighting factors have effects on the optimal results of the system. In the table, E_K (MWh) denotes the pumping energy demand of the system which is the summation of HK pumping energy, E_{hk} (MWh), and grid pumping energy,E_{gk} (MWh), over the 24 h control horizon. The optimal energy output, E_{opt} (MWh), is the result of the summation of hydro-turbine energy output, E_g, excess HK energy supplied to the grid load, E_{hg}, less the grid pumping energy demand, E_{gk}. From Table 3.6, the objective function simulated using measured values for the case when $\omega_1 = \omega_2 = \omega_3 = \omega_4 = 0.25$ results in an optimal hydro-turbine energy output, $E_g = \sum P_g t_s = 859.5723$ MWh, where $P_g = g\rho_w \eta_e q_o h\, o10^{-6}$. In this chapter, weighting factors are not optimised, therefore, to ascertain their effects, different combinations of weights are considered. An equal weight to each of the four objective vectors results in grid pumping energy, E_{gk}, of 35.60 MWh and E_{opt} of 1264.30 MWh per day, which translates to 47.09% increase in the daily energy yield of the resultant system.

Table 3.6. Daily optimal energy flows for a cascaded system in dry season

$\sum_{i=1}^{4} \omega_i = 1$	E_g (MWh)	E_{hg} (MWh)	E_{hk} (MWh)	E_{gk} (MWh)	E_K (MWh)	E_{opt} (MWh)	Increase (%)
$\omega_1 = \omega_2 = \omega_3 = \omega_4 = 0.25$	859.57	440.29	78.69	35.60	114.30	1264.30	47.09
$\omega_2 = \omega_3 = \omega_4 = 0; \omega_1 = 1$	859.57	440.29	79.36	34.94	114.30	1264.92	47.16
$\omega_1 = \omega_3 = \omega_4 = 0; \omega_2 = 1$	816.16	518.99	0.00	114.98	114.98	1184.90	45.18
$\omega_1 = \omega_2 = \omega_4 = 0; \omega_3 = 1$	781.12	518.99	0.00	220.59	220.59	1078.30	38.05
$\omega_1 = \omega_2 = \omega_3 = 0; \omega_4 = 1$	943.00	356.30	162.68	57.91	220.59	1241.39	31.64

On the other hand, allocating full priority to minimisation of the grid pumping energy, E_{gk}, by setting $\omega_1 = 1; \omega_2 = \omega_3 = \omega_4 = 0$, results in the best optimal solution with the lowest grid pumping energy demand of 34.94 MWh. This optimisation scenario also results in the lowest overall pumping energy demand of 114.3 MWh with 47.16% increase in the overall energy yield of the resultant system; which is the highest gain when compared to other operation strategies. On the other hand, setting

$\omega_1 = \omega_2 = \omega_4 = 0; \omega_3 = 1$, which maximises the restoration of the dam volume by the pumping action of $K2$ results in the highest grid pumping energy demand, E_{gk}, of 220.59 MWh and 38.05% increase in the overall energy output of the system. This is expected because maximisation of restoration of the water level of the main dam results in continuous pumping operation by both pumps $K1$ and $K2$ throughout the 24 h control horizon resulting in the highest pumping energy demand of 220.59 MWh with the OC opting to meet it fully by E_{gk}.

The case of weights $\omega_1 = \omega_2 = \omega_3 = 0, \omega_4 = 1$ results in the optimal solution with the lowest E_{hg} of 356.3 MWh with 31.64% gain in the overall energy output of the system, which is the lowest performance index when compared to other combinations of weights. This is because maximisation of HK pumping energy, E_{hk}, minimises grid HK energy export, E_{hg}, resulting in the low gain in overall energy yield, E_{opt}, despite high E_g. These results with ranging values of weights provide a framework of reference for decision makers when faced with multiple objectives so that effective trade-offs and choices are made with regard to the priority of each of the sub-objectives.

Finally, this proposed OC model yields results with uncertainty error in the performance index based on true values discussed in subsection 3.4.3.5 and 3.5.1.4 equal to:$E_g = \sum P_g t_s = 859.5684$ MWh against the energy output simulated from the measured values of 859.5723 MWh, which are in close agreement. This proves a low risk of uncertainty implying that the model's results have high confidence level to the margin of:

$$\triangle E = \sum P_g t_s \times 0.022 \times 10^{-2} = 0.1891, \tag{3.39}$$

where 0.022×10^{-2} is the weakest link. A value of $\triangle E = 0.1891$ gives this model the energy output results with the marginal uncertainty error of $E = (859.5723 \pm 0.1891)$.

3.5.1.6 Comparison with the classical single pump pumpback system

The pumpback system for the classical PS system employs a single high lift pump for pumping water from the afterbay to the forebay of the power plant. Figure 3.7 shows optimal switching and flow rates of the classical PS system when the weights $\omega_1 = \omega_2 = \omega_3 = \omega_4 = 0.25$. As shown, for the same initial conditions of the dam and grid load demand, the optimal control keeps pump K in ON mode throughout the control horizon to maintain the same level of system performance achieved by the cascaded pumpback system.

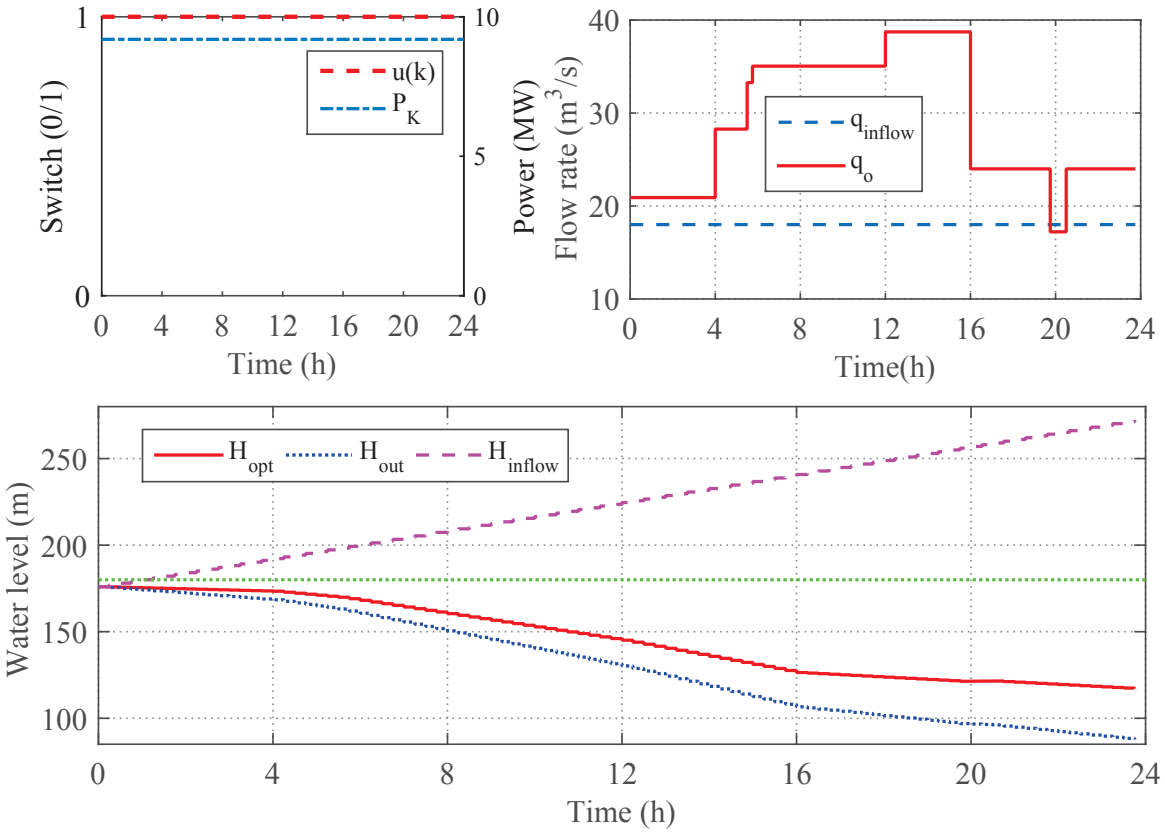

Figure 3.7. Optimal decay of the dam for the classical PS system in dry season

Figure 3.8 shows the optimal power flows of the classical PS system when the weights $\omega_1 = \omega_2 = \omega_3 = \omega_4 = 0.25$. As shown, the pumping power demand of 9.19 MW is met solely by the grid import power, P_{gk}, between 00:00 and 05:30 and between 19:45 and 20:30, otherwise it is met by the HK power, P_{hk}.

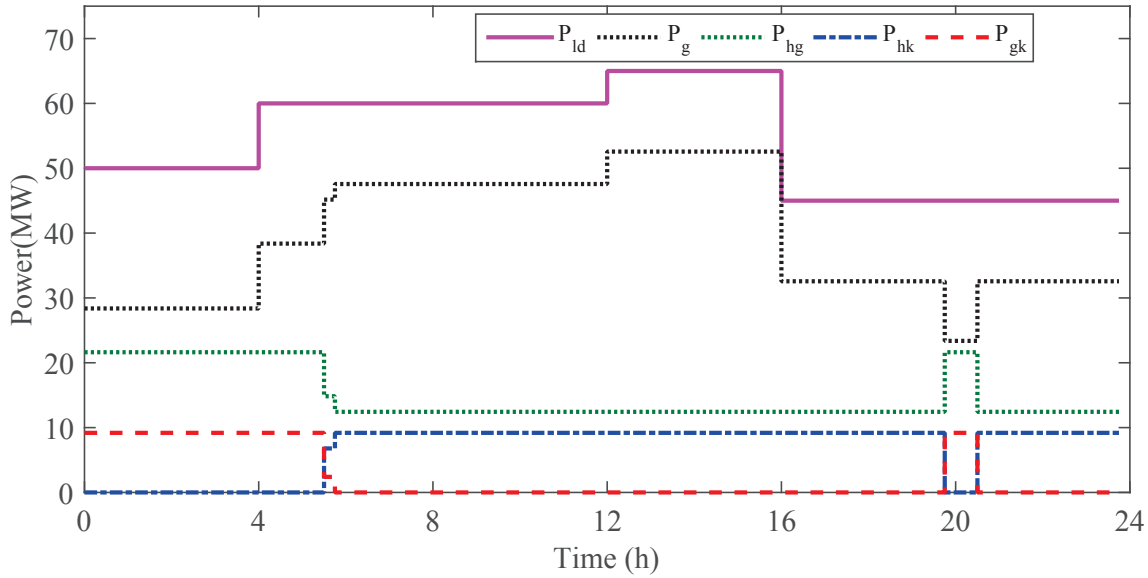

Figure 3.8. System power balance of the classical PS system in dry season

Table 3.7 shows the energy flows of the classical PS system for the same weighting factors used to simulate the results of the plant with the cascaded pumping system shown in Table 3.6. As shown, for the same weighting factors, the pumping energy demand for the classical PS system is far higher for the first three operation strategies as compared to the cascaded pumping system. For instance, for the case when the weights $\omega_1 = \omega_2 = \omega_3 = \omega_4 = 0.25$, the classical PS systems' pumping energy demand, E_K, is 220.59 MWh as compared to 114.30 MWh demanded by the cascaded pumping system.

Table 3.7. Daily optimal energy flows for a classical PS in dry season

$\sum_{i=1}^{4} \omega_i = 1$	E_g (MWh)	E_{hg} (MWh)	E_{hk} (MWh)	E_{gk}(MWh)	E_K (MWh)	E_{opt} (MWh)	Increase (%)
$\omega_1 = \omega_2 = \omega_3 = \omega_4 = 0.25$	943.56	356.44	162.54	58.05	220.59	1242.00	31.63
$\omega_2 = \omega_3 = \omega_4 = 0; \omega_1 = 1$	908.63	299.05	219.94	0.00	219.94	1207.68	32.91
$\omega_1 = \omega_3 = \omega_4 = 0; \omega_2 = 1$	873.92	325.79	173.20	47.28	220.48	1152.43	31.87
$\omega_1 = \omega_2 = \omega_4 = 0, \omega_3 = 1$	867.51	432.49	0.00	220.59	220.59	1079.40	24.43
$\omega_1 = \omega_2 = \omega_3 = 0; \omega_4 = 1$	943.56	356.44	162.54	58.05	220.59	1242.00	31.63

In this regard, using the classical PS system as the baseline, the cascaded pumpback system saves 106.29 MWh of pumping energy, which translates to a saving potential of 48.18%. Similarly, the case when the weights $\omega_1 = 1; \omega_2 = \omega_3 = \omega_4 = 0$ results in 114.30 MWh of pumping energy demand

for the cascaded system as compared to 219.94 MWh of the single pump classical PS system. This translates to 48.03% energy savings when the classical PS system is used as the baseline. In similar veins, allocation of full optimisation priority to the restoration of the dam volume, that is by setting the weights $\omega_1 = \omega_2 = \omega_4 = 0; \omega_3 = 1$ results in an optimal solution with pumping energy demand of 220.59 MWh for both cascaded and classical PS systems for the same weighting factors. This is because this operation strategy results in continuous pumping throughout the control period in both systems resulting in the highest pumping energy demand. In comparison, the use of a cascaded pumping system for this case results in 38.05% increase in energy yield of the cascaded pumpback system as compared to 24.43% gain realised by the classical PS model. This underscores that the cascaded model has a comparative advantage over the classical PS system even under the worst operational scenario.

In general, the high pumping energy demand for the classical single pump PS system when compared to the cascaded pumping system in the first three operational scenarios shown in Table 3.6 and Table 3.7 is as a result of the high pumping head bridged by a single high lift pump for the classical case. Optimal operation of the cascaded pumpback system reduces the pumping power and pumping energy demand by alternating the operating schedule of the two pumps at some point over the control horizon as shown in Figure 3.2 and Figure 3.3 resulting in lower daily pumping energy demand.

3.5.2 Operation scenario II

This scenario simulates the performance of the proposed optimal control system on a typical day in the rainy season with high in-stream discharge, q_{in}. Under this operation scenario, the OC should opt to keep the pumping system in OFF mode throughout the control horizon since the high in-stream discharge is sufficient to optimally meet the committed grid load demand.

3.5.2.1 Optimal flow rates of the main dam in rainy season

During the rainy season, Pangani River discharge increases to an average of 25 m^3/s, which is high enough to maintain a high water level in the dam to meet the committed load demand of the HPP. Figure 3.9 shows the optimal power flows for the cascaded pumpback system on a typical day in the rainy season. As shown, the OC keeps all the pumps $K1$ and $K2$ in OFF mode and as a result, all the

518.99 MWh of on-site generated HK energy is exported to the grid. Figure 3.11 shows the optimal flow rates and the corresponding change in water level of the dam throughout the control period. The constant supply of 21.62 MW of HK power results in low demand for P_g between 16:00 and 24:00 and as a result, a sharp decrease in q_o from 31.95 m^3/s to 17.22 m^3/s is observed.

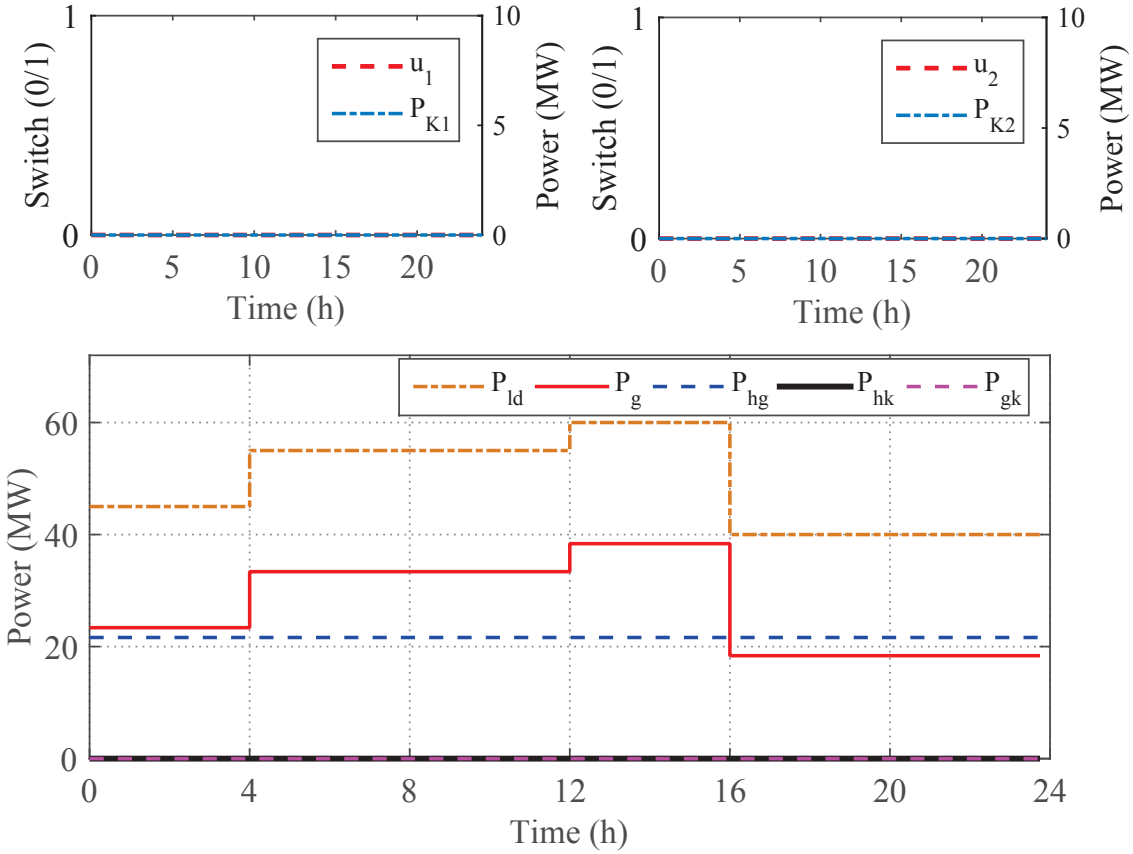

Figure 3.9. Optimal power balance of the system in rainy season

Because of the high q_{in} of 25.0 m^3/s as compared to the turbine discharge rate, q_o, of 17.22 m^3/s, the water level in the dam rises from 171.9 m, to 184.7 m between 16:00 and 24:00 as shown in Figure 3.11. Table 3.8 shows the optimal energy flows of the proposed model on a typical day in the rainy season for the case when the weights $\omega_1 = \omega_2 = \omega_3 = \omega_4 = 0.25$ for both the cascaded and the classical PS systems.

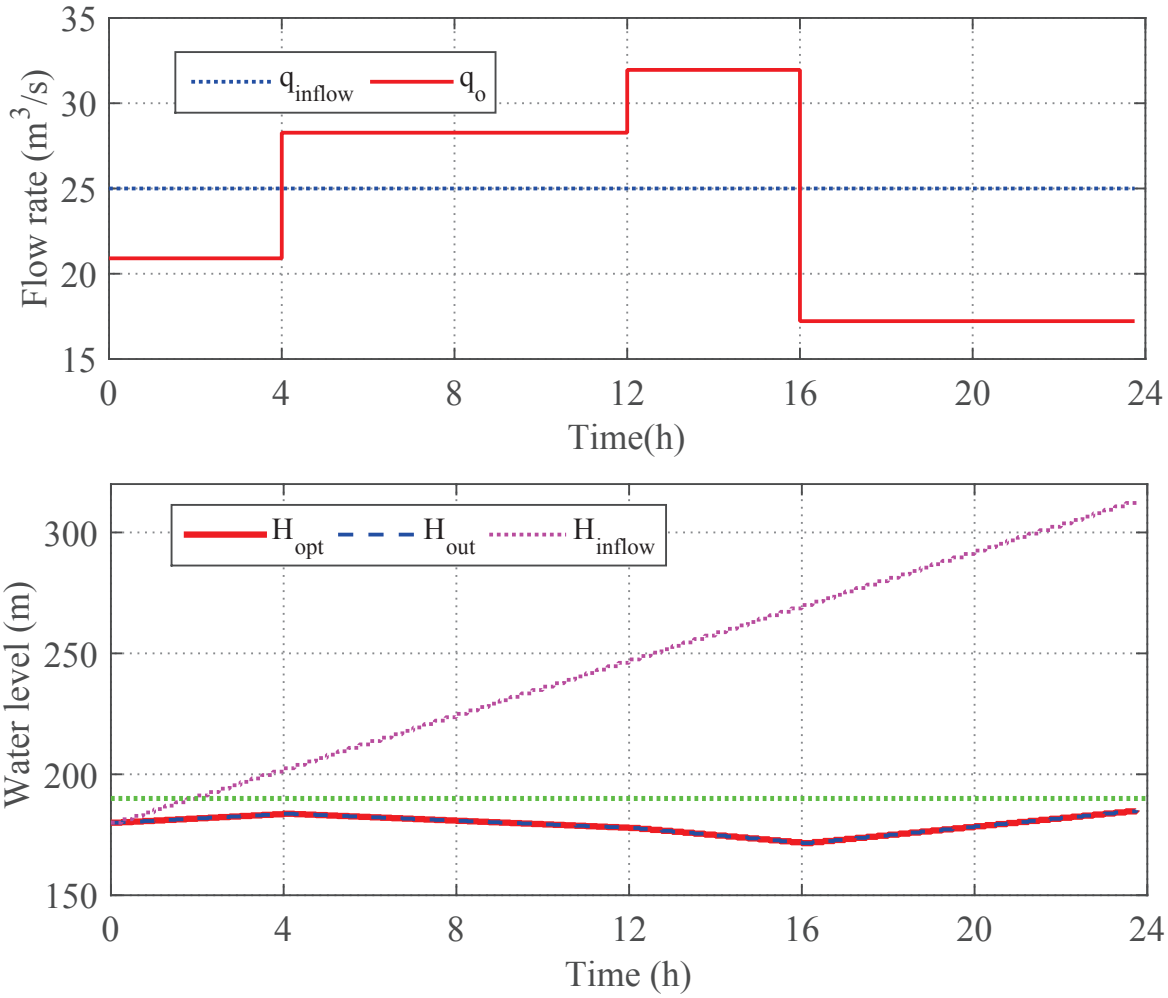

Figure 3.10. Optimal flow rates and change in water level of the dam in rainy season

Figure 3.11. Optimal flow rates and change in water level of the dam in rainy season

As shown in the table, pumping energy, E_K, is zero throughout the control horizon because the OC opts to operate the pumping system only during the dry season when there is low q_{in}. As a result, all the generated HK energy of 518.99 MWh is exported to the grid resulting in 66.45% increase in the overall energy yield of the resultant system.

Table 3.8. Daily optimal energy flows in the rainy season

$\sum_{i=1}^{4} \omega_i = 1$	E_g (MWh)	E_{hg} (MWh)	E_{hk} (MWh)	E_{gk} (MWh)	E_K (MWh)	E_{opt} (MWh)	Increase (%)
$\omega_1 = \omega_2 = \omega_3 = \omega_4 = 0.25$	781.02	518.99	0.0	0.0	0.0	1300.0	66.45

3.6 SUMMARY

This chapter presented an optimal control for a conventional hydropower plant (HPP) retrofitted with a hydrokinetic-powered pumpback system in the dry season. The objective of the study was to maximise the energy output of the plant for meeting a deterministic time varying load by simultaneously; minimising the grid imported pumping energy demand; minimising the wear and tear of the pumps; maximising the use of the on-site generated hydrokinetic (HK) energy for pumping operation; and maximising the restoration of the volume of the dam through pumpback operation. Simulation results based on a practical case study showed the potential of the proposed optimal control to save pumping energy up to 48.18% and increase the overall energy output of the resultant hybrid system by 30 to 48% in dry seasons and up to 66.45% in the rainy season. The high increase in energy yield of the HPP in the rainy season is occasioned by the exportation of all the on-site generated HK energy to the grid because the pumpback system was in OFF mode. When compared to the single pump classical pumped storage (PS) system, the cascaded pumping system showed superior performance with lower pumping energy demand. For the optimisation scenario when the weights $\omega_1 = \omega_2 = \omega_3 = \omega_4 = 0.25$, the cascaded pumping system resulted in an overall pumping energy demand of 114.30 MWh as compared to 220.59 MWh demanded by the classical PS system. Using the classical model as the operation baseline, the use of cascaded pumping system resulted in an energy saving potential of up to 48.18%. For the cascaded pumpback system, the optimal control was observed to alternate the operation of pumps $K1$ and $K2$ throughout the control horizon in order to reduce the overall maximum pumping power demand and the overall pumping energy of the system. This is one of the main advantages of the cascaded pumping system. Furthermore, simulation results showed that integration of the auxiliary constraint in the switching transitions of the pumps reduces the switching frequency of the pumps in the pumpback system, thereby reducing the wear and tear associated with pump switches.

CHAPTER 4 EFFECTS OF FLOW CONSTRAINTS ON THE PERFORMANCE OF A HYDROPOWER PLANT WITH PUMPBACK OPERATION

4.1 CHAPTER OVERVIEW

Chapter 3 presented an optimal control model of a high head hydropower plant (HPP) with a hydrokinetic-powered cascaded pumpback retrofit. Simulation results based on a practical case study showed that a cascaded pumpback system is economical in terms of pumping energy demand when compared to the classical single pump pumped storage system. In chapter 3, the downstream river flow of the system was assumed un-regulated and thus the HPP operator had the full flexibility to vary the turbine discharge rate in response to the changes in system load demand to maximise the economic value of the available water. In this chapter, downstream ecological flow constraints are introduced in the optimal control model of the HPP. Wind power is also introduced to form a hybrid HK-wind power system for powering the pumpback operation. The main objective of the chapter is to assess the effects of downstream flow constraints to the performance of a HPP. The plant operator seeks to maximise the economic value of the available water in meeting deterministic time-varying consumer load.

4.2 INTRODUCTION

The main objective of optimal operation of hydropower plants (HPPs) is to maximise the energy and revenue yield of the reservoirs. In deregulated energy markets, optimal control may entail adjusting

the turbine discharge rate in response to changes in energy prices to maximise power generation when it is most profitable [79]. Where power generation is the sole purpose and the reservoir release rate is not regulated, the facility operators can maximise their reservoirs' value by storing sufficient water during off-peak hours for optimal peak generation [80]. However, this operation strategy, technically known as hydropeaking [81], has adverse effects to the downstream riverine ecosystem [6, 8, 82, 83, 84]. Generally, dams serve multiple purposes including provision of a downstream habitat for aquatic biodiversity, recreational navigation, water abstraction for irrigation farming and supply for both domestic and industrial use [85]. Therefore, without environmental constraints, operation of peak HPPs can cause large variations in downstream flow regimes with negative consequences to human settlement and farming, recreational navigation and aquatic biodiversity [7, 86, 87, 88, 89, 90]. According to [86, 91, 92, 93], low downstream flow during off-peak hours and high flow during peak hours can cause stranding of fishes and other aquatic species. To minimise the effects of operation of HPPs to the downstream riverine ecosystem, environmental flow policies are incorporated in their operation policies [9]. The minimum flow constraint, the maximum ramp-up and ramp-down rates, and maximum water allocation for power generation over a given control horizon are the commonly used ecological constraints to the operation of hydropower systems [9].

Therefore, it is proposed in this chapter that optimal operation of a HPP entails striking a balance between environmental protection and maximisation of energy output of the reservoir. These conflicting objectives underscore the need to assess the impacts of regulatory policies and develop mitigation strategies that can maximise the reservoir utility while at the same time effecting maximum downstream riverine ecosystem protection.

The effects of pumpback operation and the downstream re-regulation reservoir to the performance of a HPP are investigated in [19]. However, the drawback of this model is the use of the much needed hydro reservoir generated power for pumping operation. Unlike the model presented in [19], in this chapter, a hydrokinetic-wind hybrid power system is proposed for powering the pumpback operation. Also investigated in this chapter is the effects of the downstream discharge rate to the performance of the combined hybrid power system. Ramp rate constraint is not considered in this chapter since the penstock discharge rate is already constrained by the technical constraints of the turbine-generator. In general, the aim of the proposed optimal control model is to meet the contracted power demand at all times taking into account the technical, operational and downstream river flow constraints.

4.3 MODEL FORMULATION OF THE SYSTEM

4.3.1 Schematic layout of the system

The schematic layout of the proposed hydropower system with a hydrokinetic-wind powered pumpback retrofit is shown in Figure 4.1. It should be noted that the re-regulation reservoir is constructed far downstream the power house to ensure that its state dynamics does not have an effect on the hydraulic head of the HPP upstream.

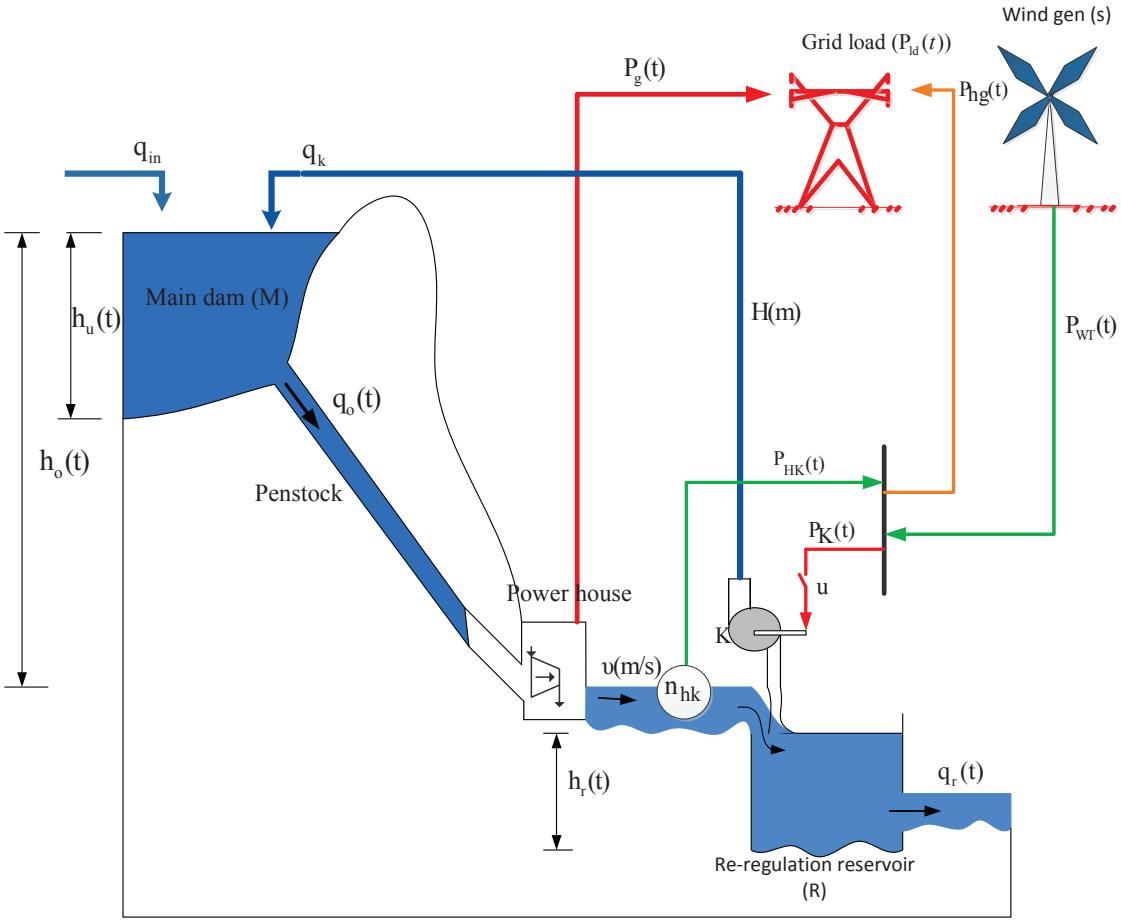

Figure 4.1. Layout of the hydropower system with pumpback operation

As shown, the pump K is primarily powered by the wind generated power, $P_{WT}(t)$, supplemented by the hydrokinetic (HK) power, $P_{hk}(t)$. The excess HK power after meeting pumping power deficit

unmet by the wind generator, $P_{hg}(t)$, is supplied to the grid to meet the system load. In the proposed model, the speed of water released from the powerhouse, υ m/s, is assumed constant and therefore, the total HK power output, $P_{HK}(t)$, is a variable which depends on the number of installed generators in parallel operation, n_{hk}. On the other hand, wind generator power output, $P_{WT}(t)$, depends on the wind speed, v $(\mathrm{m/s})$. In Figure 4.1, $P_g(t)$ and $P_K(t)$ denote the hydro-turbine generator power output and the pumping power demand of pump K supplied through control switch u respectively. In this model, the control variables include, the turbine discharge rate through the penstock, $q_o(t)$, the number of HK generators, $n_{hk}(t)$, the HK pumping power supply, $P_{hk}(t)$, the excess HK power supplied to the system load, $P_{hg}(t)$, and the state of the pump switch, $u(t)$. The water level in the main dam, $h_u(t)$, and the level in the re-regulation reservoir, $h_r(t)$, constitute the state variables of the system. A control horizon of 24 h is chosen to give accurate optimal operational predictions rather than a year long horizon.

4.3.2 Sub-system models and constraints

4.3.2.1 Conventional hydropower system

A conventional hydropower system comprises a dam reservoir and a hydro-turbine generator system as shown in Figure 2.2. The theoretical power output of a HPP, $P_g(t)$, is a nonlinear function of the water head, $h_o(t)$, which depends on the available volume of water, $W(t)$, and the turbine discharge rate, $q_o(t)$, expressed by equation (3.3). At any given time t, $P_g(t)$ is constrained by the turbine technical capacity as follows:

$$P_g^{min} \leq P_g(t) \leq P_g^{max}, \tag{4.1}$$

where P_g^{min} and P_g^{max} are respectively, the minimum and the maximum bounds of the variable, $P_g(t)$.

4.3.2.2 Main dam

In this chapter, a cylindrical model for the main dam with a base area, A_u, is assumed. The water mass balance of a hydro reservoir over a short scheduling period is given by equation (3.4) in section 3.3.3.1. Therefore, using the relationships and assumptions described in section 3.3.2, the water mass balance of the dam for the baseline optimisation scenario is expressed as follows:

$$h_u(t) = h_u(0) + \frac{1}{A_u}\int_{t_0}^{t} \big(q_{in}(t) - q_o(t)\big)dt, \tag{4.2}$$

where $h_u(t)$ and $h_u(0)$ are respectively, the level of water in the main reservoir at the end of time t and the initial water level at time $t = 0$.

For the model with a pumpback retrofit, the level of water in the main dam is a function of the natural in-stream flow, pumped discharge and the turbine discharge for hydropower generation expressed as follows:

$$h_u(t) = h_u(0) + \frac{1}{A_u}\int_{t_0}^{t} \big(q_{in}(t) + q_k u(t) - q_o(t)\big)dt, \tag{4.3}$$

where q_k is the discharge rate of pump K expressed in m^3/s while u is a binary variable [0,1] denoting the ON/OFF status of the switch that controls pump K. For a short control period, the in-stream flow rate, q_{in}, is assumed constant in this chapter.

4.3.2.3 Re-regulation reservoir

The main function of the re-regulation reservoir is to control the downstream discharge rate back to the river without significant alteration of its flow regimes as well as to provide a temporary storage to ensure pumping continuity of the system. To maximise the economic value of the available water; zero spillage is assumed; all water discharged is utilised for hydropower generation. Therefore, the water mass balance equation of the re-regulation reservoir is expressed as follows:

$$h_r(t) = h_r(0) + \frac{1}{A_r}\int_{t_0}^{t}\big((1-\alpha)q_o(t) - q_r(t) - q_k u(t)\big)dt, \tag{4.4}$$

where $h_r(0)$ and $h_r(t)$ are respectively, the initial water level of the reservoir at time $t = 0$ and the level at the end of time period t. The quantity $q_r(t)$ denotes the re-regulation reservoir release rate to the downstream river flow, while α denotes the fraction of the turbine discharge lost in cooling and spillage in the machine house. In this chapter, a 20% loss is assumed.

The minimum environmental flow constraint imposed on the operation of the hydro reservoir is defined as follows:

$$q_o(t) \geq q_r^{min} \quad ; \quad q_r(t) \geq q_r^{min}, \tag{4.5}$$

where q_r^{min} denotes the minimum discharge rate of water from the re-regulation reservoir into the downstream river flow. Equation (4.5) shows that at any given time t, the hydro-turbine discharge rate, $q_o(t)$, must be greater than the defined minimum downstream release rate, q_r^{min}, which is less than the instantaneous re-regulation reservoir release rate, $q_r(t)$. For optimal reservoir operation, the total daily turbine discharge must not exceed the daily water allocation for hydropower generation expressed as follows:

$$\frac{1}{A_u}\int_{t_0}^{t} q_o(t)dt \leq W_u, \tag{4.6}$$

where W_u denotes the total daily volume of water allocated for hydropower generation.

4.3.2.4 Wind power generator

The power output of a wind turbine, $P_{WT}(t)$, is dependent on the wind speed at the given location the air density, ρ_a, the area swept by the turbine rotor and the energy extraction efficiency of the turbine, η_{wt}. There are various models developed in the current literature for computing the power output of a wind turbine generator [38, 94] based on various assumptions such as linear and quadratic turbine power functions [95]. However, in this chapter, the simplified model used in [96] is adopted:

$$P_{WT}(t) = \begin{cases} P_{WT,r}\frac{v^{\chi}-v_i^{\chi}}{v_r^{\chi}-v_i^{\chi}}, & (v_i \leq v \leq v_r) \\ P_{WT,r}, & (v_r \leq v \leq v_o) \\ 0, & (0 \leq v_i \quad \text{and} \quad v \leq v_o), \end{cases} \tag{4.7}$$

where v is the wind speed at the desired height, h_{hub}, while χ is the Weibull shape parameter, which in this chapter it takes the value of 2. $P_{WT,r}$, v_r, v_i and v_o are respectively, the rated power output of the wind generator, the rated wind speed, the cut-in wind speed and the cut-out wind speed.

At any given time t, the power output of the wind generator, $P_{WT}(t)$, is bounded to lie between a minimum value, P_{WT}^{min}, and a maximum value, P_{WT}^{max}, expressed by equation (4.8).

$$P_{WT}^{min} \leq P_{WT}(t) \leq P_{WT}^{max}. \tag{4.8}$$

4.3.2.5 Hydrokinetic generator

A hydrokinetic turbine operates on a similar principle like that of a wind turbine except that it is powered by the kinetic energy of the water currents. Therefore, the instantaneous power output of the hydrokinetic energy conversion (HKEC) system, $P_{HK}(t)$, is expressed as a function of the river current velocity υ,(m/s) and the area swept by the HK turbine rotor, A_{hk}, given by equation (2.2). The instantaneous power output of the HKEC system is governed by the following constraint:

$$P_{HK}^{min} \leq P_{HK}(t) \leq P_{HK}^{max}, \tag{4.9}$$

where P_{HK}^{min} and P_{HK}^{max} are respectively, the minimum and the maximum power output of the HKEC system. In the proposed model, a fraction of the HK power produced is supplied to meet the pumping power demand, $P_{hk}(t)$, while the surplus, $P_{hg}(t)$, is exported to meet the grid demand. Therefore, the power balance of the HKEC system is expressed as follows:

$$P_{HK}(t) = P_{hk}(t) + P_{hg}(t). \tag{4.10}$$

The HK pumping power demand, $P_{hk}(t)$, is constrained by equation (4.11):

$$P_{hk}^{min} \leq P_{hk}(t) \leq P_{hk}^{max}, \tag{4.11}$$

where P_{hk}^{min} and P_{hk}^{max} are respectively, the minimum and maximum bounds of the variable $P_{hk}(t)$. Similarly, the excess HK power supplied to the grid at any given time is bounded by equation (4.12) where P_{hg}^{min} and P_{hg}^{max} denote the lower and the upper bounds of the variable $P_{hg}(t)$ respectively:

$$P_{hg}^{min} \leq P_{hg}(t) \leq P_{hg}^{max}. \tag{4.12}$$

4.3.2.6 Pumpback system and constraints

In the proposed hydropower system, pumpback operation is employed to maintain a high reservoir water level required for optimal power generation. In the optimal control model, the pump K is powered primarily by the wind power, $P_{WT}(t)$, supplemented by $P_{hk}(t)$. Therefore, the power balance of the pumping system is written as follows:

$$P_{WT}(t) + P_{hk}(t) = P_K u(t), \tag{4.13}$$

where P_K is the nominal power rating of pump K while $u(t)$ is a binary notation for the ON/OFF status of the switch through which the pump is powered. The relationship between the pumping power demand, the discharge rate of the pump and the net differential head to be bridged by the pump is given by equation (2.5).

4.3.2.7 System power balance

For the baseline optimisation model, the system load demand, $P_{ld}(t)$, is met fully by the hydro-turbine power output, $P_g(t)$. Therefore, at any given time t, $P_g(t)$ must be equal to $P_{ld}(t)$ expressed as follows:

$$P_g(t) = P_{ld}(t). \tag{4.14}$$

In the optimisation scenario with a pumpback retrofit, the total system load demand, $P_{ld}(t)$ is met primarily by the hydro-turbine generator power supply, $P_g(t)$, supplemented by the surplus HK power above the pumping power demand, $P_{hg}(t)$. Therefore, the system load power balance is expressed as follows:

$$P_g(t) + P_{hg}(t) = P_{ld}(t). \tag{4.15}$$

4.4 DISCRETE MODEL FORMULATION AND OPTIMISATION

4.4.1 Objective function

The objective of the proposed optimal control model is to meet contractual power supply to the grid over a 24 h control horizon in the dry season. The optimisation problem is first formulated for the baseline operation scenario as follows:

$$\max \quad J = t_s \sum_{j=1}^{N} P_{g,j}, \tag{4.16}$$

where j is the discrete time instant while t_s is the system sampling interval, which is 0.25 h in this chapter and the number of samples, $N = \frac{24}{t_s} = 96$. The objective function expressed by equation (4.16) is solved subject to the following constraints:

$$P_{g,j} = P_{ld,j}, \tag{4.17}$$

$$h_u^{min} \leq h_{u,0} + \frac{t_s}{A_u}\left(q_{in} - \sum_{i=1}^{j} q_{o,i}\right) \leq h_u^{max}, \tag{4.18}$$

$$P_g^{min} \leq P_{g,j} \leq P_g^{max} \quad ; \quad 0 \leq q_{o,j} \leq A_c\sqrt{2gh_o^{max}}, \tag{4.19}$$

where h_u^{min}, h_u^{max} and respectively, the minimum and the maximum bounds of the water level in the main dam for optimal operation. P_g^{min} and P_g^{max} denote respectively, the minimum and maximum power output of the hydro-turbine generator.

In the second scenario, a hydrokinetic-wind-powered pumpback retrofit is incorporated in the optimal control of the hydro reservoir. A fraction of the total HK power generated is supplied to the pumpback system while the surplus HK power is exported to meet contractual load demand. Therefore, the optimisation problem is formulated to maximise the energy yield of the resultant system as follows:

$$\max \quad J = t_s \sum_{j=1}^{N} \left(P_{g,j} + P_{hg,j}\right), \tag{4.20}$$

subject to the following constraints expressed in discrete time domain:

$$P_{g,j} + P_{hg,j} = P_{ld,j}, \tag{4.21}$$

$$P_{HK,j} = P_{hk,j} + P_{hg,j}, \tag{4.22}$$

$$P_{hk,j} + P_{WT,j} = P_K u_j, \tag{4.23}$$

$$h_u^{min} \leq h_{u,0} + \frac{t_s}{A_u}\left(q_{in} + q_k \sum_{i=1}^{j} u_i - \sum_{i=1}^{j} q_{o,i}\right) \leq h_u^{max}, \tag{4.24}$$

$$P_g^{min} \leq P_{g,j} \leq P_g^{max} \quad ; \quad 0 \leq q_{o,j} \leq A_c\sqrt{2gh_o^{max}}, \tag{4.25}$$

$$P_{HK}^{min} \leq P_{HK,j} \leq P_{HK}^{max} \quad ; \quad n_{hk}^{min} \leq n_{hk,j} \leq n_{hk}^{max}, \tag{4.26}$$

$$P_{hg}^{min} \leq P_{hg,j} \leq P_{hg}^{max}, \tag{4.27}$$

$$P_{hk}^{min} \leq P_{hk,j} \leq P_{hk}^{max}, \tag{4.28}$$

$$P_{WT}^{min} \leq P_{WT,j} \leq P_{WT}^{max}, \tag{4.29}$$

$$u_j \in [0,1], \quad (1 \leq j \leq N), \tag{4.30}$$

For the optimisation scenario with a pumpback retrofit and downstream flow restrictions, besides the constraints 4.21– 4.30, the objective function (4.20) is solved subject to the following constraints:

$$h_r^{min} \leq h_{r,0} + \frac{t_s}{A_r}\left((1-\alpha)\sum_{i=1}^{j} q_{o,i} - q_k \sum_{i=1}^{j} u_i - \sum_{i=1}^{j} q_{r,i}\right) \leq h_r^{max}, \quad (1 \leq i \leq j), \tag{4.31}$$

$$q_{o,j} \geq q_r^{min} \quad ; \quad q_{r,j} \geq q_r^{min}, \tag{4.32}$$

$$\sum_{j=1}^{N} q_{o,j} \leq W_u, \tag{4.33}$$

4.4.2 Optimisation algorithm formulation

The baseline optimisation model of the hydro reservoir has only one real number control variable, $q_{o,j}$, while the model incorporating a pumpback retrofit and a down-stream re-regulation reservoir comprises five real number control variables: $n_{hk,j}$, $q_{o,j}$, $q_{r,j}$, $P_{hg,j}$ and $P_{hk,j}$ and one binary variable, u_j, solvable by the *OPTI toolbox* SCIP algorithm in MATLAB.

4.4.2.1 The objective function

The objective functions expressed by equation (4.16) and equation (4.20) can be expressed in canonical form as follows:

$$\max \quad f^T \mathbf{X} \quad \text{subject to} \quad \begin{cases} \boldsymbol{AX} \leq \boldsymbol{b} \\ \boldsymbol{A}_{eq}\boldsymbol{X} = \boldsymbol{b}_{eq} \\ \boldsymbol{L}_B \leq \boldsymbol{X} \leq \boldsymbol{U}_B, \end{cases} \tag{4.34}$$

where $f^T \mathbf{X}$ is the objective function to be solved subject to inequality constraints, $\boldsymbol{AX} \leq \boldsymbol{b}$, equality constraints, $\boldsymbol{A}_{eq}\boldsymbol{X} = \boldsymbol{b}_{eq}$, and the lower and the upper bounds of the control variables, $\boldsymbol{L}_B \leq \boldsymbol{X} \leq \boldsymbol{U}_B$.

For the baseline optimisation model, the vector $\mathbf{X}$ contains the single control variable defined by equation (4.35):

$$\mathbf{X} = \left[q_{o,1}...q_{o,N}\right]'_{N\times 1}. \tag{4.35}$$

For the optimisation model with a pumpback retrofit and the re-regulation reservoir, the vector $\mathbf{X}$ is given by equation (4.36).

$$\mathbf{X} = \left[u_1...u_N,\quad n_{hk,1}...n_{hk,N},\quad q_{o,1}...q_{o,N},\quad q_{r,1}...q_{r,N},\quad P_{hk,1}...P_{hk,N},\quad P_{hg,1}...P_{hg,N}\right]'_{6N\times 1}. \tag{4.36}$$

From the objective function expressed in equation (4.16),

$$f^T = \left[-\tfrac{9.81}{1000}\eta_m\eta_e h_{o,1}... - \tfrac{9.81}{1000}\eta_m\eta_e h_{o,N},\right]_{1\times N}. \tag{4.37}$$

In the same vein, from the objective function expressed by equation (4.20),

$$f^T = \left[0_1...0_N,\quad 0_1...0_N,\quad -\tfrac{9.81}{1000}\eta_m\eta_e h_{o,1}... - \tfrac{9.81}{1000}\eta_m\eta_e h_{o,N},\quad 0_1...0_N,\quad 0_1...0_N,\quad -1_1... - 1_N,\right]_{1\times 6N}. \tag{4.38}$$

The lower and the upper bounds of the control variable of the baseline model are expressed by equation (4.39) and equation (4.40).

Lower bounds

$$lb^T = \left[8.5_1...8.5_N\right]_{N\times 1}. \tag{4.39}$$

Upper bounds

$$ub^T = \left[45_1...45_N\right]_{1\times N}. \tag{4.40}$$

Similarly, the lower and the upper bounds of the control variables of the model with a pumpback retrofit are expressed by equation (4.41) and equation (4.42) respectively.

Lower bounds

$$lb^T = \left[0_1 ... 0_N, \quad 0_1 ... 0_N, \quad 8.5_1 ... 8.5_N, \quad 8.5_1 ... 8.5_N, \quad 0_1 ... 0_N, \quad 0_1 ... 0_N\right]_{6N\times 1}. \tag{4.41}$$

Upper bounds

$$ub^T = \left[1_1 ... 1_N, \quad 12_1 .... 12_N, \quad 45_1 ... 45_N, \quad 25_1 ... 25_N, \quad P_{K,1} ... P_{K,N} \quad (P_{HK} n_{hk})_1 ... (P_{HK} n_{hk})_N\right]_{1\times 6N}. \tag{4.42}$$

The detailed formulation of the inequality and equality constraints of the baseline optimisation problem and the proposed model with a pumpback retrofit are attached to Addendum B.

4.4.3 Description of the case study

The case study for validation of the proposed optimal control model is based on Hale hydropower plant (HPP), a 21 MW HPP located on Pangani River in Tanzania. Hale HPP is one of the three HPPs that form the cascade of Pangani hydropower system. The total water discharged into Hale hydropower dam is the sum total of discharge from NyM HPP plus discharges from Mkomazi and Luengela seasonal rivers, less abstraction for irrigation farming and losses at Kirua swamp [77]. The combined effects of the on-going climate change and increased abstraction for irrigation farming upstream have resulted in a drastic decline in Hale dam inflows in recent years. For instance, Luengela and Mkomazi rivers have reduced into seasonal streams that dry up during dry seasons leading to very low inflows into the Hale dam. The dwindling inflows make Hale HPP a perfect case study for the application of the pumpback retrofit to maximise the energy value of the available water. The Hale HPP is installed with 2×10.5 MW Vertical Francis turbines with a total generation of 2×12.350 MVA. Table 4.1 shows the salient features of the Hale HPP [77].

Table 4.1. Salient features of Hale HPP

Storage (m^3)	h_u^{max} (masl)	h_u^{min} (masl)	Head (m)	$P_{g,r}$ (MW)	q_o^{max} (m^3/s)	q_o^{min} (m^3/s)	q_{in} (m^3/s)
1.9×10^6	331.0	329.8	63.0	21.0	45.0	8.5	16.5

4.4.3.1 Re-regulation reservoir parameters

The proposed optimal control model of a HPP incorporates a re-regulation reservoir downstream beyond the powerhouse to control the release rate back to the river as well as to provide a temporary storage for pumpback operation. The aim of the pumpback operation is to maintain a high water level in the main dam required for optimal power generation [70]. The amount of water discharged for each unit of hydropower generated is inversely proportional to the system head (water level in the dam). For optimal operation of the system, the capacity of the re-regulation reservoir must be big enough to maintain a minimum downstream discharge even with low discharge from the powerhouse and provide capacity for pumpback operation. In this chapter, the reservoir is designed by the rule of thumb with a capacity of 3.85×10^5 m^3 and height is 35.0 m. In the model, the minimum reservoir level for pumpback operation as well as the downstream discharge is set at 5.0 m.

4.4.3.2 Pumping system parameters

The proposed model employs the Sulzar Ltd's SJT vertical turbine pumps for pumpback operation. Their performance features are shown in Table 3.3. The proposed model is applied to the Hale HPP which has a net hydraulic head of 63.0 m. In the model, the design pump flow rate is set at 6.5 m^3/s to optimise restoration of the dam water level in the dry season for optimal operation of the system [21].

4.4.3.3 Hydrokinetic system parameters

The hydrokinetic energy conversion system used in the case study comprise of twelve CC025A river-in-stream HK turbines developed by the Clean Current Renewable Energy Systems Inc [1] and the flooded, permanent magnet generators. The CC025A turbine has a rotor diameter of 2.2 m and requires a minimum river depth of 2.8 m for effective deployment. The technical specifications of the hydrokinetic turbines (HKTs) used in the case study are given in Table 4.2. The CC025A HK turbine model has a rated power output of 33 kW and a nominal speed of 75 rpm.

[1] http://www.cleancurrent.com/river-turbines

Table 4.2. Hydrokinetic turbine specifications

Model	n_{hk}	$P_{HK,r}$ (kW)	A_{hk} (m^2)	υ_r (m/s)	η_t (%)	η_g (%)	C_p
CC035A	12	33	3.8	3.0	90.0	80.0	0.48

4.4.3.4 Wind generator parameters

The case study employs the 75 kW ZECWP horizontal wind turbines manufactured by ZEC wind Power [2] for powering the pumpback system. In the table, n_{wt}, v_i, v_o and v_s are respectively, the number of wind turbines in parallel operation, the cut-in wind speed, the cut-out wind speed and the survival wind speed . The quantities R_{wt} and v_r are respectively, the wind turbine rotor diameter and the rated wind speed. The ZECWP 75 kW wind turbines have a rotor speed of 42 rpm and a tower height of 36.0 m. To generate sufficient wind power to power the pumpback system of the proposed model, eight wind turbines are proposed. The technical specifications of the Vestas- ZECWP 75.0 kW turbines used in the case study are shown in Table 4.3.

Table 4.3. Wind turbine specifications

Model	n_{wt}	$P_{WT,r}$ (kW)	R_{wt} (m)	v_r (m/s)	v_o (m/s)	v_i (m/s)	v_s (m/s)	C_p
ZECWP	8.0	75.0	10.0	7.5	25	3.0	52.0	0.48

4.5 RESULTS AND DISCUSSION

The performance of the proposed optimal control (OC) model was analysed under different optimisation scenarios. The first scenario simulates the baseline case in the dry season while the second case incorporates wind-HK-powered pumpback operation in the operation policy of the HPP. The objective of second optimisation scenario is to assess the effects of pumpback operation to the energy yield of

[2] http://www.zecwindpower.com/zecwp-75kw-wind-turbine/technical-specifications/

the hydro reservoir. The third optimisation scenario incorporates pumpback operation and downstream flow constraints in the OC policy of the hydro reservoir. The objective this third scenario is to assess the effects of environmental flow constraints to the performance of the hydropower plant in question.

4.5.1 Optimisation scenario I

4.5.1.1 Baseline operation of the hydropower plant

In the baseline operation scenario, the objective of optimal control is to use the daily allocated water to fully meet the HPP's contractual obligation. This scenario gives the plant operator full flexibility to adjust the turbine discharge rate, q_o, in response to changes in the system load demand. Figure 4.2 shows the results of the baseline operation of the HPP in question. In the figure, q_{in} is kept constant at 16.5 m^3/s while q_o varies in response to the changes in P_{ld} throughout the control horizon. In the model, the system load, P_{ld}, is met fully by the hydro-turbine generation, P_g. For instance, q_o is 18.36 m^3/s when P_{ld} is 8.50 MW between 00:00 and 03:00. However, an increase in P_{ld} from 8.50 MW to 11.0 MW between 03:00 and 04:00 results in a corresponding increase in q_o from 18.36 m^3/s to 23.76 m^3/s. The system peak load of 419.50 MW that occurs between 10:00 and 12:00 corresponds to a peak turbine discharge of 42.11 m^3/s. Shown in the far right of the first row of Figure 4.2 is h_{opt}, which is the change in the dam water level as a result of q_{in}, less q_o. In the case study, a constant q_{in} of 16.5 m^3/s is assumed, which is a typical inflow rate of Hale dam in dry seasons experienced in recent years in the face of prolonged droughts. As shown in the figure, the water level in the dam model decays from the initial level of 300.0 m to 272.5 m at the end of the day. With the model base area of 4.0×10^4 m^2, the change in water level of the dam model translates to 1.1×10^6 m^3. This is the daily minimum amount of water allocation required for sufficient hydropower generation to meet the plant's contractual obligation.

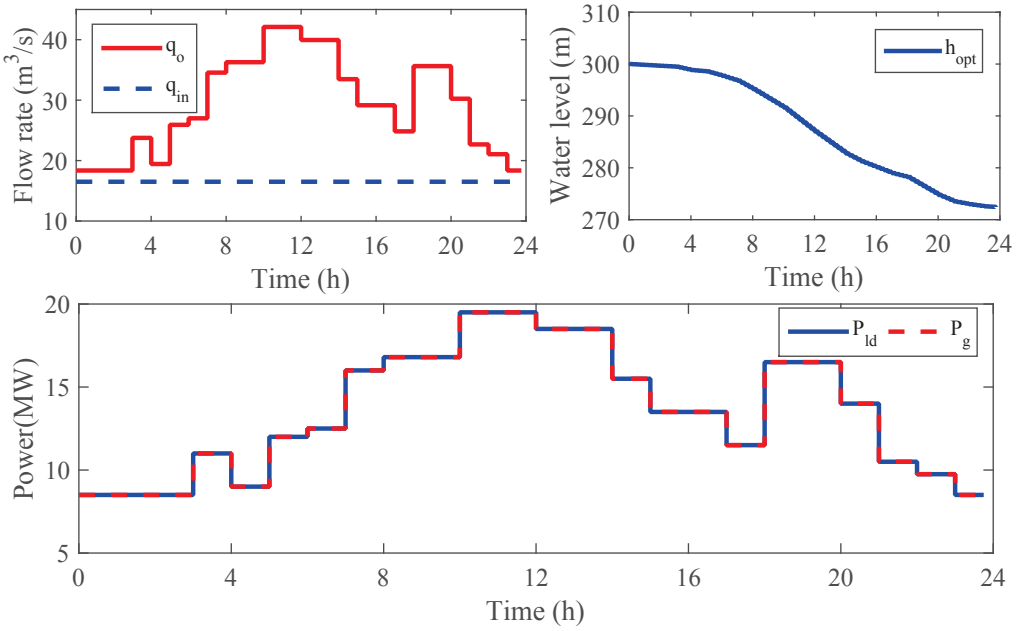

Figure 4.2. Baseline operation of Hale hydropower plant

4.5.2 Optimisation scenario II

This optimisation scenario incorporates pumpback operation in the optimal control policy of the hydro reservoir. A re-regulation reservoir is constructed downstream the powerhouse to provide a temporary storage for pumpback operation as well as re-regulate downstream flow regimes. It should be noted that the re-regulation reservoir is located downstream such that its level dynamics does not affect the hydraulic head of the hydropower system upstream. Where a daily water allocation for hydropower generation is specified, optimal pumpback operation can help maximise the reservoir energy output without violation of the daily discharge constraints.

4.5.2.1 Change in water level of the model with pumpback retrofit

The results of the optimal flow rates and their corresponding effects on the water level of the dam with a pumpback retrofit are shown in Figure 4.3. In the figure, q_{inflow} denotes the combined inflows into the dam, which is the sum of the river in-stream discharge, q_{in}, and the pumped capacity, q_k. As shown in the first row of Figure 4.3, q_{in} and q_k are constant at 16.5 m^3/s and 6.5 m^3/s respectively, giving a

constant total inflow , q_{inflow}, of 23.0 m^3/s. On the other hand, the turbine discharge, q_o, is seen to vary in response to the changes in system load, P_{ld}. As shown in Figure 4.3, the peak turbine discharge of 34.15 m^3/s occurs between 10:00 and 11:00, which corresponds to a system peak load of 19.50 MW, shown in Figure 4.5.

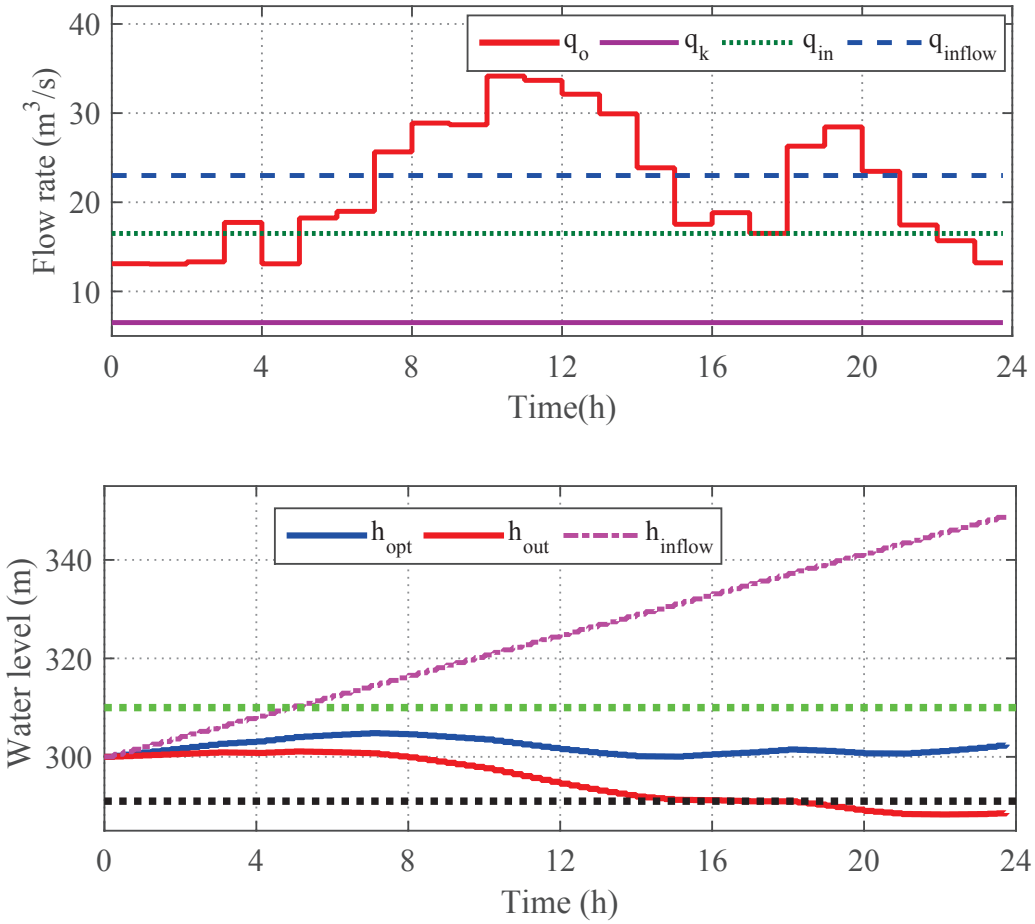

Figure 4.3. Optimal flow rates and change in reservoir water level

Shown in the second row of Figure 4.3 is the change in the dam water level in response to the combined inflows and outflows. In the figure, h_{out} is the change in the reservoir water level in response to the turbine discharge rate, q_o. h_{inflow} is the change in reservoir water level due to combined system inflows, q_{inflow}, while h_{opt} is the net optimal change in water level due to the combined inflows and outflows of the reservoir. An important observation to note is the would be operation scenario if the dam was operated without pumpback operation; the water level would fall below the minimum operational limit by 16:00 making it technically infeasible to generate power for the last eight hours of the control

period. However, pumpback operation keeps the dam water level above its minimum limit throughout the control horizon as shown in Figure 4.3. If the dam was operated without inflows, its water level would drop from the initial level of 300.0 m to 288.6 m by end of the control period. In the same vein, if there were continuous inflows without penstock discharge for hydropower generation, q_{inflow} would raise the water level of the dam above its operation limit by 05:00 leading to spillage. However, the combined effects of q_{inflow} and q_o raises the optimal water level, h_{opt}, from the initial level of 300.0 m to 302.3 m by end of the control horizon.

4.5.2.2 Optimal WEC and HKEC power flows of the pumpback model

Figure 4.4 shows the power flows of the wind energy conversion (WEC) and the hydrokinetic energy conversion (HKEC) systems for the model simulated with the pumpback operation. As shown in the figure, P_{HK} and P_K are constant at 5.05 MW and 4.22 MW respectively. The OC switches ON all the 12 installed HK generators to maximise their beneficial use in meeting the system power demand. In the model P_K is met primarily by P_{WT} supplemented by P_{hk}. The surplus HK power, P_{hg}, is supplied to meet the contractual grid load. In the figure, P_{hk} is seen to change inversely in response to the changes in P_{WT} to maximise the use of wind power for pumping operation. An increase in P_{WT} causes a corresponding decrease in P_{hk} and increase in P_{hg}; and an increase in P_{hg} causes a decrease in P_g as shown in Figure 4.5. For instance, an increase in P_{WT} from 0.83 MW to 1.99 MW between 13:00 and 14:00 causes a corresponding decrease in P_{hk} from 3.39 MW to 2.24 MW and an increase in P_{hg} from 1.64 MW to 2.80 MW. This increase in P_{hg} results in a decrease in P_g from 16.86 to 15.70 MW as shown in Figure 4.5.

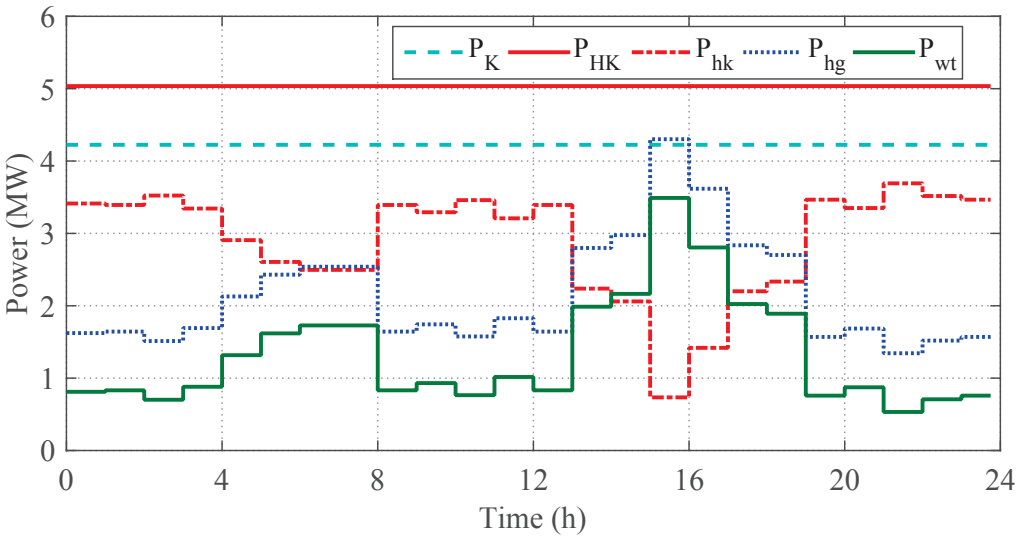

Figure 4.4. Pumping power flows of the system

The inverse complementary relationship between between P_{WT} and P_{hk} underscores the ability of the proposed model to maximise the use of wind power for pumping operation and maximise HK grid power export, P_{hg}.

4.5.2.3 Power flows of the system with pumpback operation

Figure 4.5 shows the results of the load balance of the model with a pumpback retrofit operated without ecological flow constraints. As shown, P_g and P_{hg} have a complementary inverse relationship; an increase in P_{hg} results in a corresponding decrease in P_g by the same magnitude, which maximises the use of P_{hg} in meeting the system load demand. For instance, between 12:00 and 13:00, the system load demand of 18.5 MW is met by 16.86 MW supplied by P_g supplemented by 1.64 MW supplied by P_{hg}. However, an increase in P_{hg} to 2.80 MW at 13:00 results in a corresponding decrease in P_g from 16.86 to 15.57 MW. This inverse complementary relationship is also seen between 15:00 and 17:00 and between 18:00 and 20:00.

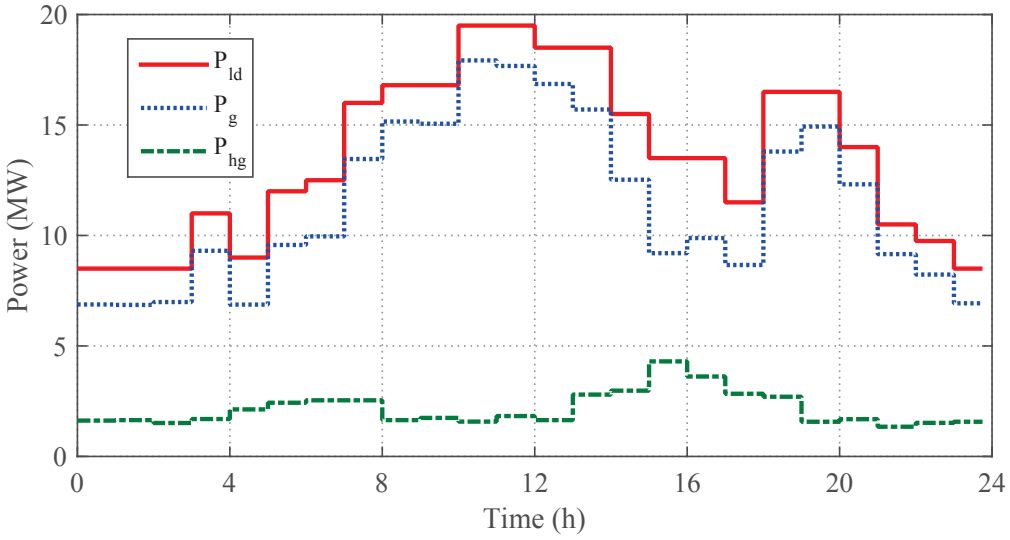

Figure 4.5. System load balance

Table 4.4 shows the daily energy flows of the proposed OC model. In the table, E_{ld}, E_g, E_{HK}, E_{WT}, E_{hg}, E_{hk} and E_K are respectively, the daily committed energy demand, the energy generated from the hydro reservoir, the energy flow from the HKEC system, the energy flow from the WEC system, the fraction of HK energy supplied to the grid, the fraction of HK energy supplied to the pumpback system and the overall pumping energy demand over the control horizon. As shown in the table, the HKEC system supplied 51.46 MWh to meet the system load demand, P_{ld}, of 325.35 MWh. This is equivalent to 15.85% of the system load.

Table 4.4. Optimal system energy flows

E_{ld} (MWh)	E_g (MWh)	E_{HK} (MWh)	E_{hg} (MWh)	E_{hk} (MWh)	E_{WT} (MWh)	E_K(MWh)
325.35	273.89	120.86	51.46	69.40	31.99	101.39

4.5.3 Optimisation scenario III

Under this operation scenario, the minimum downstream flow constraint is incorporated in the OC policy of the HPP with a pumpback retrofit. In section 4.5.2, the optimal performance of the model

was simulated with downstream flow constraint of q_r^{min} and q_r^{max} of 8.5 m^3/s and 45 m^3/s respectively, which coincides with the technical constraints of the turbine discharge of the Hale HPP as shown in Table 4.1. Thus, under this optimisation scenario, the HPP operator has the full flexibility to adjust q_o to effectively respond to the changes in the system load demand, P_{ld}. To assess the effects of downstream environmental flow policy to the operation of the HPP in question, q_r^{min} is raised to 17.00 m^3/s while q_r^{max} is lowered to 25.0 m^3/s. This downstream flow restriction limits the operational flexibility of the reservoir operator to vary q_o in response to the system load demand.

4.5.3.1 Optimal pumpback model operation with downstream flow constraints

Figure 4.6 shows the comparative results of the turbine discharge rates and their corresponding hydropower generation levels for the system when operated with and without minimum downstream flow restrictions. In the figure, $q_{o,1}$ and $q_{o,2}$ are respectively, the turbine discharge for the model without and with minimum environmental flow constraints while $P_{g,1}$ and $P_{g,2}$ are their corresponding hydropower generation levels. As shown in the figure, $q_{o,2} > q_{o,1}$ throughout the day. This is occasioned by the high downstream flow requirement of the model with environment flow restrictions. Correspondingly, as shown in the second row of Figure 4.6, $P_{g,2} > P_{g,1}$ throughout the control period. For a deterministic and fixed load, an increase in P_g output has a direct opportunity cost of a corresponding decrease in free HK energy in the model.

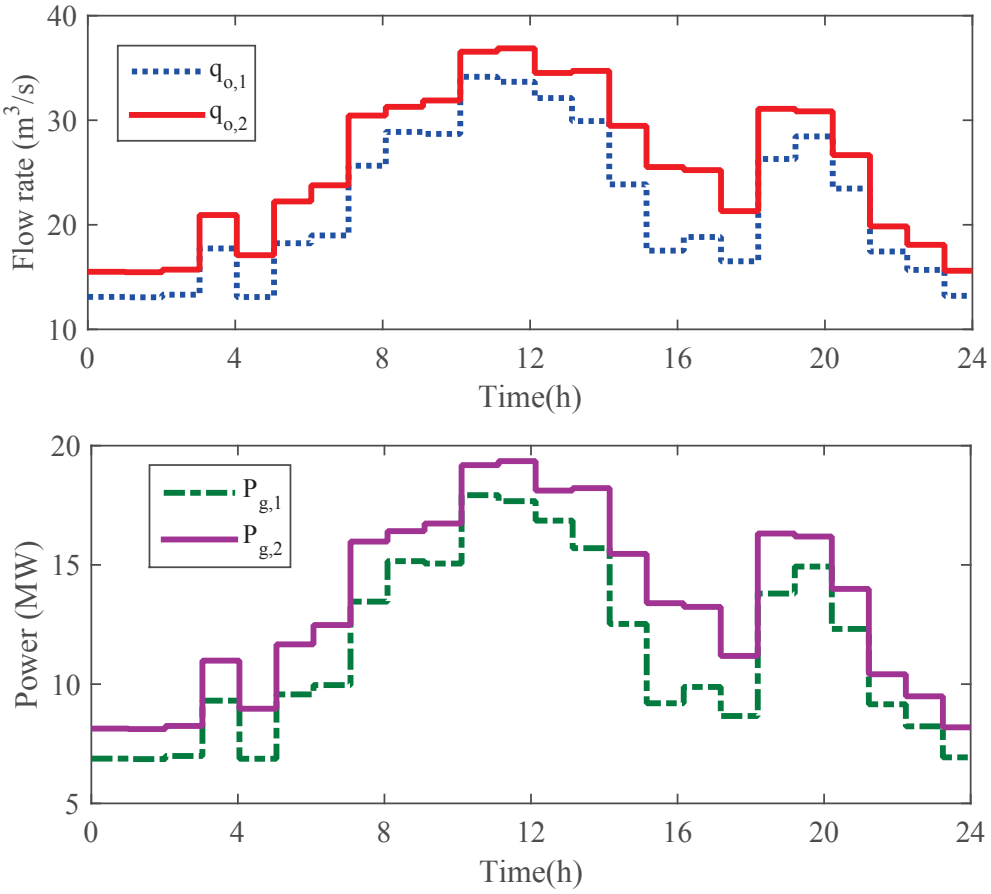

Figure 4.6. Effects of minimum ecological flow to the performance of the system

The peak turbine discharge for the model with q_r constraint, which occurs between 11:00 and 12:00, is 36.87 m^3/s. The peak turbine discharge for the model without minimum flow constraint is 34.15 m^3/s and it occurs between 10:00 and 11:00. Correspondingly, as shown in the second row of Figure 4.6, peak $P_{g,2}$ is 19.35 MW while peak $P_{g,1}$ is 17.92 MW. In general, the high q_r required for the model with downstream flow restriction compels the OC to release more water consequently resulting in high $P_{g,2}$ generation.

An important comparative observation made when the proposed OC model is simulated with downstream flow constraint, q_r, is the differences in the decay rate of the water level in the dam. In Figure 4.7, $h_{out,2}$ and $h_{out,1}$ denote the change in water level of the dam in response to turbine discharge, q_o, for the case with and without q_r constraint respectively. In the second row of the figure, $h_{opt,2}$ and $h_{opt,1}$ are respectively, the net optimal change in water level of the dam for the case with and without q_r constraint. As shown in the first row of Figure 4.7, when operated without environmental flow restriction, the dam water level, $h_{out,1}$, would drop from the initial level of 300.0 to 288.6 m by the end of the control

horizon. However, when the HPP is operated with downstream environmental flow constraint, the dam water level, $h_{out,2}$ would fall from the initial level of 300.0 to 280.0 m. Correspondingly, the net optimal water level of the dam for the operation case with q_r constraint, $h_{opt,2}$, falls from the initial level of 300.0 to 294.2 m at the end of the control horizon. This contradicts with the optimisation case without q_r constraint where $h_{opt,1}$ rises to 302.3 m by end of day. Of interest to note is the rise in $h_{opt,1}$ to 302.3 m at the end of the control period because of the high net inflows, $q_{inflows}$, as compared to outflow, q_o, for the optimisation scenario without q_r constraint.

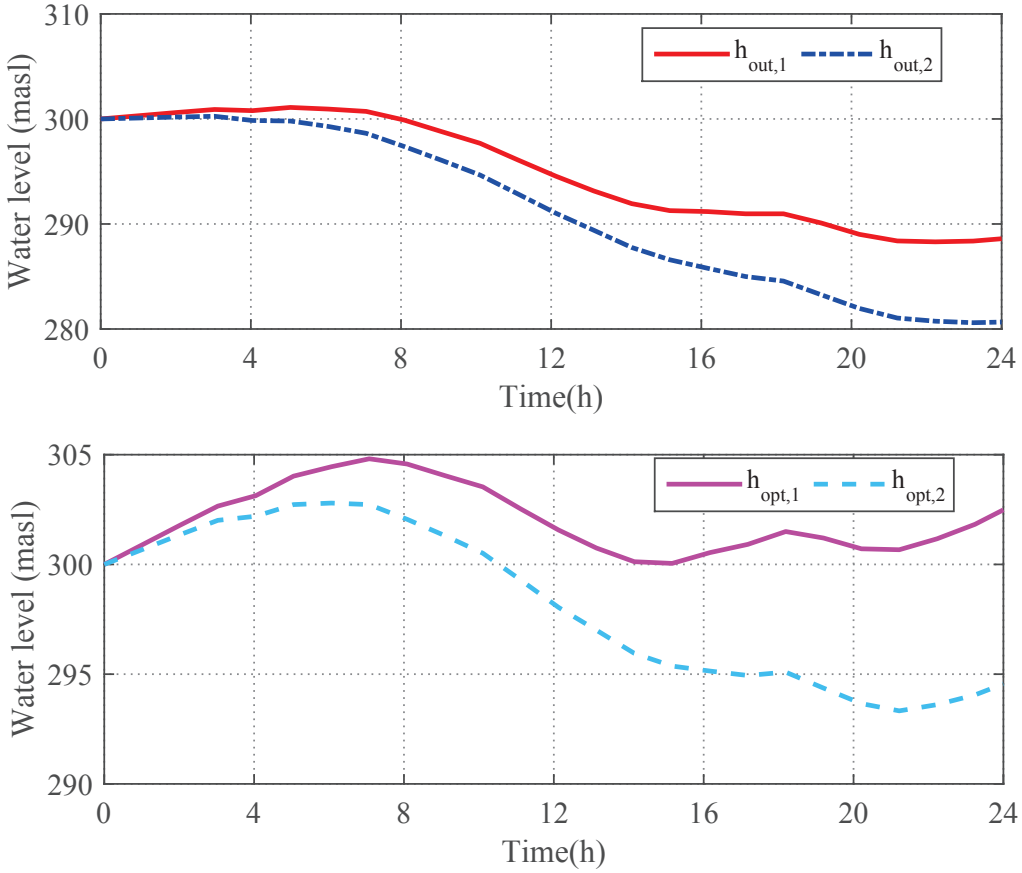

Figure 4.7. Decay rate of the reservoir under minimum flow constraint

The difference in the dam water level at the end of the day for the two cases, as shown in Figure 4.7, underscores the opportunity cost of environmental flow constraints to the operation of a HPP in terms of water economy. For the case with q_r constraint, the plant operator releases more water to meet the downstream flow requirements resulting in the high decay rate of the dam. For instance, at 16:00, the dam water level had risen to 300.4 m for the case without q_r constraint while it fell to a low of 295.2 m for the case with downstream flow constraint.

Another important operational aspect of the proposed OC model is the initial conditions and system dynamics of the re-regulation reservoir. Figure 4.8 shows the optimal change in water level of the re-regulation reservoir for the optimisation case without q_r constraint, $h_{r,opt-1}$ and for the case with q_r constraint, $h_{r,opt-2}$. As shown in Figure 4.8, despite the comparatively high initial point of 35.0 m for the case with q_r constraint,$h_{r,opt-2}$ decays to a minimum of 11.2 m at the end of the control horizon. This contrasts with the optimisation case without q_r constraint; as shown in the figure, $h_{r,opt-1}$ rises from the initial point of 15.0 to 34.55 m at the end of the day, implying that the net inflow from the powerhouse is higher than the combined reservoir outflows resulting in an increase in volume.

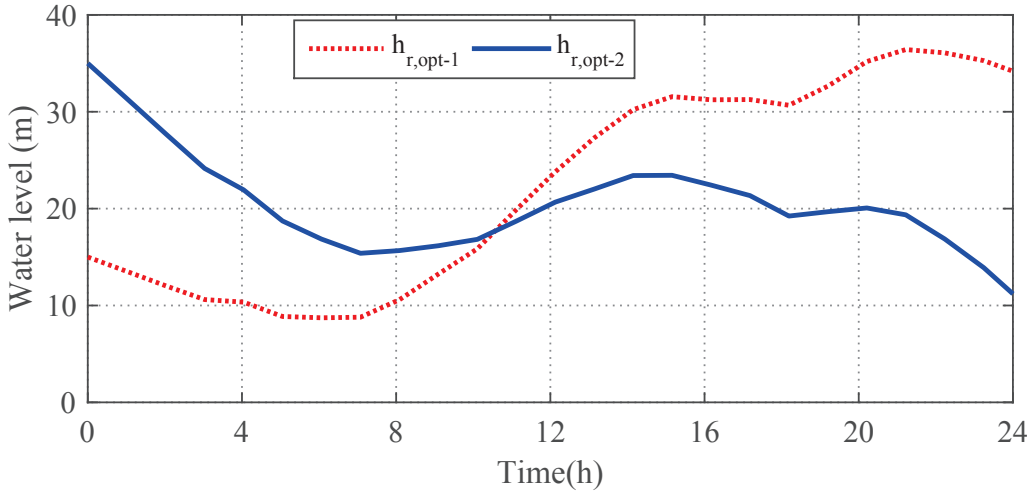

Figure 4.8. Change in water level of the re-regulation reservoir

The observable state dynamics of the re-regulation reservoir shown in Figure 4.8 underscores the importance of the initial conditions of the reservoir in ensuring un-interrupted downstream flow regimes as well as continuous pumping operation of the pumpback system over the given control horizon.

4.5.3.2 Power flows of the pumpback model with downstream flow constraints

Figure 4.9 shows the results of the effects of downstream discharge, q_r, constraints to the performance of the WEC and the HKEC systems of the proposed OC model with a pumpjack retrofit. As shown, the total HK power output, P_{HK}, varies in response to the changes in P_{hg} and P_{hk} throughout the control horizon. These results contrast with the results of the model without q_r constraint shown in Figure 4.4 in which the OC switches ON all the 12 installed HK generators, n_{hk_1} shown in Figure 4.10, to

generate a constant P_{HK} output of 3.03 MW throughout the control horizon. When q_r constraint is integrated in the OC policy of the HPP in the case study, the high turbine discharge, q_o, results in high $P_{g,2}$ as shown in Figure 4.6. This results in P_{ld} being met almost entirely by P_g and as a result, only a small supply of P_{hg} is required to meet the contractual load deficit. The high P_g caused by the high q_r constraint compels the OC to vary n_{hk-2} at each discrete time j to generate just enough P_{hg} and P_{hk} to meet the deterministic system load demand, P_{ld}, and pumping power demand unmet by the wind generator output, P_{hk}.

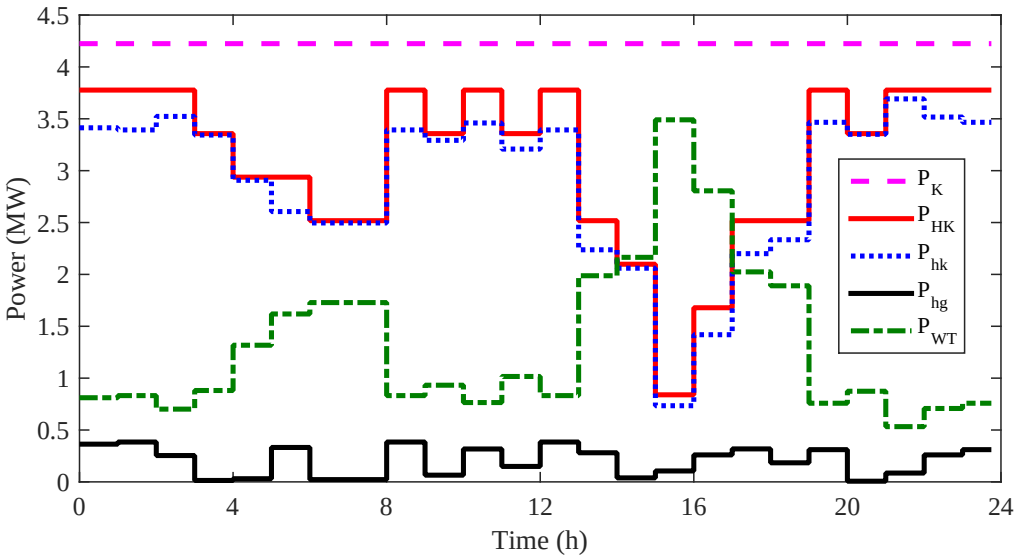

Figure 4.9. Effects of high downstream flow on HK-wind power flows

Figure 4.10 shows the results of the effects of q_r constraints to the optimal number of HK generators, n_{hk}, that can be operated at any given time, j. In the figure, n_{hk-1} and n_{hk-2} are respectively, the HK generators in parallel operation for the optimisation case without and with downstream flow, q_r, constraint. As shown, for the optimisation case without q_r constraint, the OC switches ON all the 12 installed HK generators to maximise the use of P_{hg} in meeting P_{ld}. A different scenario is observed when the model is simulated with q_r constraint: The OC varies n_{hk-2} to produce just enough P_{hk} and P_{hg} to offset the pumping power deficit and the unmet system load respectively. For instance, between 00:00 and 03:00, the OC switches ON nine HK generators to produce just enough HK power for meeting the system deficit. An increase in wind generation, P_{WT}, between 03:00 and 08:00 results in a decrease in P_{hk} and correspondingly, the OC adjusts n_{hk-2} from nine to eight and subsequently to six. The high P_{WT} between 15:00 and 16:00 results in a sharp decrease in P_{hk} with a corresponding

decrease in n_{hk-2} from five to two. Subsequently, the OC varies n_{hk-2} in response to the changes in P_{hk} and P_{hg} for the remainder of the control horizon.

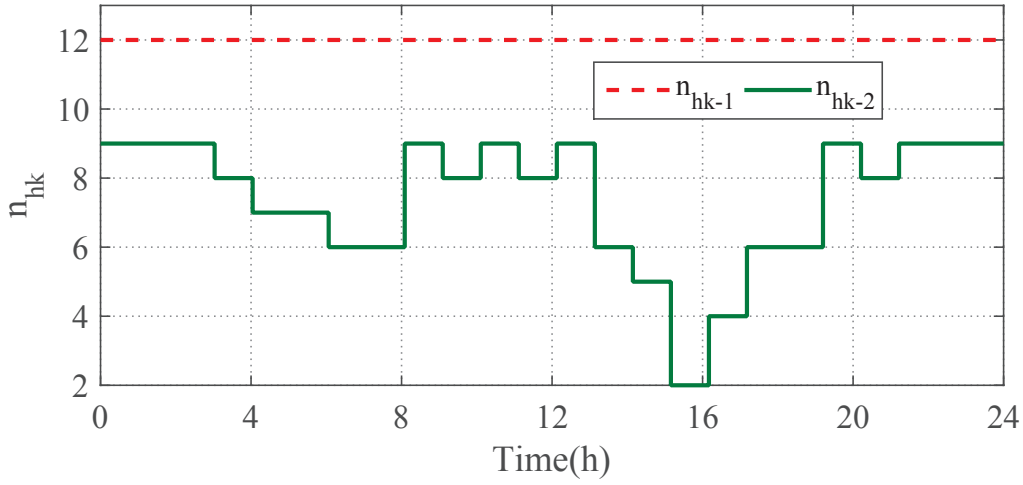

Figure 4.10. Effects of minimum ecological flow rate to the HKEC system

Figure 4.11 shows the results of the effects of downstream flow constraints to the HK power exported to the grid, P_{hg}. In the figure, $P_{hg,1}$ and $P_{hg,2}$ are respectively, the excess HK power exported to the grid when the OC model is operated without and with q_r constraints. As shown, $P_{hg,1} > P_{hg,2}$ throughout the control horizon. Because of the high q_r^{min} for the model with q_r constraint, the OC is compelled to increase the turbine discharge, q_o, resulting in high P_g generation, shown as $P_{g,2}$ in Figure 4.6. Consequently, the system load, P_{ld}, is almost entirely met by P_g and as a result, the model requires only a small quantity of P_{hg}, denoted by $P_{hg,2}$ in Figure 4.11, to meet the system load deficit. For instance, between 15:15 and 16:15, $P_{hg,1}$ supplied 4.3 MW to meet the system's contractual demand of 13.5 MW. In the same period, the OC for the model with q_r constraint supplied just 0.11 MW of $P_{hg,2}$ to cover the same demand deficit. In this chapter, the decrease in P_{hg} in response to an increase in q_r underscores the opportunity costs of environmental constraints to the economic performance of the model. The numerical differences in the total HK energy supplied to meet the system load, E_{hg}, shown in Table 4.4 and Table 4.5 underscores the measure of the opportunity cost of the downstream flow constraints.

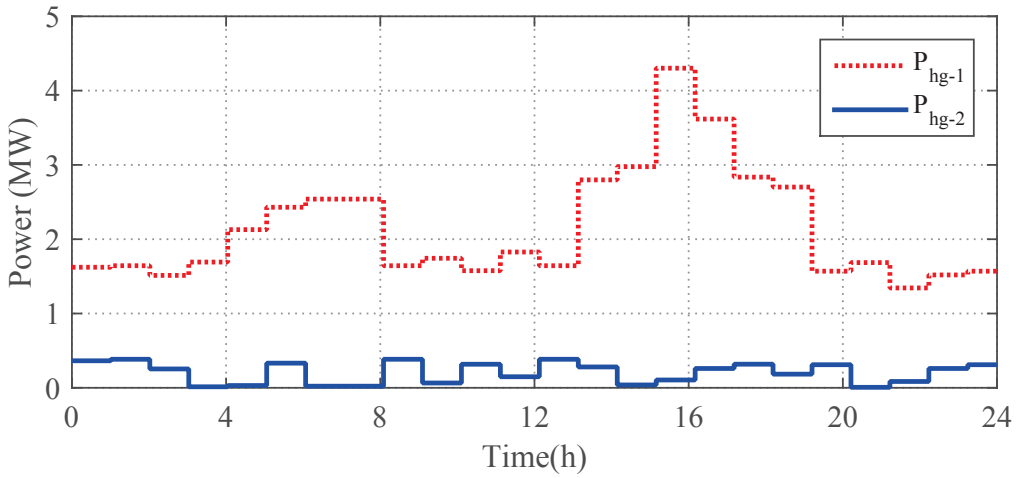

Figure 4.11. Effects of ecological flow constraints on P_{hg} flows

Table 4.5 shows the daily energy output of the model simulated with minimum q_r constraint. As shown, the total energy output of the HKEC system is 74.28 MWh, which is less than the 120.86 MWh generated by the model without q_r constraint shown in Table 4.4. If the pumpback model of section 4.5.2 is taken as the comparative baseline, it is seen that raising the minimum q_r to 17.0 m^3/s results in 38.54% decrease in the energy yield of the HKEC system. In the same vein, subjecting the hydropower reservoir to a high q_r^{min} results in an E_g output of 320.47 MWh, which is higher than 273.89 MWh of E_g generated by the model without minimum q_r constraint. This translates to 17.00% increase in hydropower generation from the hydro reservoir.

Table 4.5. Optimal system energy flows of the model with downstream flow constraint

E_{ld} (MWh)	E_g (MWh)	E_{HK} (MWh)	E_{hg} (MWh)	E_{hk} (MWh)	E_{WT} (MWh)	E_K(MWh)
325.35	320.47	74.28	4.88	69.40	31.99	101.39

Similarly, comparison of the results of Table 4.4 and Table 4.5 shows that increasing q_r^{min} to 17.0 m^3/s results in a change in E_{hg} from 51.46 MWh to 4.88 MWh which translates to 90.52% decrease in the amount of hydrokinetic energy supplied to meet the committed grid load.

4.6 SUMMARY

This chapter presented an optimal control model for assessing the effects of the pumpback operation and downstream flow constraints to the performance of a hydropower plant in dry seasons. The objective of the study was to use the available water to meet deterministic but time-varying system load over a 24 h control horizon. Three different optimisation scenarios were studied: the baseline case; the case with wind-hydrokinetic-powered pumpback capabilities; and the operation scenario incorporating the pumpback operation and the downstream ecological flow constraints. Simulation results based on a hypothetical case study showed the potential of the model with pumpback capabilities to reduce the daily amount of water allocation for hydropower generation.

Similarly, the results of the second operation scenario showed that incorporation of the wind-HK-powered pumpback operation in the optimal control of the plant in the case study reduces the energy demand from the hydro reservoir for meeting the system load by 15.82%, which is a positive performance indicator that conserves the reservoir water. This performance was caused by the exportation of the surplus hydrokinetic energy to the grid to meet the system load.

Incorporation of the downstream flow constraints in the optimal control policy of the third optimisation scenario resulted in 38.54% decrease in the energy output of the hydrokinetic systems; which is a negative performance index in this chapter considering that the hydrokinetic energy is free energy extracted from the downstream water flow that can be used to offset reliance on hydro reservoir generation. The decrease in the energy yield of the hydrokinetic system is a measure of the opportunity cost associated with environmental restrictions to the operation of a hydropower plant. In general, using the amount of hydrokinetic energy generation in the hybrid system as the performance index of the proposed model, the system performance presented in this chapter showed that incorporation of the downstream flow constraint in the operation policy of a hydropower plant has an opportunity cost of reduced utilisation of the freely available hydrokinetic energy.

CHAPTER 5 CONCLUSION

This dissertation developed two optimal control models for maximising the energy output of a conventional hydropower plant in dry season. Many hydropower plants in drought-prone regions such as Southern Africa experience low power output in dry seasons due to low water levels in the dams. Pumpback operation to maintain a high reservoir water level for optimal hydropower generation is presented in this dissertation. In the first optimal control model presented in chapter 3, a cascaded pumping system powered by the on-site hydrokinetic energy resource is proposed. The objective of the model is to meet the contractual grid obligations at minimal pumping energy demand over a 24 h control horizon. The problem is formulated as a discrete multi-objective optimisation function to simultaneously; minimise the grid pumping power demand; minimise wear and tear associated with the switching frequency of the cascaded pumps; maximise restoration of the reservoir volume through pumpback operation, and maximise the use of on-site generated hydrokinetic power for pumping operation. To validate the performance advantages of a cascaded pumping system over the classical pumped storage system, the proposed optimal control is applied to a suitable case study. Simulation results demonstrate the potential of a cascaded pumpback system to minimise the overall pumping energy demand of the control system over a 24 h control horizon by alternating the switching of the two pumps.

The second optimal control model, presented in chapter 4 investigates the effects of downstream environmental flow constraints to the performance of a conventional hydropower plant with the wind-hydrokinetic powered pumpback operation. The objective of the model is to optimise the economic value of the available water in meeting contracted consumer load. Three different optimisation scenarios were studied in this optimal control model presented in chapter 4: The baseline case; the case with the wind-hydrokinetic-powered pumpback operation; and the case integrating both pumpback capabilities and downstream flow constraints.

For the second and the third optimisation scenarios, a downstream re-regulation reservoir for temporary storage for pumping continuity as well as to re-regulate the rate of water release back into the river is incorporated in the plant's operation policy. The operation strategy was for the optimal control to meet the pumping power demand primarily by the wind power supplemented by the hydrokinetic power, while at the same time maximise the use of surplus hydrokinetic power in meeting the plant's contractual obligations.

Simulation results based on a suitable case study showed the potential of the model with a wind-hydrokinetic -powered pumpback retrofit to reduce the daily amount of water needed for the hydropower plant to meet its contractual obligations. This was occasioned by recycling of the downstream discharged water to increase its economic value as well as exportation of the surplus hydrokinetic power to the grid to offset a part of the system demand.

Simulation results of the third optimisation scenario showed that integration of environmental flow constraints in the optimal control policy of a hydropower plant reduces the hydrokinetic energy yield by 38.54%, which in this dissertation is a measure of the opportunity cost of environmental constraints: Hydrokinetic energy is considered a free energy resource that can be utilised optimally to minimise reliance on the hydro reservoir generated power.

5.1 CONTRIBUTION

In summary, this dissertation presented optimal control strategies for improving the economic value of the available reservoir water for hydropower generation in dry seasons. The cascaded pumpback system presented in chapter 3 is shown to reduce the pumping energy demand over a 24 h control horizon as compared to the classical PS model. The results of the first model, presented in chapter 3, also showed that the optimal control executed pumpback operation only during the dry season. That is, the pumpback system was OFF throughout the control horizon in the rainy season with sufficient water level in the dam to cover the plant's contractual obligations. The results of the second model, presented in chapter 4, showed that integrating environmental flow constraints in the optimal control policy of a hydropower plant reduces its economic performance as evidenced in the reduction of the generation of the free hydrokinetic power. Both the models mark the first attempt at using alternative renewable on-site wind and hydrokinetic power for pumping operation as applied in hydropower systems.

5.2 RECOMMENDATIONS AND FUTURE RESEARCH

1. The current work is based on the open-loop optimal control strategy of a hydropower plant with a pumpback retrofit. An interesting future research direction will be the application of the closed-loop optimal control strategies such as model predictive control (MPC) which have better performance in handling system uncertainties such as changes in system load, in-stream flow variability and variations in wind speed. The application of closed loop control strategies could improve the performance of the hydropower system in question.

2. In the current work, the proposed optimal control models are analysed for a 24 h control period with a constant in-stream river flow. Future research can be the extension of the optimisation horizon to a longer period, such as 12 months, to take into account seasonal variations in in-stream flows as a source of uncertainty.

3. In this dissertation, economic analysis of the proposed optimal control models is not considered. Future research work should consider life cycle cost analysis of the system to validate the economic feasibility of the proposed models.

4. The models proposed in the current work considers constant speed pumping; the pumps are assumed to work at their full rated capacity whenever in operation. Therefore, future research into the application of variable speed pumping is recommended.

5. In the current work, the objective of the optimal control is for the hydropower plant to meet deterministic system load which does not optimise the revenue generation of the facility since the hourly generation levels are capped. A future research should consider a non-deterministic HPP in a pool based market with time-varying energy prices, such as time-of-use (TOU) tariff structure, to maximise the revenue yield of the system.

REFERENCES

[1] M. T. van Vliet, D. Wiberg, S. Leduc, and K. Riahi, "Power-generation system vulnerability and adaptation to changes in climate and water resources," *Nature Climate Change*, vol. 6, pp. 375–380, 2016.

[2] G. Harrison, H. Whittington, and A. Wallace, "Sensitivity of hydropower performance to climate change," *International Journal of Power & Energy Systems*, vol. 26, no. 1, pp. 42–48, 2006.

[3] G. Ravazzani, F. Dalla Valle, L. Gaudard, T. Mendlik, A. Gobiet, and M. Mancini, "Assessing climate impacts on hydropower production: The case of the Toce River Basin," *Climate*, vol. 4, no. 2, 2016.

[4] G. P. Harrison and H. Whittington, "Vulnerability of hydropower projects to climate change," *IEE Proceedings-Generation, Transmission and Distribution*, vol. 149, no. 3, pp. 249–255, 2002.

[5] S. Niu and M. Insley, "On the economics of ramping rate restrictions at hydropower plants: Balancing profitability and environmental cost," *Energy Economics*, vol. 39, pp. 39–52, 2013.

[6] Q. Chen, X. Zhang, Y. Chen, Q. Li, L. Qiu, and M. Liu, "Downstream effects of a hydropeaking dam on ecohydrological conditions at subdaily to monthly time scales," *Ecological Engineering*, vol. 77, pp. 40–50, 2015.

[7] R. Sternberg, "Damming the river: A changing perspective on altering nature," *Renewable and Sustainable Energy Reviews*, vol. 10, no. 3, pp. 165–197, 2006.

[8] I. Guisandez, J. I. Pérez-Díaz, and J. R. Wilhelmi, "Approximate formulae for the assessment of the long-term economic impact of environmental constraints on hydropeaking," *Energy*, vol. 112, pp. 629–641, 2016.

[9] I. Guisández, J. I. Pérez-Díaz, and J. R. Wilhelmi, "Assessment of the economic impact of environmental constraints on annual hydropower plant operation," *Energy Policy*, vol. 61, pp. 1332–1343, 2013.

[10] P. M. Jacovkis, H. Gradowczyk, A. M. Freisztav, and E. G. Tabak, "A linear programming approach to water-resources optimization," *Zeitschrift für Operations Research*, vol. 33, no. 5, pp. 341–362, 1989.

[11] B. K. Edwards, S. J. Flaim, and R. E. Howitt, "Optimal provision of hydroelectric power under environmental and regulatory constraints," *Land Economics*, pp. 267–283, 1999.

[12] B. Chatterjee, R. E. Howitt, and R. J. Sexton, "The optimal joint provision of water for irrigation and hydropower," *Journal of Environmental Economics and Management*, vol. 36, no. 3, pp. 295 – 313, 1998.

[13] E. Kondili, J. Kaldellis, and C. Papapostolou, "A novel systemic approach to water resources optimisation in areas with limited water resources," *Desalination*, vol. 250, no. 1, pp. 297–301, 2010.

[14] J. Wang, "Short-term generation scheduling model of Fujian hydro system," *Energy Conversion and Management*, vol. 50, no. 4, pp. 1085–1094, 2009.

[15] A. Helseth, M. Fodstad, and B. Mo, "Optimal medium-term hydropower scheduling considering energy and reserve capacity markets," *IEEE Transactions on Sustainable Energy*, vol. 7, no. 3, pp. 934–942, 2016.

[16] G. Pritchard, A. B. Philpott, and P. J. Neame, "Hydroelectric reservoir optimization in a pool market," *Mathematical Programming*, vol. 103, no. 3, pp. 445–461, 2005.

[17] E. Gil, J. Bustos, and H. Rudnick, "Short-term hydrothermal generation scheduling model using a genetic algorithm," *IEEE Transactions on Power Systems*, vol. 18, no. 4, pp. 1256–1264, 2003.

[18] M. A. Olivares, "Optimal hydropower reservoir operation with environmental requirements," Ph.D. dissertation, UNIVERSITY OF CALIFORNIA DAVIS, 2008.

[19] J. I. Pérez-Díaz, R. Millan, D. Garcia, I. Guisandez, and J. Wilhelmi, "Contribution of re-regulation reservoirs considering pumping capability to environmentally friendly hydropower operation," *Energy*, vol. 48, no. 1, pp. 144–152, 2012.

[20] W. Li, J. Huang, G. Li, and Z. Wang, "Research on optimizing operation of the single reservoir of hybrid pumped storage power station," in *2011 4th International Conference on Electric Utility Deregulation and Restructuring and Power Technologies (DRPT)*. Weihai, China: IEEE, 2011, pp. 1389–1394.

[21] G. Zhao and M. Davison, "Optimal control of hydroelectric facility incorporating pump storage," *Renewable Energy*, vol. 34, no. 4, pp. 1064–1077, 2009.

[22] J. I. Pérez-Díaz and J. R. Wilhelmi, "Assessment of the economic impact of environmental constraints on short-term hydropower plant operation," *Energy Policy*, vol. 38, no. 12, pp. 7960–7970, 2010.

[23] E. D. Castronuovo and J. P. Lopes, "On the optimization of the daily operation of a wind-hydro power plant," *IEEE Transactions on Power Systems*, vol. 19, no. 3, pp. 1599–1606, 2004.

[24] C. Bueno and J. A. Carta, "Wind powered pumped hydro storage systems, a means of increasing the penetration of renewable energy in the Canary Islands," *Renewable and Sustainable Energy Reviews*, vol. 10, no. 4, pp. 312–340, 2006.

[25] J. S. Anagnostopoulos and D. E. Papantonis, "Pumping station design for a pumped-storage wind-hydro power plant," *Energy Conversion and Management*, vol. 48, no. 11, pp. 3009–3017, 2007.

[26] E. Barbour, I. G. Wilson, J. Radcliffe, Y. Ding, and Y. Li, "A review of pumped hydro energy storage development in significant international electricity markets," *Renewable and Sustainable Energy Reviews*, vol. 61, pp. 421–432, 2016.

[27] P. Kanakasabapathy and K. S. Swarup, "Evolutionary tristate PSO for strategic bidding of pumped-storage hydroelectric plant," *IEEE Transactions on Systems, Man, and Cybernetics, Part C (Applications and Reviews)*, vol. 40, no. 4, pp. 460–471, 2010.

[28] F. C. Figueiredo and P. C. Flynn, "Using diurnal power price to configure pumped storage," *IEEE Transactions on Energy Conversion*, vol. 21, no. 3, pp. 804–809, 2006.

[29] J. D. Hunt, M. A. V. Freitas, and A. O. P. Junior, "Enhanced-pumped-storage: Combining pumped-storage in a yearly storage cycle with dams in cascade in Brazil," *Energy*, vol. 78, pp. 513 – 523, 2014.

[30] N. Kishor, R. Saini, and S. Singh, "A review on hydropower plant models and control," *Renewable and Sustainable Energy Reviews*, vol. 11, no. 5, pp. 776–796, 2007.

[31] A. Acakpovi, E. B. Hagan, and F. X. Fifatin, "Review of hydropower plant models," *International Journal of Computer Applications*, vol. 108, no. 18, 2014.

[32] D. Ramey and J. W. Skooglund, "Detailed hydrogovernor representation for system stability studies," *IEEE Transactions on Power Apparatus and Systems*, no. 1, pp. 106–112, 1970.

[33] A. Arce, T. Ohishi, and S. Soares, "Optimal dispatch of generating units of the Itaipú hydroelectric plant," *IEEE Transactions on Power Systems*, vol. 17, no. 1, pp. 154–158, 2002.

[34] M. Güney and K. Kaygusuz, "Hydrokinetic energy conversion systems: A technology status review," *Renewable and Sustainable Energy Reviews*, vol. 14, no. 9, pp. 2996 – 3004, 2010.

[35] M. Khan, M. Iqbal, and J. Quaicoe, "River current energy conversion systems: Progress, prospects and challenges," *Renewable and Sustainable Energy Reviews*, vol. 12, no. 8, pp. 2177–2193, 2008.

[36] M. Khan, G. Bhuyan, M. Iqbal, and J. Quaicoe, "Hydrokinetic energy conversion systems and assessment of horizontal and vertical axis turbines for river and tidal applications: A technology status review," *Applied Energy*, vol. 86, no. 10, pp. 1823–1835, 2009.

[37] M. Anyi and B. Kirke, "Evaluation of small axial flow hydrokinetic turbines for remote communities," *Energy for Sustainable Development*, vol. 14, no. 2, pp. 110–116, 2010.

[38] M. R. Patel, *Wind and Solar Power Systems: Design, Analysis, and Operation*. New York, USA: Taylor & Francis, 2005.

[39] T. Burton, D. Sharpe, N. Jenkins, and E. Bossanyi, *Wind Energy Handbook*. New York: John Wiley & Sons, 2001.

[40] H. Tazvinga, "Energy optimisation and management of off-grid hybrid power supply systems," Ph.D. dissertation, UNIVERSITY OF PRETORIA, 2015.

[41] L. Lago, F. Ponta, and L. Chen, "Advances and trends in hydrokinetic turbine systems," *Energy for Sustainable Development*, vol. 14, no. 4, pp. 287–296, 2010.

[42] A. P. Engelbrecht, *Computational Intelligence: An Introduction*, 2nd ed. West Sussex, England: John Wiley & Sons, 2007.

[43] J. W. Labadie, "Optimal operation of multireservoir systems: state-of-the-art review," *Journal of Water Resources Planning and Management*, vol. 130, no. 2, pp. 93–111, 2004.

[44] A. Afshar, F. Sharifi, and M. Jalali, "Non-dominated archiving multi-colony ant algorithm for multi-objective optimization: Application to multi-purpose reservoir operation," *Engineering Optimization*, vol. 41, no. 4, pp. 313–325, 2009.

[45] J. M. González, M. A. Olivares, J. Medellín-Azuara, R. Moreno, and G. Marques, "Multi-purpose reservoir operation: A tradeoff analysis between hydropower generation and irrigated agriculture using hydro-economic models," in *World Environmental and Water Resources Congress 2016*. West Palm Beach, Florida: American Society of Civil Engineers, 2016, pp. 241–250.

[46] L. Hongling, J. Chuanwen, and Z. Yan, "A review on risk-constrained hydropower scheduling in deregulated power market," *Renewable and Sustainable Energy Reviews*, vol. 12, no. 5, pp. 1465–1475, 2008.

[47] H. Yan, P. B. Luh, X. Guan, and P. M. Rogan, "Scheduling of hydrothermal power systems," *IEEE Transactions on Power Systems*, vol. 8, no. 3, pp. 1358–1365, 1993.

[48] J.-H. Yoo, "Maximization of hydropower generation through the application of a linear programming model," *Journal of Hydrology*, vol. 376, no. 1, pp. 182–187, 2009.

[49] J. García-González, E. Parrilla, and A. Mateo, "Risk-averse profit-based optimal scheduling of a hydro-chain in the day-ahead electricity market," *European Journal of Operational Research*, vol. 181, no. 3, pp. 1354–1369, 2007.

[50] A. J. Conejo, J. M. Arroyo, J. Contreras, and F. A. Villamor, "Self-scheduling of a hydro producer in a pool-based electricity market," *IEEE Transactions on Power Systems*, vol. 17, no. 4, pp. 1265–1272, 2002.

[51] J. Catalão, H. Pousinho, and V. Mendes, "Scheduling of head-dependent cascaded hydro systems: Mixed-integer quadratic programming approach," *Energy Conversion and Management*, vol. 51, no. 3, pp. 524–530, 2010.

[52] O. Nilsson and D. Sjelvgren, "Mixed-integer programming applied to short-term planning of a hydro-thermal system," *IEEE Transactions on Power Systems*, vol. 11, no. 1, pp. 281–286, 1996.

[53] I. Farhat and M. El-Hawary, "Optimization methods applied for solving the short-term hydro-thermal coordination problem," *Electric Power Systems Research*, vol. 79, no. 9, pp. 1308–1320, 2009.

[54] H. Brännlund, J. Bubenko, D. Sjelvgren, and N. Andersson, "Optimal short term operation planning of a large hydrothermal power system based on a nonlinear network flow concept," *IEEE Transactions on Power Systems*, vol. 1, no. 4, pp. 75–81, 1986.

[55] R. C. Zambon, M. T. Barros, J. E. G. Lopes, P. S. Barbosa, A. L. Francato, and W. W.-G. Yeh, "Optimization of large-scale hydrothermal system operation," *Journal of Water Resources Planning and Management*, vol. 138, no. 2, pp. 135–143, 2011.

[56] R. J. Pinto, C. T. Borges, and M. E. Maceira, "An efficient parallel algorithm for large scale hydrothermal system operation planning," *IEEE Transactions on Power Systems*, vol. 28, no. 4, pp. 4888–4896, 2013.

[57] R.-H. Liang, "A noise annealing neural network for hydroelectric generation scheduling with pumped-storage units," *IEEE Transactions on Power Systems*, vol. 15, no. 3, pp. 1008–1013, 2000.

[58] N. Lu, J. H. Chow, and A. A. Desrochers, "Pumped-storage hydro-turbine bidding strategies in a competitive electricity market," *IEEE Transactions on Power Systems*, vol. 19, no. 2, pp. 834–841, 2004.

[59] M. Beaudin, H. Zareipour, A. Schellenberglabe, and W. Rosehart, "Energy storage for mitigating the variability of renewable electricity sources: An updated review," *Energy for Sustainable Development*, vol. 14, no. 4, pp. 302–314, 2010.

[60] A. Borghetti, C. D'Ambrosio, A. Lodi, and S. Martello, "An MILP approach for short-term hydro scheduling and unit commitment with head-dependent reservoir," *IEEE Transactions on Power Systems*, vol. 23, no. 3, pp. 1115–1124, 2008.

[61] X. Guan, P. B. Luh, H. Yen, and P. Rogan, "Optimization-based scheduling of hydrothermal power systems with pumped-storage units," *IEEE Transactions on Power Systems*, vol. 9, no. 2, pp. 1023–1031, 1994.

[62] J. J. Shaw, R. F. Gendron, and D. P. Bertsekas, "Optimal scheduling of large hydrothermal power systems," *IEEE Transactions on Power Apparatus and Systems*, vol. PAS-104, no. 2, pp. 286–294, 1985.

[63] A. I. Cohen and S. Wan, "An algorithm for scheduling a large pumped storage plant," *IEEE Transactions on Power Apparatus and Systems*, vol. PAS-104, no. 8, pp. 2099–2104, 1985.

[64] K. K. Mandal, M. Basu, and N. Chakraborty, "Particle swarm optimization technique based short-term hydrothermal scheduling," *Applied Soft Computing*, vol. 8, no. 4, pp. 1392–1399, 2008.

[65] S. Orero and M. Irving, "A genetic algorithm modelling framework and solution technique for short term optimal hydrothermal scheduling," *IEEE Transactions on Power Systems*, vol. 13, no. 2, pp. 501–518, 1998.

[66] K. E. Lansey and K. Awumah, "Optimal pump operations considering pump switches," *Journal of Water Resources Planning and Management*, vol. 120, no. 1, pp. 17–35, 1994.

[67] X. Zhuan and X. Xia, "Optimal operation scheduling of a pumping station with multiple pumps," *Applied Energy*, vol. 104, pp. 250–257, 2013.

[68] Y. Tang, G. Zheng, and S. Zhang, "Optimal control approaches of pumping stations to achieve energy efficiency and load shifting," *International Journal of Electrical Power & Energy Systems*, vol. 55, pp. 572–580, 2014.

[69] E. M. Wanjiru, L. Zhang, and X. Xia, "Model predictive control strategy of energy-water management in urban households," *Applied Energy*, vol. 179, pp. 821–831, 2016.

[70] F. Wamalwa, S. Sichilalu, and X. Xia, "Optimal control of conventional hydropower plant retrofitted with a cascaded pumpback system powered by an on-site hydrokinetic system," *Energy Conversion and Management*, vol. 132, pp. 438–451, 2017.

[71] M. Singh and A. Chanldra, "Modelling and control of isolated micro-hydro power plant with battery storage system," in *National Power Electronic Conference*, 2010.

[72] M. Sechilariu, B. C. Wang, and F. Locment, "Supervision control for optimal energy cost management in dc microgrid: Design and simulation," *International Journal of Electrical Power*

& Energy Systems, vol. 58, pp. 140–149, 2014.

[73] E. M. Wanjiru and X. Xia, "Energy-water optimization model incorporating rooftop water harvesting for lawn irrigation," *Applied Energy*, vol. 160, pp. 521–531, 2015.

[74] T. Mathaba, X. Xia, and J. Zhang, "Analysing the economic benefit of electricity price forecast in industrial load scheduling," *Electric Power Systems Research*, vol. 116, pp. 158–165, 2014.

[75] T. Achterberg, "Scip: solving constraint integer programs," *Mathematical Programming Computation*, vol. 1, no. 1, pp. 1–41, 2009.

[76] R. Kimwaga and S. Nkandi, "Evaluation of the suitability of Pangani Falls redevelopment (hydro power) project in Pangani River Basin, Tanzania: An IWRM Approach," 2007.

[77] K. Luteganya and S. Kizzy, "Hydroelectric power modelling study. Pangani River Basin flow assessment," January 2009.

[78] S. M. Sichilalu and X. Xia, "Optimal energy control of grid tied pv–diesel–battery hybrid system powering heat pump water heater," *Solar Energy*, vol. 115, pp. 243–254, 2015.

[79] J. Catalao, H. Pousinho, and J. Contreras, "Optimal hydro scheduling and offering strategies considering price uncertainty and risk management," *Energy*, vol. 37, no. 1, pp. 237–244, 2012.

[80] D. Connolly, H. Lund, P. Finn, B. V. Mathiesen, and M. Leahy, "Practical operation strategies for pumped hydroelectric energy storage (PHES) utilising electricity price arbitrage," *Energy Policy*, vol. 39, no. 7, pp. 4189–4196, 2011.

[81] M. Fette, C. Weber, A. Peter, and B. Wehrli, "Hydropower production and river rehabilitation: A case study on an Alpine River," *Environmental Modeling & Assessment*, vol. 12, no. 4, pp. 257–267, 2007.

[82] P. H. Gleick, "Environmental consequences of hydroelectric development: the role of facility size and type," *Energy*, vol. 17, no. 8, pp. 735–747, 1992.

[83] J. Korman and S. E. Campana, "Effects of hydropeaking on nearshore habitat use and growth of age-0 rainbow trout in a large regulated river," *Transactions of the American Fisheries Society*, vol. 138, no. 1, pp. 76–87, 2009.

[84] T. Meile, J. L. Boillat, and A. Schleiss, "Hydropeaking indicators for characterization of the Upper-Rhone River in Switzerland," *Aquatic Sciences*, vol. 73, no. 1, pp. 171–182, 2011.

[85] R. Mehta and S. K. Jain, "Optimal operation of a multi-purpose reservoir using neuro-fuzzy technique," *Water Resources Management*, vol. 23, no. 3, pp. 509–529, 2009.

[86] B. D. Richter and G. A. Thomas, "Restoring environmental flows by modifying dam operations," *Ecology and Society*, vol. 12, no. 1, 2007.

[87] W. Tang, Z. Li, M. Qiang, S. Wang, and Y. Lu, "Risk management of hydropower development in China," *Energy*, vol. 60, pp. 316–324, 2013.

[88] G. Berland, T. Nickelsen, J. Heggenes, F. Okland, E. Thorstad, and J. Halleraker, "Movement of wild atlantic salmon parr in relation to peaking flows below a hydropower station," *River Resource Application*, vol. 20, no. 8, pp. 957–966, 2004.

[89] M. J. Bradford, G. C. Taylor, J. A. Allan, and P. S. Higgins, "An experimental study of the stranding of juvenile coho salmon and rainbow trout during rapid flow decreases under winter conditions," *North American Journal of Fisheries Management*, vol. 15, no. 2, pp. 473–479, 1995.

[90] M. C. Bruno, B. Maiolini, M. Carolli, and L. Silveri, "Impact of hydropeaking on hyporheic invertebrates in an Alpine stream (Trentino, Italy)," *International Journal of Limnology*, vol. 45, no. 3, pp. 157–170, 2009.

[91] S. Saltveit, J. Halleraker, J. Arnekleiv, and A. Harby, "Field experiments on stranding in juvenile Atlantic salmon (Salmo salar) and brown trout (Salmo trutta) during rapid flow decreases caused by hydropeaking," *Regulated Rivers: Research & Management*, vol. 17, no. 4-5, pp. 609–622, 2001.

[92] O. Moog, "Quantification of daily peak hydropower effects on aquatic fauna and management to minimize environmental impacts," *Regulated Rivers: Research & Management*, vol. 8, no. 1-2, pp. 5–14, 1993.

[93] S. E. Bunn and A. H. Arthington, "Basic principles and ecological consequences of altered flow regimes for aquatic biodiversity," *Environmental Management*, vol. 30, no. 4, pp. 492–507, 2002.

[94] S. Ashok, "Optimised model for community-based hybrid energy system," *Renewable Energy*, vol. 32, no. 7, pp. 1155–1164, 2007.

[95] C. Bueno and J. Carta, "Technical–economic analysis of wind-powered pumped hydrostorage systems. Part I: model development," *Solar Energy*, vol. 78, no. 3, pp. 382–395, 2005.

[96] S. Sichilalu, H. Tazvinga, and X. Xia, "Optimal control of a fuel cell/wind/pv/grid hybrid system with thermal heat pump load," *Solar Energy*, vol. 135, pp. 59–69, 2016.

ADDENDUM A CHAPTER 3 DETAILED ALGORITHM FORMULATION

A.1 EQUALITY MATRICES

Equation (3.19) constitutes a sparse matrix $\mathbf{A_{eq1}}$, given in equation (A.1) and vector $\mathbf{b_{eq1}}$ shown in equation (A.2):

$$\mathbf{A_{eq1}} = \begin{bmatrix} 0 \cdots 0 & 0 \cdots 0 & 0 \cdots 0 & \frac{9.81\eta_m\eta_e h_o}{1000} \cdots 0 & 0 \cdots 0 & 0 \cdots 0 & 1 \cdots 0 & 0 \cdots 0 & 0 \cdots 0 \\ \vdots \ddots \vdots & \vdots \ddots \vdots & \vdots \ddots \vdots & \vdots \ddots \vdots & \vdots \ddots \vdots & \vdots \ddots \vdots & \vdots \ddots \vdots & \vdots \ddots \vdots & \vdots \ddots \vdots \\ 0 \cdots 0 & 0 \cdots 0 & 0 \cdots 0 & 0 \cdots \frac{9.81\eta_m\eta_e h_o}{1000} & 0 \cdots 0 & 0 \cdots 0 & 0 \cdots 1 & 0 \cdots 0 & 0 \cdots 0 \end{bmatrix}_{N\times 9N} . \tag{A.1}$$

$$\mathbf{b_{eq1}} = \begin{bmatrix} P_{ld,1} \\ \vdots \\ P_{ld,N} \end{bmatrix}_{N\times 1} . \tag{A.2}$$

Similarly, the matrix $\mathbf{A_{eq2}}$ shown in equation (A.3) and vector $\mathbf{b_{eq3}}$ shown in equation (A.4) are constituted from equality constraint (3.21) for the pump power balance.

$$\mathbf{A_{eq2}} = \begin{bmatrix} -P_{K1} \cdots 0 & -P_{K2} \cdots 0 & 0 \cdots 0 & 0 \cdots 0 & 1 \cdots 0 & 1 \cdots 0 & 0 \cdots 0 & 0 \cdots 0 & 0 \cdots 0 \\ \vdots \ddots \vdots & \vdots \ddots \vdots & \vdots \ddots \vdots & \vdots \ddots \vdots & \vdots \ddots \vdots & \vdots \ddots \vdots & \vdots \ddots \vdots & \vdots \ddots \vdots & \vdots \ddots \vdots \\ 0 \cdots -P_{K1} & 0 \cdots -P_{K2} & 0 \cdots 0 & 0 \cdots 0 & 0 \cdots 1 & 0 \cdots 1 & 0 \cdots 0 & 0 \cdots 0 & 0 \cdots 0 \end{bmatrix}_{N\times 9N} . \tag{A.3}$$

$$\mathbf{b_{eq2}} = \begin{bmatrix} 0_1 \\ \vdots \\ 0_N \end{bmatrix}_{N\times 1} . \tag{A.4}$$

Lastly, the matrix $\mathbf{A_{eq3}}$ shown in equation (A.5) and vector $\mathbf{b_{eq3}}$ shown in equation (A.6) are constituted from the HK power balance of equation (3.20).

$$\mathbf{A_{eq3}} = \begin{bmatrix} 0 \cdots 0 & 0 \cdots 0 & P_{HK} \cdots 0 & 0 \cdots 0 & -1 \cdots 0 & 0 \cdots 0 & -1 \cdots 0 & 0 \cdots 0 & 0 \cdots 0 \\ \vdots \ddots \vdots & \vdots \ddots \vdots & \vdots \ddots \vdots & \vdots \ddots \vdots & \vdots \ddots \vdots & \vdots \ddots \vdots & \vdots \ddots \vdots & \vdots \ddots \vdots & \vdots \ddots \vdots \\ 0 \cdots 0 & 0 \cdots 0 & 0 \cdots P_{HK} & 0 \cdots 0 & 0 \cdots -1 & 0 \cdots 0 & 0 \cdots -1 & 0 \cdots 0 & 0 \cdots 0 \end{bmatrix}_{N\times 9N} . \tag{A.5}$$

$$\mathbf{b_{eq3}} = \begin{bmatrix} 0_1 \\ \vdots \\ 0_N \end{bmatrix}_{N\times 1} . \tag{A.6}$$

The canonical form , $\boldsymbol{A_{eq}X} = \boldsymbol{b_{eq}}$ is given in equation (B.10).

$$\mathbf{A_{eq}} = \begin{bmatrix} \mathbf{A_{eq1}} \\ \mathbf{A_{eq2}} \\ \mathbf{A_{eq3}} \end{bmatrix}_{3N\times 7N} , \qquad \mathbf{b_{eq}} = \begin{bmatrix} \mathbf{b_{eq1}} \\ \mathbf{b_{eq2}} \\ \mathbf{b_{eq3}} \end{bmatrix}_{3N\times 1} . \tag{A.7}$$

A.2 INEQUALITY MATRICES

The general formulation of the inequality constraint is shown in equation (A.8):

$$\boldsymbol{AX} \leqslant \boldsymbol{b}. \tag{A.8}$$

Expression (3.22) constitutes the upper boundary matrix $\mathbf{A_1}$ given by equation (A.9) and the upper boundary vector $\mathbf{b_1}$ given by equation (A.10). Where the lower boundary matrix $\mathbf{A_2} = -\mathbf{A_1}$ and the lower boundary vector $\mathbf{b_2}$ is given by equation (A.11).

$$\mathbf{A_1} = \begin{bmatrix} 0 \cdots 0 & \frac{q_2 t_s}{A_u} & \cdots & 0 & 0 \cdots 0 & -\frac{t_s}{A_u} & \cdots & 0 & 0 \cdots 0 & 0 \cdots 0 & 0 \cdots 0 & 0 \cdots 0 & 0 \cdots 0 \\ \vdots \ddots \vdots & \vdots & \ddots & \vdots & \vdots \ddots \vdots & \vdots & \ddots & \vdots & \vdots \ddots \vdots & \vdots \ddots \vdots & \vdots \ddots \vdots & \vdots \ddots \vdots & \vdots \ddots \vdots \\ 0 \cdots 0 & \frac{q_2 t_s}{A_u} & \cdots & \frac{q_2 t_s}{A_u} & 0 \cdots 0 & -\frac{t_s}{A_u} & \cdots & -\frac{t_s}{A_u} & 0 \cdots 0 & 0 \cdots 0 & 0 \cdots 0 & 0 \cdots 0 & 0 \cdots 0 \end{bmatrix}_{N \times 9N} . \tag{A.9}$$

$$\mathbf{b_1} = \begin{bmatrix} h_u^{max} - h_{u,0} - \frac{q_{in} t_s, 1}{A_u} \\ \vdots \\ h_u^{max} - h_{u,0} - \frac{q_{in} t_s, N}{A_u} \end{bmatrix}_{N \times 1} . \tag{A.10}$$

$$\mathbf{b_2} = \begin{bmatrix} -h_u^{min} + h_{u,0} + \frac{q_{in} t_s, 1}{A_u} \\ \vdots \\ -h_u^{min} + h_{u,0} + \frac{q_{in} t_s, N}{A_u} \end{bmatrix}_{N \times 1} . \tag{A.11}$$

Similarly, the inequality constraint equation (3.23) constitutes the matrix $\mathbf{A_3}$ given by equation (A.12) and vector $\mathbf{b_3}$ expressed by equation (A.13):

$$\mathbf{A_3} = \begin{bmatrix} \frac{q_1 t_s}{A_m} & \cdots & 0 & \frac{-q_2 t_s}{A_m} & \cdots & 0 & 0 \cdots 0 & 0 \cdots 0 & 0 \cdots 0 & 0 \cdots 0 & 0 \cdots 0 & 0 \cdots 0 & 0 \cdots 0 \\ \vdots & \ddots & \vdots & \vdots & \ddots & \vdots & \vdots \ddots \vdots & \vdots \ddots \vdots & \vdots \ddots \vdots & \vdots \ddots \vdots & \vdots \ddots \vdots & \vdots \ddots \vdots & \vdots \ddots \vdots \\ \frac{q_1 t_s}{A_m} & \cdots & \frac{q_1 t_s}{A_m} & \frac{-q_2 t_s}{A_m} & \cdots & \frac{-q_2 t_s}{A_m} & 0 \cdots 0 & 0 \cdots 0 & 0 \cdots 0 & 0 \cdots 0 & 0 \cdots 0 & 0 \cdots 0 & 0 \cdots 0 \end{bmatrix}_{N \times 9N} . \tag{A.12}$$

$$\mathbf{b_3} = \begin{bmatrix} h_m^{max} - h_{m,0} \\ \vdots \\ h_m^{max} - h_{m,0} \end{bmatrix}_{N \times 1} . \tag{A.13}$$

The lower boundary matrix of the intermediate reservoir $\mathbf{A_4} = -\mathbf{A_3}$ and lower limit vector $\mathbf{b_4}$ is given by equation (A.14).

$$\mathbf{b_4} = \begin{bmatrix} -h_m^{min} + h_{m,0} \\ \vdots \\ -h_m^{min} + h_{m,0} \end{bmatrix}_{N\times 1} . \tag{A.14}$$

By letting

$$A_{51} = \begin{bmatrix} 1 & 0 & 0 & \dots & 0 \\ -1 & 1 & 0 & \dots & 0 \\ 0 & -1 & 1 & \dots & 0 \\ \vdots & \vdots & \ddots & \ddots & \vdots \\ 0 & 0 & \dots & -1 & 1 \end{bmatrix}_{N\times N}, \quad A_{52} = \begin{bmatrix} -1 & 0 & 0 & \dots & 0 \\ 0 & -1 & 0 & \dots & 0 \\ 0 & 0 & -1 & \dots & 0 \\ \vdots & \vdots & \vdots & \ddots & \vdots \\ 0 & 0 & 0 & \dots & -1 \end{bmatrix}_{N\times N}, \tag{A.15}$$

then, the inequality expressed by equation (3.29) can be written as

$$A_5 = \begin{bmatrix} A_{51}, & A_{51}, & 0, & 0, & 0, & 0, & 0, & A_{52}, & A_{52} \end{bmatrix}_{N\times 9N}, \tag{A.16}$$

$$\mathbf{b_5} = \begin{bmatrix} 0, & 0, & 0, & ..., & 0 \end{bmatrix}^T_{N\times 1} . \tag{A.17}$$

Therefore, the final expression of the matrix $\mathbf{A}$ and vector $\mathbf{b}$ is given by equation (A.18)

$$\mathbf{A} = \begin{bmatrix} \mathbf{A_1} \\ \mathbf{A_2} \\ \mathbf{A_3} \\ \mathbf{A_4} \\ \mathbf{A_5} \end{bmatrix}_{5N\times 9N}, \quad \mathbf{b} = \begin{bmatrix} \mathbf{b_1} \\ \mathbf{b_2} \\ \mathbf{b_3} \\ \mathbf{b_4} \\ \mathbf{b_5} \end{bmatrix}_{5N\times 1} . \tag{A.18}$$

ADDENDUM B CHAPTER 4 DETAILED ALGORITHM FORMULATION

B.1 BASELINE OPTIMISATION MODEL

B.1.1 Equality matrices

The equality matrix $\mathbf{A_{eq}}$ and the vector $\mathbf{b_{eq1}}$ of the baseline model are formulated from equation (4.14) as follows:

$$\mathbf{A_{eq}} = \begin{bmatrix} \frac{9.81\eta_m\eta_e h_o}{1000} & \cdots & 0 \\ \vdots & \ddots & \vdots \\ 0 & \cdots & \frac{9.81\eta_m\eta_e h_o}{1000} \end{bmatrix}_{N\times N}, \qquad \mathbf{b_{eq1}} = \begin{bmatrix} P_{ld,1} \\ \vdots \\ P_{ld,N} \end{bmatrix}_{N\times 1}, \tag{B.1}$$

where the vector $\mathbf{b_{eq}} = \mathbf{b_{eq1}}$.

B.1.2 Inequality matrices

From the state constraint of the dam expressed by equation (4.18), the inequality matrix $\mathbf{A_1}$ and the upper boundary vector $\mathbf{b_1}$ are constituted. The lower boundary matrix $\mathbf{A_2} = -\mathbf{A_1}$ and the lower boundary vector $\mathbf{b_2}$ are given in equation (B.3).

$$\mathbf{A_1} = \begin{bmatrix} \frac{-t_s}{A_u} & \cdots & 0 \\ \vdots & \ddots & \vdots \\ \frac{-t_s}{A_u} & \cdots & \frac{-t_s}{A_u} \end{bmatrix}_{N\times N} . \tag{B.2}$$

$$\mathbf{b_1} = \begin{bmatrix} h_u^{max} - h_{u,0} - \frac{q_{in}t_s,1}{A_u} \\ \vdots \\ h_u^{max} - h_{u,0} - \frac{q_{in}t_s,N}{A_u} \end{bmatrix}_{N\times 1} , \qquad \mathbf{b_2} = \begin{bmatrix} -h_u^{min} + h_{u,0} + \frac{q_{in}t_s,1}{A_u} \\ \vdots \\ -h_u^{min} + h_{u,0} + \frac{q_{in}t_s,N}{A_u} \end{bmatrix}_{N\times 1} . \tag{B.3}$$

The final canonical expression, $\boldsymbol{AX} = \boldsymbol{b}$ is formulated in equation (B.4).

$$\mathbf{A} = \begin{bmatrix} \mathbf{A_1} \\ \mathbf{A_2} \end{bmatrix}_{2N\times N} , \qquad \mathbf{b} = \begin{bmatrix} \mathbf{b_1} \\ \mathbf{b_2} \end{bmatrix}_{2N\times N} . \tag{B.4}$$

B.2 MODEL FOR OPTIMISATION SCENARIO II & III

B.2.1 Equality matrices

From the system power balance equation (4.21), a sparse matrix $\mathbf{A_{eq1}}$ given by equation (B.5) and a vector $\mathbf{b_{eq1}}$ is given in equation (B.1) are constituted.

$$\mathbf{A_{eq1}} = \begin{bmatrix} 0 & \cdots & 0 & 0 & \cdots & 0 & \frac{9.81\eta_m\eta_e h_o}{1000} & \cdots & 0 & 0 & \cdots & 0 & 0 & \cdots & 0 & 1 & \cdots & 0 \\ \vdots & \ddots & \vdots & \vdots & \ddots & \vdots & \vdots & \ddots & \vdots & \vdots & \ddots & \vdots & \vdots & \ddots & \vdots & \vdots & \ddots & \vdots \\ 0 & \cdots & 0 & 0 & \cdots & 0 & 0 & \cdots & \frac{9.81\eta_m\eta_e h_o}{1000} & 0 & \cdots & 0 & 0 & \cdots & 0 & 0 & \cdots & 1 \end{bmatrix}_{6N\times N} . \tag{B.5}$$

Similarly, the sparse matrix, $\mathbf{A_{eq2}}$ given by equation (B.6), and a vector, $\mathbf{b_{eq2}}$ given in equation (B.7) are constituted from the pumping power balance equation (4.23).

$$\mathbf{A_{eq2}} = \begin{bmatrix} -P_K & \cdots & 0 & \vdots & 0 & \cdots & 0 & \vdots & 0 & \cdots & 0 & \vdots & 0 & \cdots & 0 & \vdots & 1 & \cdots & 0 & \vdots & 0 & \cdots & 0 \\ \vdots & \ddots & \vdots & \vdots & \vdots & \ddots & \vdots & \vdots & \vdots & \ddots & \vdots & \vdots & \vdots & \ddots & \vdots & \vdots & \vdots & \ddots & \vdots & \vdots & \vdots & \ddots & \vdots \\ 0 & \cdots & -P_K & \vdots & 0 & \cdots & 0 & \vdots & 0 & \cdots & 0 & \vdots & 0 & \cdots & 0 & \vdots & 0 & \cdots & 1 & \vdots & 0 & \cdots & 0 \end{bmatrix}_{6N \times N} . \tag{B.6}$$

$$\mathbf{b_{eq2}} = \begin{bmatrix} -P_{WT,1} \\ \vdots \\ -P_{WT,N} \end{bmatrix}_{N \times 1} . \tag{B.7}$$

From the hydrokinetic energy conversion system power balance equation (4.22), the matrix $\mathbf{A_{eq3}}$ shown in equation (B.8) and the vector $\mathbf{b_{eq3}}$ shown in equation (B.9) are constituted.

$$\mathbf{A_{eq3}} = \begin{bmatrix} 0 & \cdots & 0 & \vdots & -P_{HK} & \cdots & 0 & \vdots & 0 & \cdots & 0 & \vdots & 0 & \cdots & 0 & \vdots & 1 & \cdots & 0 & \vdots & 1 & \cdots & 0 \\ \vdots & \ddots & \vdots & \vdots & \vdots & \ddots & \vdots & \vdots & \vdots & \ddots & \vdots & \vdots & \vdots & \ddots & \vdots & \vdots & \vdots & \ddots & \vdots & \vdots & \vdots & \ddots & \vdots \\ 0 & \cdots & 0 & \vdots & 0 & \cdots & -P_{HK} & \vdots & 0 & \cdots & 0 & \vdots & 0 & \cdots & 0 & \vdots & 0 & \cdots & 1 & \vdots & 0 & \cdots & 1 \end{bmatrix}_{6N \times N} . \tag{B.8}$$

$$\mathbf{b_{eq3}} = \begin{bmatrix} 0_1 \\ \vdots \\ 0_N \end{bmatrix}_{N \times 1} . \tag{B.9}$$

The final canonical expression , $\boldsymbol{A_{eq}X} = \boldsymbol{b_{eq}}$ is formulated in equation (B.10).

$$\mathbf{A_{eq}} = \begin{bmatrix} \mathbf{A_{eq1}} \\ \mathbf{A_{eq2}} \\ \mathbf{A_{eq3}} \end{bmatrix}_{3N \times N} , \qquad \mathbf{b_{eq}} = \begin{bmatrix} \mathbf{b_{eq1}} \\ \mathbf{b_{eq2}} \\ \mathbf{b_{eq3}} \end{bmatrix}_{3N \times N} . \tag{B.10}$$

B.2.2 Inequality matrices

Equation (B.11) shows the upper boundary matrix $\mathbf{A_1}$ constituted from the dam's water level constraint equation (4.24). The lower boundary matrix $\mathbf{A_2} = -\mathbf{A_1}$. The upper and the lower boundary vectors $\mathbf{b_1}$ and $\mathbf{b_2}$ are expressed in equation (B.3).

$$\mathbf{A_1} = \begin{bmatrix} \frac{q_k t_s}{A_u} & \cdots & 0 & \vdots & 0 & \cdots & 0 & \vdots & \frac{-t_s}{A_u} & \cdots & 0 & \vdots & 0 & \cdots & 0 & \vdots & 0 & \cdots & 0 & \vdots & 0 & \cdots & 0 \\ \vdots & \ddots & \vdots & \vdots & \vdots & \ddots & \vdots & \vdots & \vdots & \ddots & \vdots & \vdots & \vdots & \ddots & \vdots & \vdots & \vdots & \ddots & \vdots & \vdots & \vdots & \ddots & \vdots \\ \frac{q_k t_s}{A_u} & \cdots & \frac{q_k t_s}{A_u} & \vdots & 0 & \cdots & 0 & \vdots & \frac{-t_s}{A_u} & \cdots & \frac{-t_s}{A_u} & \vdots & 0 & \cdots & 0 & \vdots & 0 & \cdots & 0 & \vdots & 0 & \cdots & 0 \end{bmatrix}_{N \times 6N} . \tag{B.11}$$

Similarly, the re-regulation reservoir water level constraint equation (4.31) constitutes the matrix $\mathbf{A_3}$ given by equation (B.12). The lower boundary matrix of the intermediate reservoir $\mathbf{A_4} = -\mathbf{A_3}$ while the upper boundary vector $\mathbf{b_3}$ and the lower boundary vector $\mathbf{b_4}$ are expressed in equation (B.13)

$$\mathbf{A_3} = \begin{bmatrix} \frac{-q_k t_s}{A_r} & \cdots & 0 & \vdots & 0 & \cdots & 0 & \vdots & \frac{t_s}{A_r} & \cdots & 0 & \vdots & \frac{-t_s}{A_r} & \cdots & 0 & \vdots & 0 & \cdots & 0 & \vdots & 0 & \cdots & 0 \\ \vdots & \ddots & \vdots & \vdots & \vdots & \ddots & \vdots & \vdots & \vdots & \ddots & \vdots & \vdots & \vdots & \ddots & \vdots & \vdots & \vdots & \ddots & \vdots & \vdots & \vdots & \ddots & \vdots \\ \frac{-q_k t_s}{A_r} & \cdots & \frac{-q_k t_s}{A_r} & \vdots & 0 & \cdots & 0 & \vdots & \frac{t_s}{A_r} & \cdots & \frac{t_s}{A_r} & \vdots & \frac{-t_s}{A_r} & \cdots & \frac{-t_s}{A_r} & \vdots & 0 & \cdots & 0 & \vdots & 0 & \cdots & 0 \end{bmatrix}_{N \times 6N} . \tag{B.12}$$

$$\mathbf{b_3} = \begin{bmatrix} h_r^{max} - h_{r,0} \\ \vdots \\ h_r^{max} - h_{r,0} \end{bmatrix}_{N \times 1} , \qquad \mathbf{b_4} = \begin{bmatrix} -h_r^{min} + h_{r,0} \\ \vdots \\ -h_r^{min} + h_{r,0} \end{bmatrix}_{N \times 1} . \tag{B.13}$$

Thus, the final expression of the matrix $\mathbf{A}$ and vector $\mathbf{b}$ is given by equation (B.14)

$$\mathbf{A} = \begin{bmatrix} \mathbf{A_1} \\ \mathbf{A_2} \\ \mathbf{A_3} \\ \mathbf{A_4} \end{bmatrix}_{4N \times N} , \qquad \mathbf{b} = \begin{bmatrix} \mathbf{b_1} \\ \mathbf{b_2} \\ \mathbf{b_3} \\ \mathbf{b_4} \end{bmatrix}_{4N \times N} . \tag{B.14}$$